20981

NATIONAL LIBRARY
OTTAWA

CANADA

BIBLIOTHÈQUE NATIONALE
OTTAWA

NAME OF AUTHOR........CHAN, CHARLES F.S.........

TITLE OF THESIS...CRITICAL BEHAVIOUR OF THE THREE-

DIMENSIONAL, SPIN 1/2 ISING MODEL

ON THE HYDROGEN PEROXIDE LATTICE.

UNIVERSITY.......UNIV. OF ALBERTA.........

DEGREE FOR WHICH THESIS WAS PRESENTED...M.Sc........

YEAR THIS DEGREE GRANTED.......1974..........

Permission is hereby granted to THE NATIONAL LIBRARY OF CANADA to microfilm this thesis and to lend or sell copies of the film.

(Signed)....Charles Chan.........

PERMANENT ADDRESS:

805 GALBRAITH HSE

MICHENER PARK

EDMONTON, ALBERTA

DATED...29 APRIL.........1974.

NL-91 (10-68)

THE UNIVERSITY OF ALBERTA

CRITICAL BEHAVIOUR OF THE THREE-DIMENSIONAL, SPIN 1/2 ISING MODEL ON THE HYDROGEN PEROXIDE LATTICE

by

© C.F.S. CHAN

A THESIS

SUBMITTED TO THE FACULTY OF GRADUATE STUDIES AND RESEARCH IN PARTIAL FULFILMENT OF THE REQUIREMENTS FOR THE DEGREE OF MASTER OF SCIENCE

IN

THEORETICAL PHYSICS

DEPARTMENT........PHYSICS..........................

EDMONTON, ALBERTA

SPRING, 1974

THE UNIVERSITY OF ALBERTA

FACULTY OF GRADUATE STUDIES AND RESEARCH

The undersigned certify that they have read, and recommend to the Faculty of Graduate Studies and Research, for acceptance, a thesis entitled Critical Behaviour of the Three-Dimensional, Spin 1/2 Ising Model on the Hydrogen Peroxide Lattice submitted by C. F. S. Chan in partial fulfilment of the requirements for the degree of Master of Science in Theoretical Physics.

Donald D. Betts
Supervisor

....

....

....

....
External Examiner

Date 22 APRIL 1974

Abstract

The low temperature configurational data obtained by Betts et al (1974) for the spin 1/2 Ising model on the hydrogen peroxide lattice are used to derive series in $z = \exp(-2J/kT)$, along the coexistence curve for the magnetization, M, and its first five derivatives, $\partial^{\ell}M/\partial\mu^{\ell}$, where $\mu = \exp(-2mH/kT)$. Series in μ along the critical isotherm are also derived for M and its first five derivatives, $\partial^{\ell}M/\partial z^{\ell}$. Critical exponents and critical amplitudes are estimated by Padé approximant analysis. Except for a few estimates which are not in good agreement with scaling, the majority of the estimated critical exponents support scaling theory.

Acknowledgement

The author would like to thank Dr. D.D. Betts for suggesting the problem, for his guidance, and for his encouragement. The author is also very grateful to Dr. C.J. Elliott and Mr. L. Filipow for their help with the computational work, and to Mrs. Doris Nordheimer for typing the thesis.

TABLE OF CONTENTS

LIST OF FIGURES

Figure | Page

Figure		Page

LIST OF TABLES

CHAPTER 1

Introduction

Phase transitions are common enough occurrences that the layman is well aware of them. Yet his curiosity does not extend beyond a mere acknowledgement of the fact. The physicist however is impelled by a strong curiosity to get to the bottom of things. We know gases can undergo condensation to liquids under the right conditions; solids can be melted; and the components of a mixture in solution can be made to separate. Transitions of such assemblies belong to a special category which may be appropriately labelled as cooperative phenomena, or critical phenomena. We shall use both terms interchangeably. We use the description "cooperative" because a detailed investigation reveals that the peculiar behaviour of such assemblies result from the interactions between individual microscopic systems. These interactions cause the cooperation of large numbers of systems to give rise to the phenomena listed above. In many of such phenomena, singularities or discontinuities are encountered in the thermodynamic description of these assemblies, and so an alternative term for such phenomena has been "critical phenomena".

The classical era of critical phenomena began with Andrews' 1869 publication of experiments on the critical point of carbon dioxide. A classic theoretical attempt to describe the critical region was made by van der Waals three years later, in his Ph.D. dissertation, "On the continuity of the liquid and gaseous states." To this day this description is fairly accurate for temperatures that are not too close to T_c, the critical temperature. Unfortunately there is a certain shortcoming in the van der Waals' theory. For all subcritical isotherms ($T < T_c$) there exists a region where the slope $\partial V/\partial P$ is positive, corresponding to the unphysical occurrence of a negative isothermal compressibility, $K_T = -V^{-1}(\partial V/\partial P)_T$. The theory was saved by the ad hoc construction named after its famous proposer, James Clerk Maxwell. For further details of the Maxwell construction one should refer to Huang (1963).

Following the spirit of van der Waals' work, the next development of importance to the understanding of critical phenomena came from theoretical efforts to understand magnetic transitions. In the early twentieth century, important pioneering work on experimental magnetism was done by Curie, Hopkinson and others. Of interest to us are the physical properties of ferromagnets. At temperatures lower than a certain critical temperature known as the Curie temperature, T_c, a ferromagnet possesses a spontaneous magnetization. For temperatures above T_c, the spontaneous magnetization vanishes, but the paramagnetic susceptibility becomes infinite at T_c, while the specific heat exhibits a λ-type singularity. To explain and consolidate the experimental findings, a number of important theories were advanced. Pierre Weiss (1907) proposed a phenomenological theory of ferromagnetism in which he suggested the spins interact with one another through an effective molecular field. Moreover, this field is proportional to the average magnetization.

Later modifications of this idea of interacting magnetic moments assume the constituent magnetic moments to be localized on fixed lattice sites, with pairwise interaction of the spins. In particular, the Ising model has been exceptionally successful in explaining magnetic cooperative phenomena. The model was suggested by Wilhelm Lenz to his student E. Ising in the early 1920's, which is why the model is occasionally referred to as the Lenz-Ising model. The spins are assumed capable of two orientations: "up" or "down"; with parallel alignment of neighbouring spins energetically favoured.

Ising (1925) succeeded in solving the model with nearest neighbour interactions only for the case of a linear chain (i.e. a one-dimensional lattice with coordination number 2). The solution did not display a phase transition at finite temperatures greater than zero. Peierls (1936) demonstrated that a two-dimensional or three-dimensional model would exhibit ferromagnetism. This was substantiated in part by a major breakthrough by Onsager (1944) when he obtained the exact solution of the two-dimensional Ising model in the absence of a magnetic field.

At the time of writing there is as yet no exact solution to the three-dimensional Ising model. Fortunately, approximation methods are available in the form of series expansions of the partition function at low and high temperatures (Domb, 1960). More recent reviews can be found in Fisher (1967), Stephenson (1971), and Domb and Green (1974). With the aid of high temperature series expansions, the critical temperatures and the critical index, γ, of the initial susceptibility for the f.c.c., b.c.c., s.c. and diamond lattices (coordination numbers 12, 8, 6 and 4 respectively) have been investigated and are well known for some time now (Domb and Sykes, 1957; Essam and Sykes, 1963). However investigations on the low temperature side have been quite scarce until recently (Essam and Hunter, 1968; Betts and Filipow, 1973; Betts and Chan, 1974).

The general theory of low temperature series expansions have been laid out in a series of papers: Sykes, Essam and Gaunt, 1965 (paper I); Sykes, Essam, Gaunt and Hunter, 1973 (paper II); and Sykes, Gaunt, Essam, Mattingly and Elliott, 1973 (paper III). Now the hydrogen peroxide lattice (Heesch and Laves, 1933; and Wells, 1954), is the three dimensional lattice with the smallest coordination number ($q = 3$). Using it as a lattice for extending the three-dimensional model to the lowest limit of coordination number possible for a three dimensional lattice, Leu, Betts and Elliott (1969) investigated the critical properties on the high temperature side ($T > T_c$). The high field (low temperature) series expansions for the Ising model on the hydrogen peroxide lattice were derived in a later paper by Betts, Elliott and Sykes (1974). We shall make use of the configurational data obtained by Betts et al (1974) to investigate the following. For $T < T_c$, we shall study the critical behaviour of the magnetization M, and its first five derivatives with respect to the field variable, $\mu = \exp(-2mH/kT)$ on the coexistence curve (H = 0). We shall also derive series expansions in μ along the critical isotherm ($T = T_c$), for M and its first five derivatives with respect to the temperature variable, $z = \exp(-2J/kT)$. The techniques of Padé approximant analysis will be applied to the series so obtained to estimate critical exponents and critical amplitudes.

CHAPTER 2

Theory of the critical region.

2.1 Critical exponents

In the study of critical phenomena it has been found that most of the thermodynamic functions of interest, such as the specific heat, the magnetization and its higher derivatives, usually vary with temperature or some other independent thermodynamic variable according to the form:

$$f(x) \sim A\{(x-x_c)/x_c\}^{\lambda} \text{ +less singular terms, } x>x_c$$

$$A'\{(x_c-x)/x_c\}^{\lambda'} \text{ +less singular terms, } x<x_c, \quad (2.1)$$

where A, or A', a numerical constant, is called the critical amplitude, x is a general, independent thermodynamic variable, x_c is the value of the independent thermodynamic variable at the critical point, and f(x) is a general thermodynamic function of interest. Then the numerical constant, λ, or λ', is defined as the critical exponent characterizing the asymptotic behaviour of the thermodynamic function, f(x), at the critical point. In view of the less singular terms in (2.1), the critical exponents, λ or λ', are sometimes defined more rigorously as:

$$\lambda = \lim_{x\to x_c^+} \frac{\ln f(x)}{\ln(x-x_c)/x_c}, \quad x>x_c$$

$$\lambda' = \lim_{x\to x_c^-} \frac{\ln f(x)}{\ln(x_c-x)/x_c}, \quad x<x_c \quad (2.2)$$

We look next at a few selected critical exponents and amplitudes. We define $t= (T-T_c)/T_c$, where T is the temperature, and T_c the temperature at the critical point. Since we are interested in regions close to the critical point we ignore less singular terms in the definitions that follow. For a magnetic system the specific heat at constant magnetic field, H = 0, has the following asymptotic functional form near $T = T_c$.

$$\frac{C_H}{Nk} \sim \begin{cases} A\ (t)^{-\alpha}, & T > T_c \text{ (i.e. } t > 0) \\ A'\ (-t)^{-\alpha'}, & T < T_c \text{ (i.e. } t < 0) \end{cases} \qquad (2.3)$$

The dimensionless quantities A and A' are the critical amplitudes. The critical exponents α and α' characterize the behaviour of the specific heat at constant field when the critical point is approached from above and below T_c respectively. For the three dimensional Ising model it is believed that (Sykes, Hunter, McKenzie and Heap, 1972)

$$\alpha \simeq 1/8 \qquad (2.4)$$

The temperature dependence of the reduced zero field magnetization, M(t) near the critical point is described by

$$M_0(t) = \mathfrak{M}_0(t)/\mathfrak{M}_0(-1) \sim B\ (-t)^{\beta}, \quad t<0 \qquad (2.5)$$

($\mathfrak{M}$ is used here to denote the magnetization in the ordinary sense.)

We note that B, the critical amplitude, is again dimensionless and β is the critical exponent characterizing the behaviour of the zero field magnetization in the neighbourhood of the critical point. The estimates of β (Fisher, 1965) lie in the range $0.303 \leq \beta \leq 0.318$. The conjecture is

$$\beta \simeq 5/16 = 0.312500 \qquad (2.6)$$

The exponent δ describes the variation of the reduced magnetization, M, with the reduced field ($h = mH/kT_c$) on the critical isotherm t=0 ($T=T_c$) :

$$|M| \sim \mathcal{D}|h|^{1/\delta} \qquad (2.7)$$

(k is Boltzmann's constant, and m is the magnetic moment per spin). Sometimes the above expression is written as

$$h \sim D\, M^{\delta} \qquad (2.8)$$

It is believed (Gaunt and Sykes, 1973) that for the three-dimensional Ising model:

$$\delta \simeq 5 \qquad (2.9)$$

Consider the H-M isotherms for a magnetic system. The slopes of these isotherms are proportional to the inverse isothermal susceptibility, χ_T^{-1}, and χ_T diverges to infinity as T approaches T_c. So we define critical exponents, γ and γ', and critical amplitudes, C and C' to describe this behaviour.

$$\chi_T/\chi_T^0 \sim \begin{cases} C(t)^{-\gamma} & , \quad T > T_c,\ H \to 0 \\ C'(-t)^{-\gamma'} & , \quad T < T_c,\ H \to 0 \end{cases} \tag{2.10}$$

χ_T^0 is the isothermal susceptibility of a system of non-interacting magnetic moments (paramagnet) at the critical point. It is believed that (Fisher, 1967; Sykes, Gaunt, Roberts and Wyles, 1972):

$$\gamma \simeq 5/4 \ , \quad \text{and } \gamma' \simeq 5/4 \tag{2.11}$$

For convenience let:

$$\Delta = \beta\delta \ . \tag{2.12}$$

2.2 Exponent Inequalities

The work of Rushbrooke (1963), Essam and Fisher (1963), Fisher (1964, 1967, 1969), Griffiths (1965a,b, 1968) and Griffiths, Hurst and Sherman (1970), among others, have focused attention on a number of rigourous relations among critical exponents expressed in the form of inequalities.

The Rushbrooke Inequality

For a magnetic system we may define specific heats at constant magnetization, C_M, or at constant field, C_H. Then:

$$C_M \equiv T\left(\frac{\partial S}{\partial T}\right)_M = \left(\frac{\partial U}{\partial T}\right)_M = -T\left(\frac{\partial^2 A}{\partial T^2}\right)_M \tag{2.13}$$

and:

$$C_H \equiv T\left(\frac{\partial S}{\partial T}\right)_H = \left(\frac{\partial E}{\partial T}\right)_H = -T\left(\frac{\partial^2 G}{\partial T^2}\right)_H \tag{2.14}$$

The isothermal susceptibility is given by:

$$\chi_T \equiv \left(\frac{\partial M}{\partial H}\right)_T = -\left(\frac{\partial^2 G}{\partial H^2}\right)_T \tag{2.15}$$

while the adiabatic susceptibility is:

$$\chi_S \left(\frac{\partial M}{\partial H}\right)_S = -\left(\frac{\partial^2 E}{\partial H^2}\right)_S \tag{2.16}$$

In the four expressions above we have:

U ≡ internal energy

S ≡ entropy

A ≡ Helmholtz potential

G ≡ Gibbs potential

E ≡ enthalpy

From thermodynamic considerations it can be shown that

$$C_H - C_M = \frac{T}{\chi_T} \cdot \left(\frac{\partial M}{\partial T}\right)_H^2 \tag{2.17}$$

Griffiths (1964) showed that (i) the Gibbs potential, G(T,H), is a concave function of both magnetic field and temperature, and (ii) the Helmholtz potential, A(T,M), is a concave function of the temperature and a convex function of the magnetization, for a magnetic system whose Hamiltonian is of the form:

$$\mathcal{H} = \mathcal{H}_0 - H\mathcal{M} \tag{2.18}$$

$\mathcal{M}$ is the magnetization operator.

(The Ising model has a Hamiltonian of the form (2.18).)

Using the convexity property of A(T,M) it can be shown that C_M must be positive. Then taking equation (2.17) it is found that

$$C_H \geq T \left(\frac{\partial M}{\partial T}\right)_H^2 / \chi_T \tag{2.19}$$

From (2.19) and the definitions of the critical exponents discussed in section 2.1, Rushbrooke (1963) showed that

$$\alpha' + 2\beta + \gamma' \geq 2. \qquad (2.20)$$

(2.20) is called the Rushbrooke inequality.

<u>The Griffiths Inequality</u>

The other inequality of interest to us is the Griffiths inequality:

$$\alpha' + \beta(1 + \delta) \geq 2. \qquad (2.21)$$

We omit the proof here, and instead refer the reader to Griffiths (1965a, 1965b).

2.3 Scaling Ideas

An immediate question is, "When are the inequalities discussed in section 2.2 equalities?" Approaches investigating whether these inequalities are indeed equalities were first described by Widom (1965a,b), Patashinskii and Pokrovskii (1966), Domb and Hunter (1965) and Kadanoff (1966). Today these ideas are embodied in what has come to be described as scaling theory.

It should be pointed out that standard scaling theory is essentially a theory for critical exponents. It has also come to be called the homogeneous function approach. At the heart of this approach is the assertion that the Gibbs potential, or free energy, is a generalized homogeneous function. Then from the form of the Gibbs potential and the properties of homogeneous functions it becomes apparent that all of the critical exponents can be expressed in terms of two parameters, if we consider a magnetic system where the Gibbs free energy is a function of the temperature and the applied field. Two critical exponents, β and δ, have already been introduced in the preceding section. Two methods will be used to show how the critical exponents of the higher derivatives of the magnetization are related to β and δ.

We begin with the approach due to Widom(1965a,b). The basic postulate of static scaling theory tells us that the Gibbs free energy is a generalized homogeneous function of the field, and the temperature. Without loss of generality, we shall work with the reduced temperature, $t = (T-T_c)/T_c$, and the reduced field $h = mH/kT_c$. Introducing two general parameters, a_t and a_h, the Gibbs free energy may be written:

$$G(\lambda^{a_t}t,\ \lambda^{a_h}h) = \lambda\ G(t,h) \tag{2.22}$$

The above is then differentiated with respect to h:

$$\lambda^{a_h}\ \partial\{G(\lambda^{a_t}t,\ \lambda^{a_h}h)\}/\ \partial(\lambda^{a_h}h) = \lambda\quad \partial G(t,h)/\partial h \tag{2.23}$$

But the reduced magnetization is defined as:

$$M(t,h) = -\ \partial G(t,h)/\partial h \tag{2.24}$$

Hence (2.23) simplifies to:

$$\lambda^{a_h}\quad M(\lambda^{a_t}t,\ \lambda^{a_h}h) = \lambda . M(t,h) \tag{2.25}$$

It now becomes apparent that there are 2 critical exponents associated with the behaviour of the magnetization near the critical point depending on whether

(i) $\lambda^{a_t}t/\lambda^{a_h}h \to 0$,

or (ii) $\lambda^{a_h}h/\lambda^{a_t}t \to 0$.

Case (i)

When $\lambda^{a_t} t/\lambda^{a_h} h \rightarrow 0$, equation (2.25) becomes:

$$M(0,h) = \lambda^{a_h - 1} M(0, \lambda^{a_h} h) \tag{2.26}$$

Setting $\lambda = h^{-1/a_h}$, one obtains:

$$M(0,h) = h^{(1-a_h)/a_h} \cdot M(0,1)$$

But from (2.7), $M(0,h) \sim h^{1/\delta}$

Therefore: $$a_h = \delta(1-a_h) \tag{2.27}$$

or $$\delta = a_h/(1-a_h) \tag{2.28}$$

Case (ii)

When $\lambda^{a_h} h/\lambda^{a_t} t \rightarrow 0$, equation (2.25) reduces to:

$$M(t,0) = \lambda^{a_h - 1} M(\lambda^{a_t} t, 0) \tag{2.29}$$

Now upon choosing $\lambda = (-1/t)^{1/a_t}$, we get:

$$M(t,0) = (-t)^{(1-a_h)/a_t} M(-1,0)$$

However when $\lambda^{a_h} h/\lambda^{a_t} t \rightarrow 0$, the reduced magnetization becomes such that:

$$M(t,0) \sim (-t)^{\beta} \tag{2.30}$$

(Note that less singular terms are neglected as before.)

Thus $$\beta = (1-a_h)/a_t \tag{2.31}$$

Solving for a_t:

$$a_t = \beta^{-1}(\delta + 1)^{-1} \tag{2.32}$$

Solving (2.27) for a_h:

$$a_h = \delta/(\delta + 1) \tag{2.33}$$

Substituting for a_t and a_h in equation (2.25) yields:

$$M(t,h) = \lambda^{-1/(\delta+1)} M(\lambda^{1/\beta(\delta+1)}t, \lambda^{\delta/(\delta+1)}h) \tag{2.34}$$

With a choice of $\lambda = \S^{\delta+1}$, (2.34) becomes:

$$M(t,h) = \S^{-1}M(\S^{1/\beta}t, \S^{\delta}h) \tag{2.35}$$

The above can be simplified into two convenient expressions by either choosing $\S = t^{-\beta}$ or $\S = h^{-1/\delta}$.

With $\S = t^{-\beta}$,

$$M(t,h) = t^{\beta} M(1,h/t^{\Delta}) \quad , \quad \Delta = \beta\delta. \tag{2.36}$$

Since we are interested in the low temperature ($T < T_c$) side of the critical point, equation (2.36) is modified to read

$$M(t,h) = (-t)^{\beta} \phi^{-}(h/(-t)^{\Delta}) \tag{2.37}$$

When a choice of $\S = h^{-1/\delta}$ in (2.35) is made:

$$M(t,h) = h^{1/\delta} M(t/h^{1/\Delta} , 1) \tag{2.38}$$

The above is consistent with the form obtained by Betts and Filipow (1972).

A second and shorter approach is to say that in general, for a magnetic system, one may write:

$$\left.\begin{array}{l} M = M(t,h) \\ \text{or} \quad h = h(t,M) \end{array}\right\} \tag{2.39}$$

Scaling theory tells us that instead of (2.39) any two of the variables h/M^{δ} , M/t^{β}, h/t^{Δ}, may be used to describe the functional form of M or h.

Thus one may write:

$$h/M^{\delta} = f_1(M/t^{\beta}) \ , \tag{2.40}$$

or

$$h/M^{\delta} = f_2(h/t^{\Delta}) \ , \qquad (2.41)$$

or

$$M/t^{\beta} = f_3(h/t^{\Delta}) \ . \qquad (2.42)$$

Also scaling theory tells us that as $h/t^{\Delta} \to 0$, $f_3 \to$ constant in (2.42) and, modifying the equation for $t \leq 0$, we find along the coexistence curve:

$$M_0(t) \sim (-t)^{\beta} \qquad (2.43)$$

The isothermal susceptibility, χ_T, is given by $\chi_T = (\partial M/\partial h)_T$. From (2.25), on differentiating with respect to h keeping T (and hence t) constant:

$$\chi_T/t^{\beta} \sim t^{-\Delta} f_3'(h/t^{\Delta}) \qquad (2.44)$$

But by definition of the critical exponent γ:

$$\chi_T \sim t^{-\gamma} \qquad (2.45)$$

Setting $h/t^{\Delta} \to 0$ in (2.44),

$$\chi_T \sim t^{\beta-\Delta} \qquad (2.46)$$

Comparing (2.45) and (2.46):

$$\gamma = \Delta - \beta \tag{2.47}$$

In three-dimensions no critical exponents have been established exactly. The work of Sykes, Gaunt, Roberts and Wyles (1972) however, strongly indicates that the susceptibility exponent, γ, is very likely 5/4. We shall assume $\gamma = 5/4$.

Thus:
$$\Delta - \beta = 5/4 \tag{2.48}$$

On differentiating (2.22) twice with respect to t, and using (2.14) and (2.3), it can be shown that:

$$\alpha + 2\beta + \gamma = 2 \tag{2.49}$$

As mentioned earlier in section 2.1, there is every indication from Sykes, Hunter, McKenzie and Heap (1972), that α is probably 1/8. We shall assume $\alpha = 1/8$. Then using (2.49) and (2.48), we have:

$$\beta = 5/16, \quad \text{and} \quad \Delta = 25/16 \tag{2.50}$$

The next step is to compute the critical exponents for the higher derivatives of the magnetization. Two cases are considered. In one case the critical point is approached

Figure 2.1 Paths along which the critical point is approached.

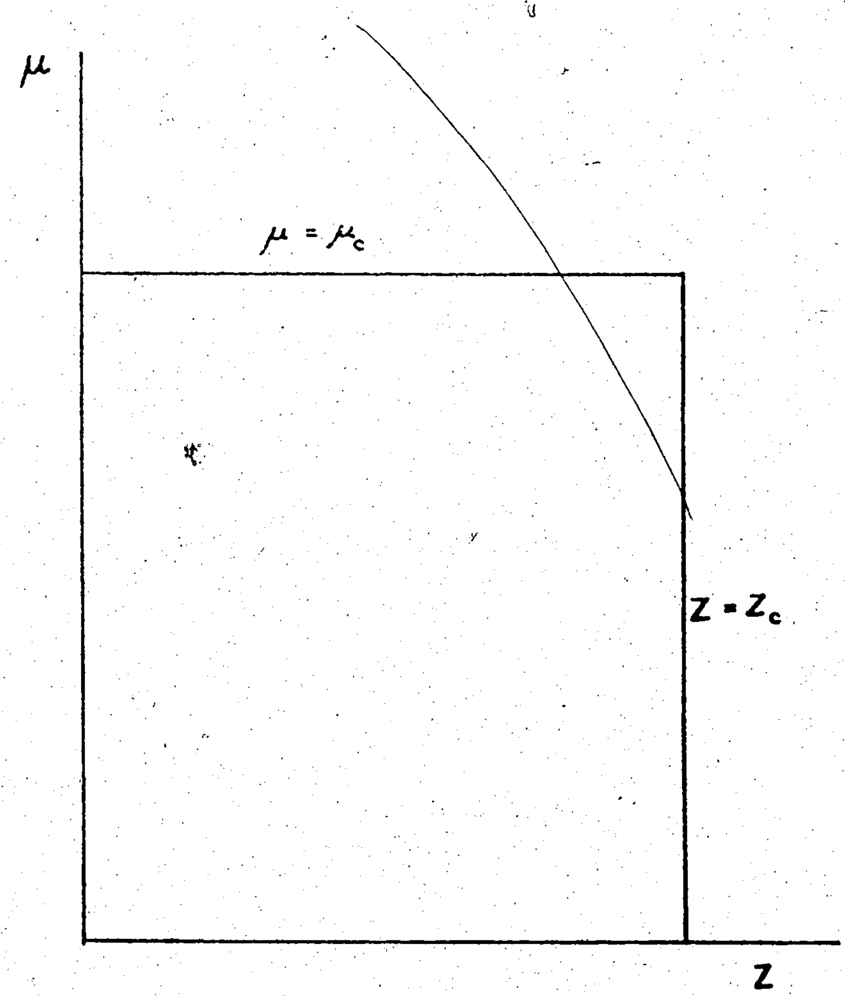

along the critical isotherm. In the second case it is approached along the coexistence curve. See figure 2.1.

Case (i) critical isotherm,

To examine the temperature derivatives of the magnetization on the critical isotherm, it is more convenient to write (2.38) as:

$$M(t,h) = h^{\beta/\Delta}\, g(t/h^{1/\Delta}) \tag{2.51}$$

Ignoring less singular terms:

$$(\partial^{\ell} M/\partial t^{\ell})_{t=0} \sim h^{(\beta-\ell)/\Delta} \tag{2.52}$$

$$\text{i.e. } (\partial^{\ell} M/\partial t^{\ell})_{t=0} \sim h^{-\varepsilon_{\ell}} \tag{2.53}$$

where $\varepsilon_{\ell} = (\ell-\beta)/\Delta$. Table 2.1 gives the scaling predictions for ε_{ℓ}, $\ell=0,1,2,3,4,5$.

Case (ii) coexistence curve

Recall equation (2.37):

$$M(t,h) = (-t)^{\beta}\phi^{-}(h/(-t)^{\Delta})$$

Therefore, taking derivatives with respect to h, and omitting less singular terms:

$$(\partial^{\ell} M/\partial h^{\ell})_{h=0} \sim (-t)^{\beta-\ell\Delta} \tag{2.54}$$

$$\text{i.e.} \quad (\partial^{\ell} M/\partial h^{\ell})_{h=0} \sim (-t)^{-\gamma'_{\ell}} \tag{2.55}$$

where $\gamma'_{\ell} = \ell\Delta-\beta$. Table 2.1 gives the scaling predictions for γ'_{ℓ} , $\ell=0,1,2,3,4,5$. We note that:

$$\gamma = \gamma'_{1} = \beta(\delta-1) \quad ,$$

$$\gamma'_{0} = -\beta \quad .$$

Table 2.1. Scaling predictions for ε_ℓ and γ'_ℓ, ℓ=0, 1, 2, 3, 4, 5.

ℓ	0	1	2	3	4	5
γ'_ℓ	-0.3125	1.25	2.8125	4.375	5.9375	7.5
ε_ℓ	-0.2	$\frac{11}{25}$=0.44	$\frac{27}{25}$=1.08	$\frac{43}{25}$=1.72	$\frac{59}{25}$=2.36	3

CHAPTER 3

The three-dimensional Ising model on the hydrogen peroxide lattice

3.1 Configurational Energy

We present here a brief outline of a method due to Sykes, Essam and Gaunt (1965) for deriving the free energy of the three dimensional spin 1/2, Ising model. Let 2J be the energy gained if 2 first neighbour spins alter alignment from parallel to antiparallel orientation, H be the applied magnetic field, q be the coordination number (3, in the case of the hydrogen peroxide lattice), and m be the magnetic moment per spin. At absolute zero there is complete order and all the spins point one way, thus giving rise to a spontaneous magnetization. The energy of the ground state for N sites is

$$-N(1/2\ qJ + mH) \tag{3.1}$$

As the temperature rises, thermal disorder occurs. The overturning of s spins with r first neighbour bonds will lead to an increase in energy of

$$2(qs - 2r)J + 2msH \tag{3.2}$$

We define

$$\left.\begin{aligned} z &= \exp(-2J/kT) \\ \mu &= \exp(-2mH/kT) \end{aligned}\right\} \tag{3.3}$$

where k is Boltzmann's constant, and T is the temperature in degrees Kelvin.

The probability for the thermal perturbation is given by the Boltzmann factor:

$$\exp\{[-2(qs-2r)J - 2smH]/kT\} = z^{qs-2r}\ \mu^{s} \qquad (3.4)$$

Let Λ_N be the partition function for N sites, and Λ be the partition function per site. For large N, $\Lambda_N \sim \Lambda^N$. At low temperatures Λ, which involves the sum of product of factors like those appearing in (3.4), can be expanded in terms of successive deviations (corresponding to more and more overturned spins) from the lowest energy state, as Domb (1960) has pointed. So the free energy per spin may be written as (log implies taking the natural logarithm):

$$\mathcal{F} = -\tfrac{1}{2}\, qJ - mH - kT \log \Lambda(\mu,z) \qquad (3.5)$$

Once the partition function is known, the formalism of statistical mechanics enables us to calculate the various thermodynamic functions of interest.

3.2 The Low Temperature, High Field Polynomials

We are now faced with the problem of obtaining a series expansion for the natural logarithm of the partition function per site. To derive this series, perturbations of the ordered state must be studied. In general, the number of perturbations of a given configuration on a large lattice of N sites will be some polynomial in N. Domb (1960) showed that $\Lambda_N(\mu,z)$ can be expanded in the form:

$$\Lambda_N(\mu,z) = 1 + \mu F_1(N,z) + \mu^2 F_2(N,z) + \ldots + \mu^s F_s(N,z) \ldots \tag{3.6}$$

Each $F_s(N,z)$ is a polynomial which can be expanded in powers of N. Domb also showed that if instead an expansion of $\log\Lambda(\mu,z)$ is preferred, then:

$$\log\Lambda(\mu,z) = \mu L_1(z) + \mu^2 L_2(z) + \ldots + \mu^s L_s(z) + \ldots \tag{3.7}$$

where $L_s(z)$ is but the coefficient of N in $F_s(N,z)$. $L_s(z)$ is itself a polynomial in z. The set of polynomials, $\{L_s(z)\}$, is the set of low temperature (high field) polynomials.

To specify a given $L_s(z)$ we require the contributions from perturbations with s overturned spins. The s spins may occur with zero first-neighbour bond, 1 first neighbour bond, 2 first neighbour bonds, ... and so on. Accordingly, following Sykes, Essam and Gaunt (1965), we write:

$$L_s(z) = \sum_{r=0}^{\frac{1}{2}s(s-1)} [s;r]\, z^{qs-2r} \tag{3.8}$$

The complete high field polynomials for the hydrogen peroxide lattice for $s < 24$ were obtained by Betts, Elliott and Sykes (1974), and are presented in appendix 2 for reference.

Take the hydrogen peroxide lattice. Consider a single site of the lattice. Then if the three nearest neighbour sites are taken as vertices of a triangle it is possible, by omitting the site we started with, to derive a sublattice of second neighbour vertices. The sublattice so obtained is called the hypertriangular lattice by Betts, Elliott and Sykes (1974). The hypertriangular lattice derived from the H_2O_2 lattice is analogous to the triangular lattice derived from the honeycomb lattice. In appendix 1 the hypertriangular lattice graphs and low temperature lattice constants needed for obtaining F_s ($s < 12$) are given.

On examining the hydrogen peroxide lattice one sees that it may be easy to determine visually the number of ways in which a polygon of ten edges may be embedded in the lattice. However as polygons of more edges are considered, the task of deciding how many ways a polygon may be embedded in the hydrogen peroxide lattice becomes more difficult. To handle this difficulty sophisticated book-keeping has to be developed. To see how this is done, one should refer to the work of Leu, Betts and Elliott (1969), and Betts, Elliott and Sykes (1974).

Armed with the low temperature (high field) polynomials we are now ready to derive various thermodynamic functions of interest from the free energy given in (3.5).

3.3 The Magnetization and its Derivatives

By definition the magnetization per spin is given by:

$$\mathcal{M} = -(\partial \mathcal{G}/\partial H)_T$$

We shall work with the reduced free energy per spin:

$$\begin{aligned} G &= \mathcal{G}/kT \\ &= -(q \log z)/4 - hT_c/T - \sum_s L_s(z)\mu^s \end{aligned} \qquad (3.9)$$

Thus we have for the reduced magnetization per spin ($h = mH/kT_c$):

$$\begin{aligned} M &= -(\partial G/\partial h)_T \\ &= -(\partial G/\partial \mu)_T \quad (\partial \mu/\partial h)_T \end{aligned} \qquad (3.10)$$

i.e. $M(\mu,z) = 1 - 2 \sum_s s \quad L_s(z)\mu^s$

Among the possible paths one can take in approaching the critical point, two are particularly convenient. One is a path along the coexistence curve and the other is along the critical isotherm. Figure 2.1 shows these two paths. The estimate of the critical point z_c is necessary before one proceeds with the analysis of the Ising model on the hydrogen peroxide lattice. Leu, Betts and Elliott (1969) have estimated $v_c = \tanh(J/kT_c)$, from which they obtained $z_c = 0.317401 \pm 0.000010$ for the hydrogen peroxide lattice.

They did this by analysing the high temperature expansion of the susceptibility.

(a) on the critical isotherm.

By setting $z = z_c$ in (3.10) one obtains:

$$M(\mu) = 1 - 2 \sum_s sL_s(z_c)\mu^s \tag{3.12}$$

In general the ℓth derivative of the magnetization with respect to z can be written as, ($\ell > 0$):

$$[\partial^{\ell} M(\mu,z)/\partial z^{\ell}]_{z=z_c} = -2\sum_s \mu^s [\partial^{\ell} L_s(z)/\partial z^{\ell}]_{z=z_c} \tag{3.13}$$

Therefore upon summarizing (3.12) and (3.13)

$$[\partial^{\ell} M(\mu,z)/\partial z^{\ell}]_{z=z_c} = \sum_{n=0}^{23} a_n^{(\ell)} \mu^n \tag{3.14}$$

The summation is truncated at s = 23 because at the moment we know $L_s(z)$ only up to s = 23. The series (3.14) for ℓ = 0, 1...5 are given in Appendix 3. The coefficients are quoted to only six figures because they are dependent on z_c which is known to only six figures.

(b) on the coexistence curve.

When (3.11) is differentiated with respect to μ, keeping z constant we have for the ℓth derivative:

$$\partial^{\ell} M(\mu,z)/\partial\mu^{\ell} = -2 \sum_{s=\ell}^{23} s^2(s-1)\ldots(s-\ell+1)\; L_s(z)\mu^{s-\ell} \tag{3.15}$$

Along the coexistence curve we set $\mu = \mu_c = 1$ (zero field, $h = 0$), and write:

$$[\partial^{\ell} M(\mu,z)/\partial\mu^{\ell}]_{\mu=\mu_c} = -2 \sum_{s=\ell}^{23} s^2(s-1)\ldots(s-\ell+1)L_s(z) \qquad (3.16)$$

Hence:

$$[\partial^{\ell} M(\mu,z)/\partial\mu^{\ell}]_{\mu=\mu_c} = \sum_{n=0}^{17} b_n^{(\ell)} z^n \qquad (3.17)$$

The reason for truncating the series in z is that we know $L_s(z)$ only up to $s = 23$. Each $L_s(z)$ when written out in ascending powers of z, begins with a leading term $w(s,p)z^p$, where $w(s,p)$ is the first non-zero numerical coefficient of z^p in $L_s(z)$. When s is tabulated against p we notice that the trend indicates that with $L_{24}(z)$, p is 18. So it is sensible to retain terms in z up to z^{17} only. Hence the series in z in (3.17) are truncated at z^{17}. The series for $\ell = 0, 1, 2\ldots5$ in (3.17) are given in Appendix 4.

Table 3.1. A table of p vs. s where p is the smallest power of z in $L_s(z)$.

s	16	17	18	19	20	21	22	23
p	14	15	14	15	16	17	16	17

From (2.52) and (2.54), scaling theory predicts that: on the critical isotherm,

$$(\partial^{\ell} M/\partial t^{\ell})_{t=0} \sim h^{-\varepsilon_{\ell}} \quad ,$$

and on the coexistence curve,

$$(\partial^{\ell} M/\partial h^{\ell})_{h=0} \sim (-t)^{-\gamma'_{\ell}} \quad .$$

Since our series expansion variables are μ and z, then, provided less singular terms are omitted:

$$(\partial^{\ell} M/\partial t^{\ell})_{t=0} \sim (\partial z/\partial t)^{\ell}_{t=0} \; (\partial^{\ell} M/\partial z^{\ell})_{z=z_c}$$

and

$$(\partial^{\ell} M/\partial h^{\ell})_{h=0} \sim (\partial \mu/\partial h)^{\ell}_{h=0} \; (\partial^{\ell} M/\partial \mu^{\ell})_{\mu=\mu_c} \quad .$$

Hence by studying the asymptotic behaviour of $(\partial^{\ell} M/\partial z^{\ell})_{z=z_c}$ and $(\partial^{\ell} M/\partial \mu^{\ell})_{\mu=\mu_c}$ we would know the corresponding behaviour of $(\partial^{\ell} M/\partial t^{\ell})_{t=0}$ and $(\partial^{\ell} M/\partial h^{\ell})_{h=0}$.

CHAPTER 4

Analysis for Critical Exponents and Amplitudes

4.1 Padé Approximants

We have seen that the magnetization and its derivatives with respect to z and μ are expressible in the form of series expansions. Since the high field polynomials $L_s(z)$ are known only to s = 23, there are unavoidable truncations of terms of the series for $(\partial^{\ell}M/\partial z^{\ell})_{z=z_c}$ and $(\partial^{\ell}M/\partial\mu^{\ell})_{\mu=\mu_c}$. Our problem then is to extract the critical behaviour from a given finite series. We hope that in spite of its finiteness it already contains the characteristics of the critical behaviour. This is not a vain hope as the success of several workers in this field has shown.

Consider a function $f(x) = \sum_{n=0}^{\infty} w_n x^n$. Suppose we truncate it at n = L. The Padé approximant to f(x), [N,D], (Baker, 1961; Gammel, Marshall and Morgan, 1963; Baker, 1965) is the ratio of 2 polynomials of orders N and D respectively,

$$\text{i.e.} \quad [N,D]\ (x) = \frac{p_0 + p_1 x + \ldots + p_N x^N}{q_0 + q_1 x + \ldots + q_D x^D} \tag{4.1}$$

such that

$$\sum_{n=0}^{L} w_n x^n = \sum_{n=0}^{N} p_n x^n \Big/ \sum_{n=0}^{D} q_n x^n \tag{4.2}$$

The coefficient q_0 is chosen to be 1 without loss of generality. If each w_n is known (n = 0, 1, 2...L) then the other coefficients can be determined provided $N + D \leq L$.

This is done in the following manner. From (4.2) we have:

$$(w_0 + w_1 x + \ldots + w_L x^L)(1 + q_1 x + \ldots + q_D x^D) = p_0 + p_1 x + \ldots + p_N x^N$$

By equating coefficients of the constant term up to x^N we find that:

$$w_0 = p_0$$

and

$$\begin{pmatrix} w_1 \\ w_2 \\ \cdot \\ \cdot \\ \cdot \\ w_N \end{pmatrix} + \begin{pmatrix} w_0 & & & \\ w_1 & w_0 & & \\ \cdot & \cdot & & \\ \cdot & \cdot & & \\ \cdot & \cdot & & \\ w_{N-1} & w_{N-2} & \ldots & w_0 \end{pmatrix} \begin{pmatrix} q_1 \\ q_2 \\ \cdot \\ \cdot \\ \cdot \\ q_N \end{pmatrix} = \begin{pmatrix} p_1 \\ p_2 \\ \cdot \\ \cdot \\ \cdot \\ p_N \end{pmatrix} \qquad (4.3)$$

where, if $D < N$, we get $q_{D+1}, q_{D+2}, \ldots q_N = 0$.
By equating coefficients of x^{N+1} to x^{N+D} we have:

$$\begin{pmatrix} w_{N+1} \\ w_{N+2} \\ \cdot \\ \cdot \\ \cdot \\ w_{N+D} \end{pmatrix} + \begin{pmatrix} w_N & w_{N-1} & \ldots & w_{N-D+1} \\ w_{N+1} & w_N & & w_{N-D} \\ \cdot & \cdot & & \cdot \\ \cdot & \cdot & & \cdot \\ \cdot & \cdot & & \cdot \\ w_{N+D-1} & w_{N+D-2} & & w_N \end{pmatrix} \begin{pmatrix} q_1 \\ q_2 \\ \cdot \\ \cdot \\ \cdot \\ q_D \end{pmatrix} = 0 \qquad (4.4)$$

where if $N < D$ we set $w_{-1}, w_{-2} \ldots$ to zero. Equations (4.3) and (4.4) may be solved on the computer.

Due to the Padé approximant being a rational function it is very suitable for applications to thermodynamic functions which have a power law singularity. For example we may consider

$$\chi(T) = \sum_{n=0}^{\infty} a_n T^n \sim A(T_c - T)^{-\gamma} \tag{4.5}$$

Taking logarithmic derivative of the above yields:

$$d\log\chi(T)/dT \sim \gamma/(T_c - T) \tag{4.6}$$

We see by the expression (4.6) that the Padé approximant to the logarithmic derivative of $\chi(T)$ will have a simple pole at $T = T_c$ and that the negative of the residue of this Padé approximant is the critical exponent, γ.

Suppose the negative of the residue (i.e. γ) is plotted on the ordinate axis, and the pole (an approximation of T_c) on the abscissa axis. Each Padé approximant to (4.6) provides us with a point. A smooth curve can be drawn usually through the collection of points due to the set of Padé approximants, {[N,D]}, used to approximate (4.6). The best estimate of γ is that ordinate on the curve for which the abscissa is the true T_c (assuming T_c is known).

4.2 Logarithmic Derivatives

We now wish to apply the method mentioned in the preceding section to the series (ℓ = 0, 1, 2, 3, 4, 5):

$$(a)\ (\partial^{\ell} M/\partial z^{\ell})_{z=z_c} = \sum_{n=0}^{23} a_n^{(\ell)} \mu^n, \tag{4.7}$$

and

$$(b)\ (\partial^{\ell} M/\partial \mu^{\ell})_{\mu=\mu_c} = \sum_{n=0}^{17} b_n^{(\ell)} z^n. \tag{4.8}$$

Case (a).

The most singular parts of (4.7) are expected to diverge as

$$(\partial^{\ell} M/\partial z^{\ell})_{z=z_c} \sim \bar{E}(1-\mu)^{-\varepsilon_{\ell}} \tag{4.9}$$

When the logarithmic derivatives to (4.7) are formed we would expect them to diverge as

$$(d/d\mu)\{\log(\partial^{\ell} M/\partial z^{\ell})_{z=z_c}\} \sim \varepsilon_{\ell}/(1-\mu) \tag{4.10}$$

Each Padé approximant to (4.10) should yield a pole close to $\mu_c = 1$, and a corresponding residue that is an estimate of ε_{ℓ}.

Figures 4.1 to 4.5 are plots of the negative of the residues of the Padé approximants to $d\{\log(\Sigma a_n^{(\ell)} \mu^n)\}/d\mu$ versus their corresponding poles closest to the physical singularity, $\mu_c = 1$, for $\ell = 0, 1, 2, 4, 5$. The results for $\ell = 3$ are so scattered that the meaningless plot has been omitted. Note that $\varepsilon_0 = -1/\delta$, where δ is defined in section 2.1. In table 4.1 estimates of ε_ℓ with their confidence limits, as obtained from the graphs, are listed.

It can be seen from figure 4.1 that the points are crowded into a region well below $\mu_c = 1$. This makes for difficult estimation of ε_0. Similarly the concentration of points above $\mu_c = 1$ in figure 4.2 renders a precise estimation of ε_1 impossible. The ε_ℓ's so estimated ($\ell = 0, 1, 2, 4, 5$) are used as guides to the choices of powers made in a more precise technique that of neighbouring powers.

Case (b).

The analysis of $(\partial^\ell M/\partial\mu^\ell)_{\mu=\mu_c}$ proceeds in a similar fashion to that of $(\partial^\ell M/\partial z^\ell)_{z=z_c}$. The most singular parts of 4.8 are supposed to diverge as

$$(\partial^\ell M/\partial\mu^\ell)_{\mu=\mu_c} \sim \bar{C}'_\ell(1 - z/z_c)^{-\gamma'_\ell} \qquad (4.11)$$

When the logarithmic derivatives to (4.11) are computed the following divergent behaviour would be expected:

$$(d/dz)\{\log(\partial^\ell M/\partial\mu^\ell)_{\mu=\mu_c} \sim \gamma_\ell'/(z_c - z) \qquad (4.12)$$

A given Padé approximant to (4.12) may have a number of poles, but the pole of interest is that one closest to $z = z_c$. The negative of the residue computed for this pole is plotted against the pole. Figures 4.6 to 4.11 are such graphs of the negative of the residues versus the poles of the Padé approximants to $d\{\log(\Sigma b_n^{(\ell)} z^n)\}/dz$ for $\mu_c = 1$, $\ell = 0, 1, 2, 3, 4, 5$. The estimates of γ_ℓ' obtained from these graphs are displayed in table 4.2, together with their confidence limits.

In figure 4.6 the poles cluster well below $z_c = 0.317401$, making it difficult to pinpoint γ_0' precisely. It is readily seen that the scatter in the points of the graphs used for estimating γ_4' and γ_5' are quite bad (figures 4.10, 4.11). One possible reason for the erratic behaviour of the Padé approximants used for these estimations is the presence of non-physical singularities. These non-physical singularities prove troublesome when their locations in the complex plane of the independent variable (in this instance the complex z plane) are nearer to the origin than z_c, or are clustered very close to the physical singularity at $z = z_c$. In a subsequent section we will look at transformations that may facilitate analysis of series expansions with such problems.

Figure 4.1 Estimates of μ_c and ϵ_0 from poles and residues of Padé approximants to $(d/d\mu) \log M(\mu,z_c)$.

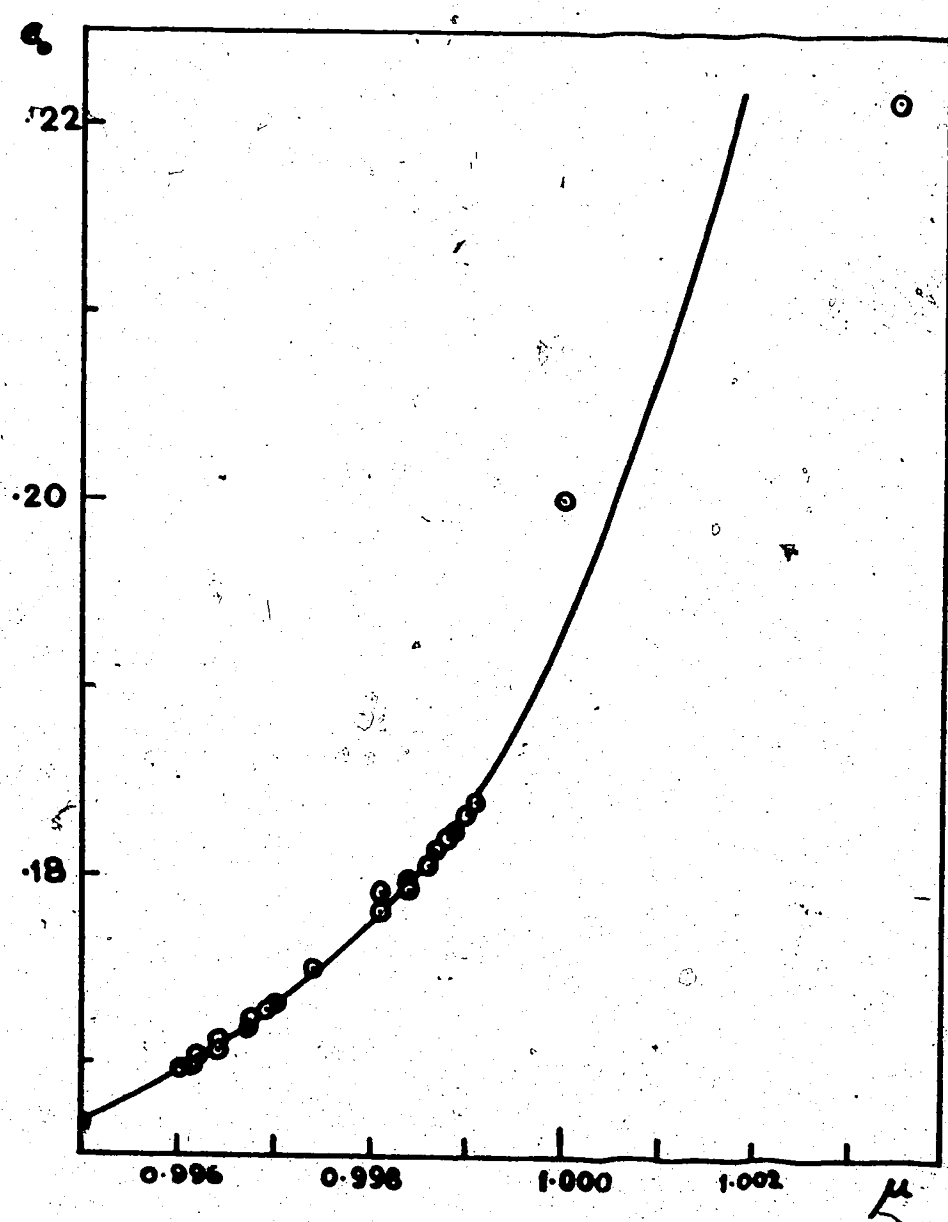

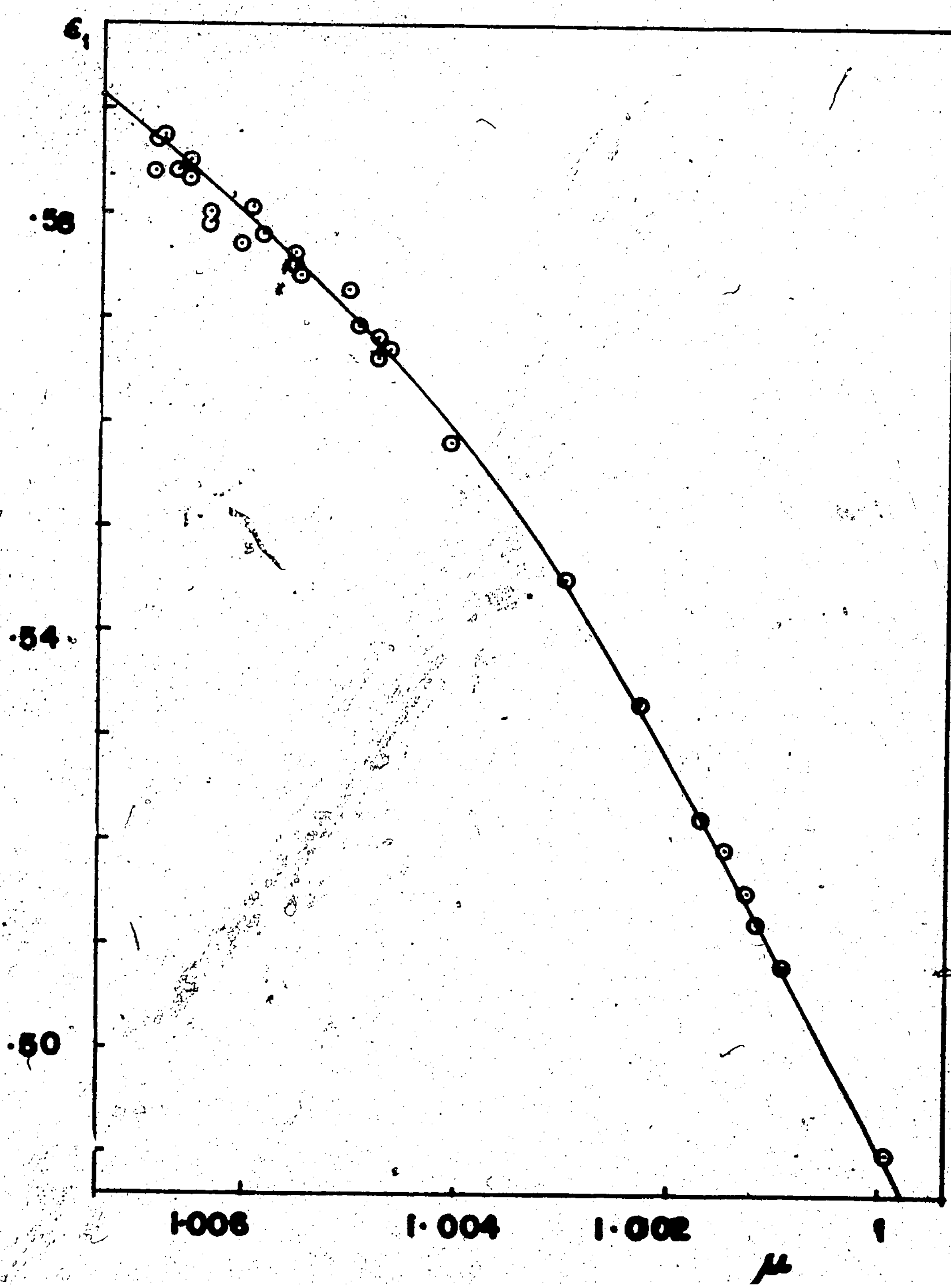

Figure 4.2 Estimates of μ_c and ϵ_1 from poles and residues of Padé approximants to $\frac{d}{d\mu}\left\{\log \frac{1}{\mu}\left[\frac{\partial M(\mu,z)}{\partial z}\right]_{z=z_c}\right\}$.

Figure 4.3 Estimates of μ_c and ε_2 from poles and residues of Padé approximants to $\frac{d}{d\mu}\left\{\log \frac{1}{\mu}\left[\frac{\partial^2 M(\mu,z)}{\partial z^2}\right]_{z=z_c}\right\}$.

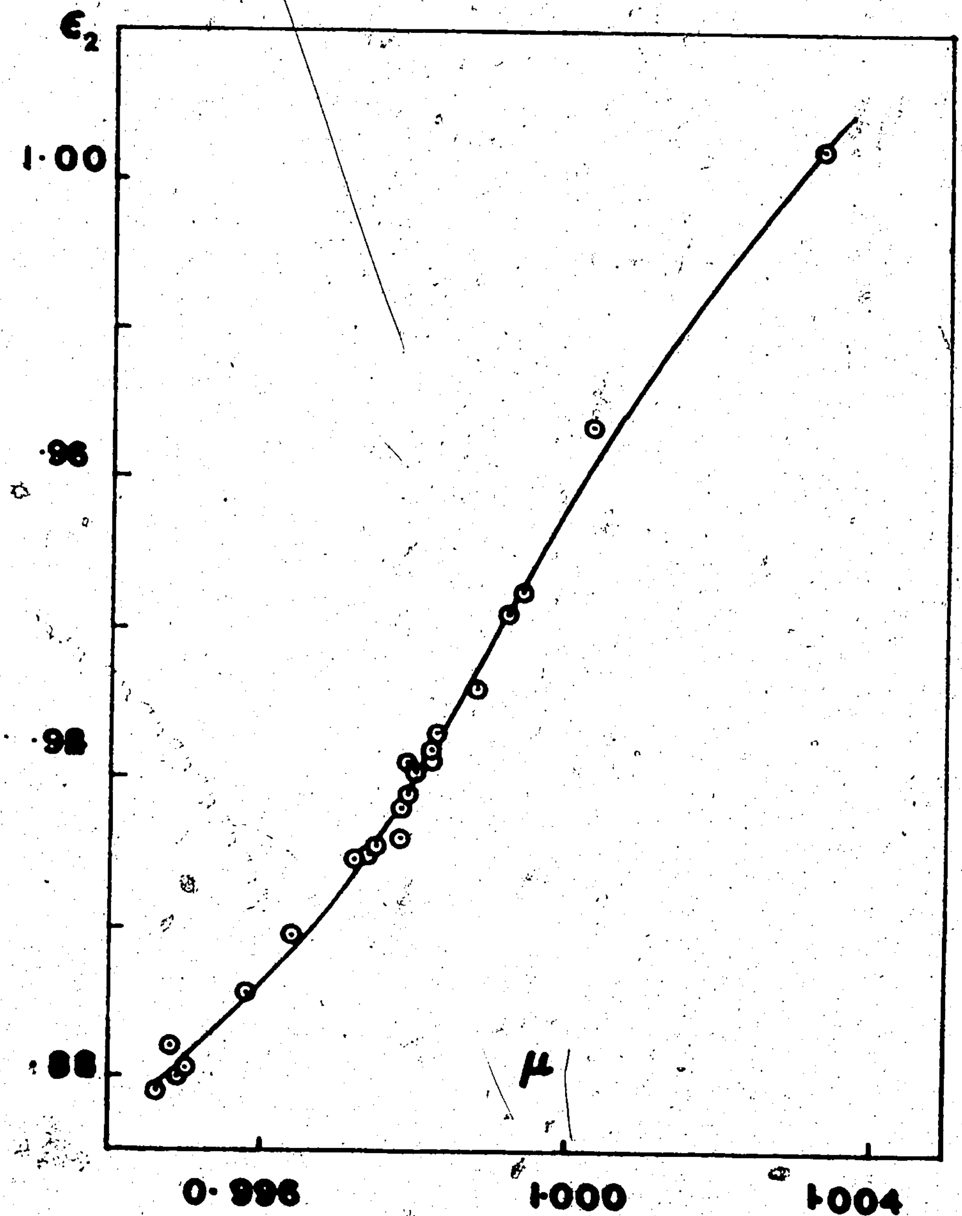

Figure 4.4 Estimates of μ_c and ϵ_4 from poles and residues of Padé approximants to

$$\frac{d}{d\mu}\left\{\log \frac{1}{\mu}\left[\frac{\partial^4 M(\mu,z)}{\partial z^4}\right]_{z=z_c}\right\}.$$

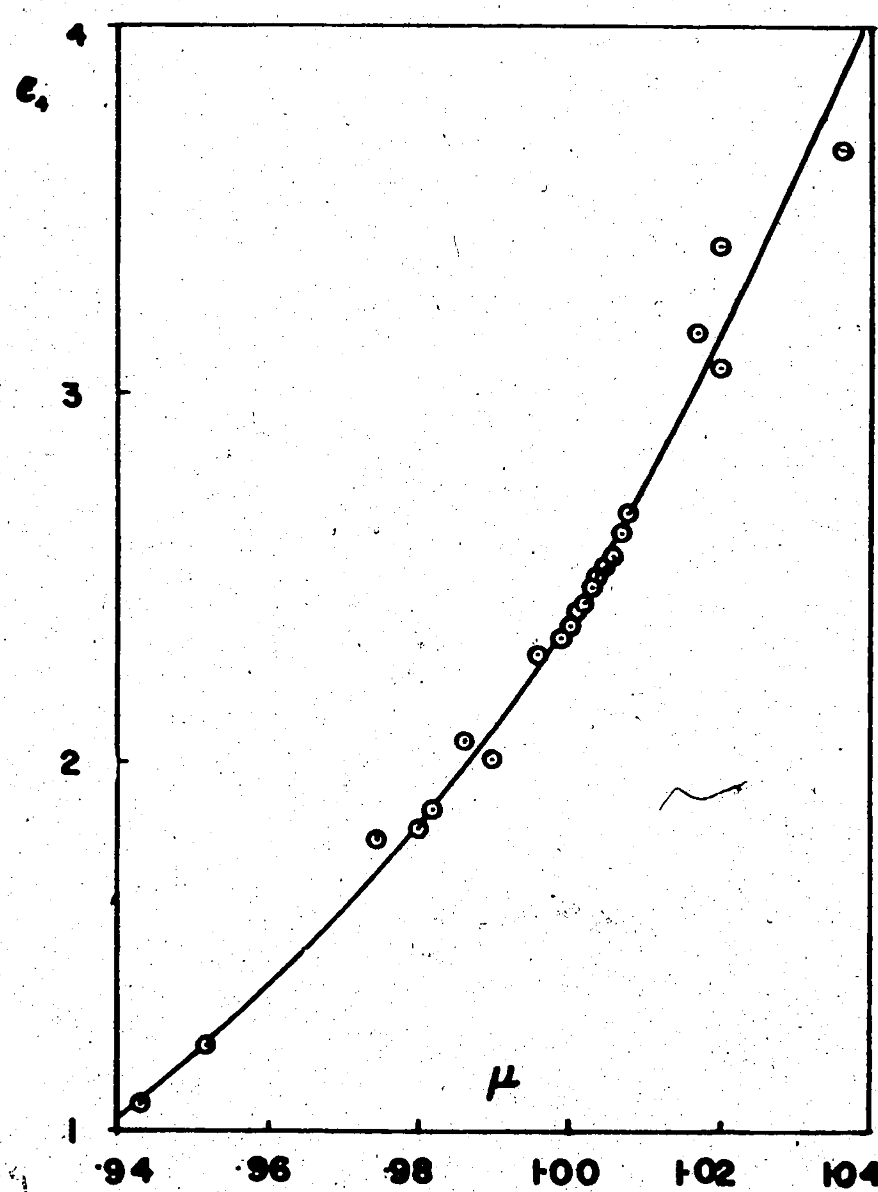

Figure 4.5 Estimates of μ_c and ε_5 from poles and residues of Padé approximants to

$$\frac{d}{d\mu}\left\{\log \frac{1}{\mu}\left[\frac{\partial^5 M(\mu,z)}{\partial z^5}\right]_{z=z_c}\right\}.$$

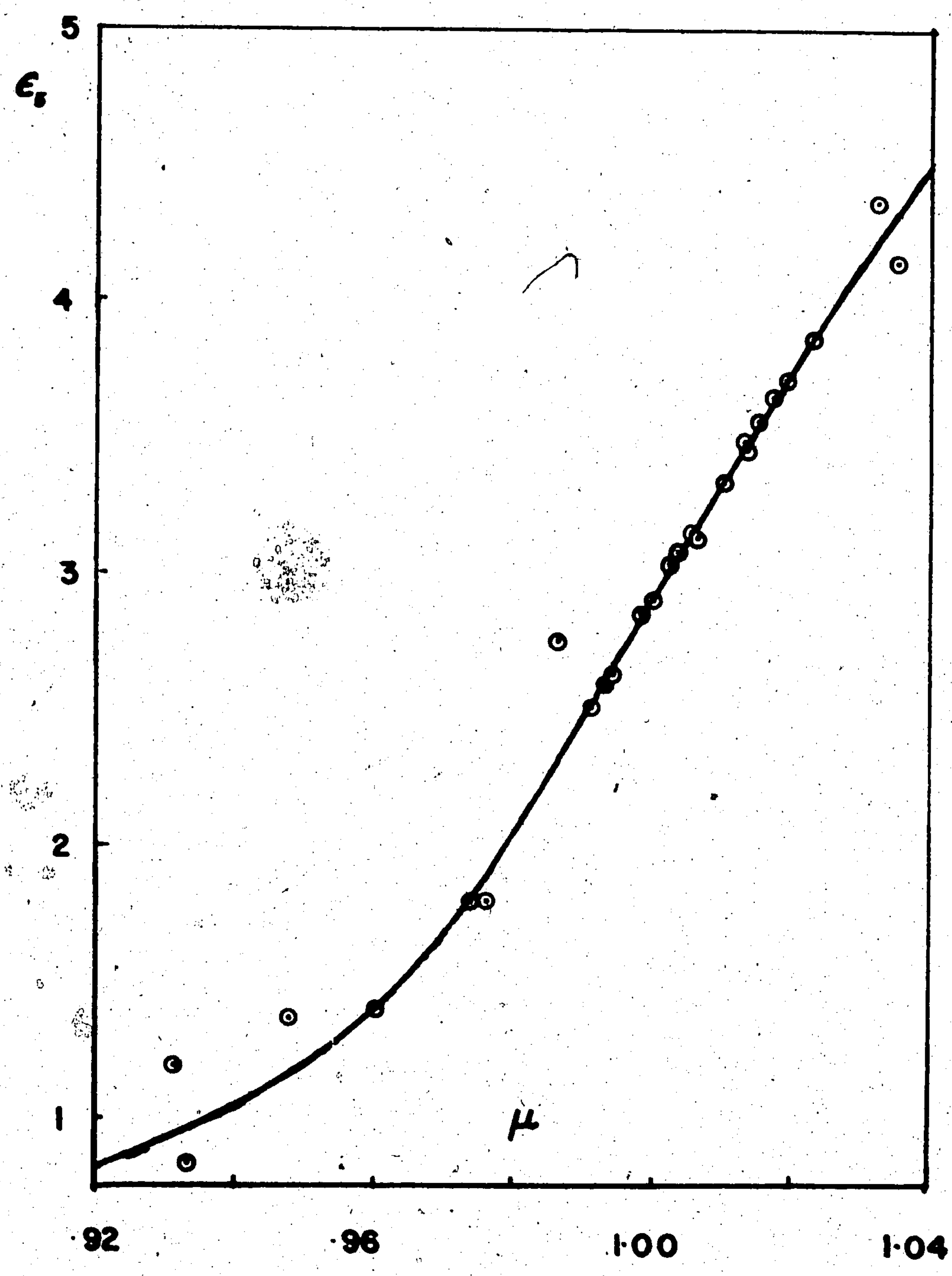

Figure 4.6 Estimates of z_c and γ_0' from poles and residues of Padé approximants to $\frac{d}{dz}\left\{\log M(z)\right\}$.

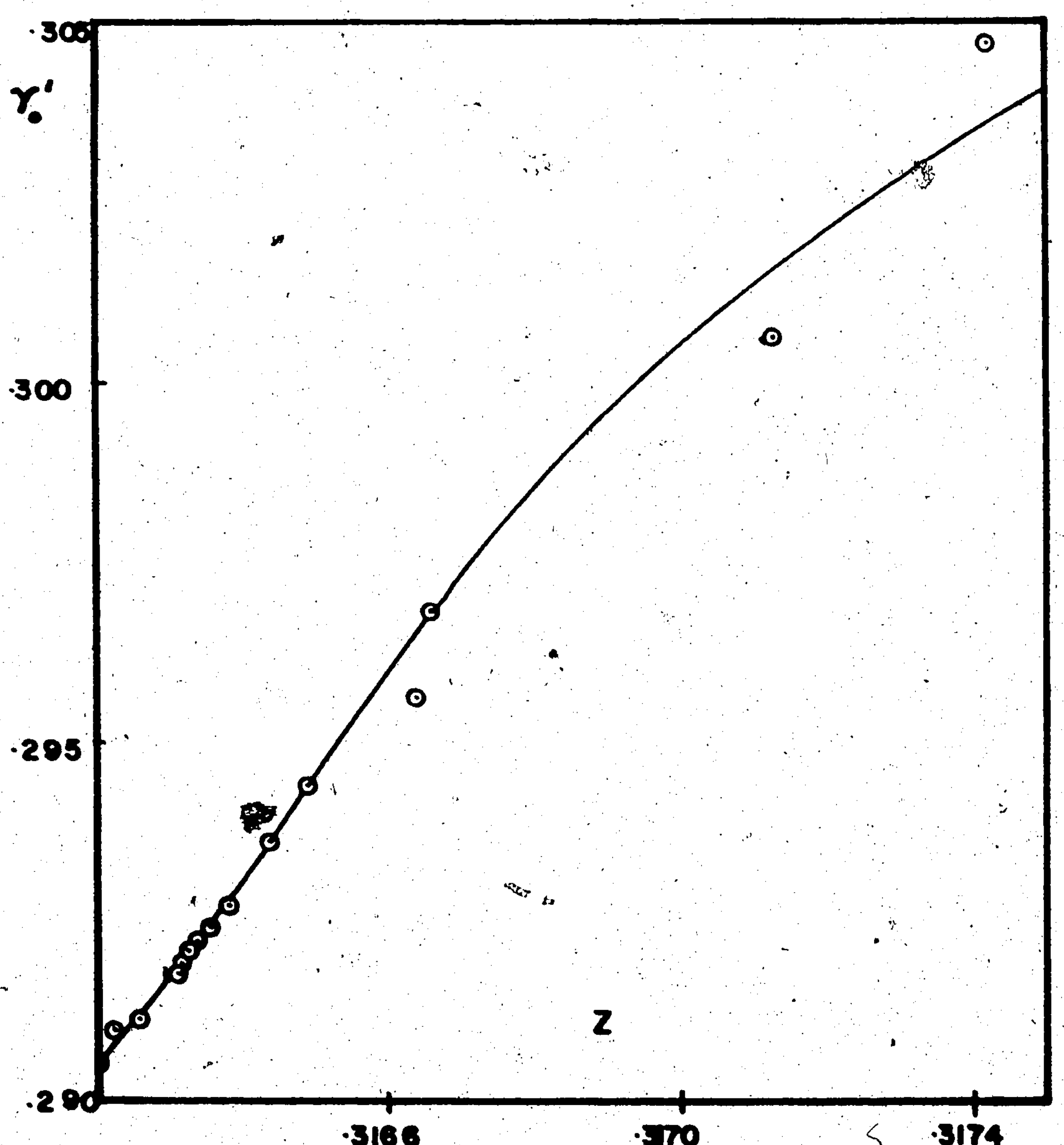

Figure 4.7 Estimates of z_c and γ_1' from poles and residues of Padé approximants to

$$\frac{d}{dz}\left\{\log \frac{1}{z^3}\left[\frac{\partial M(\mu,z)}{\partial \mu}\right]_{\mu=\mu_c}\right\}.$$

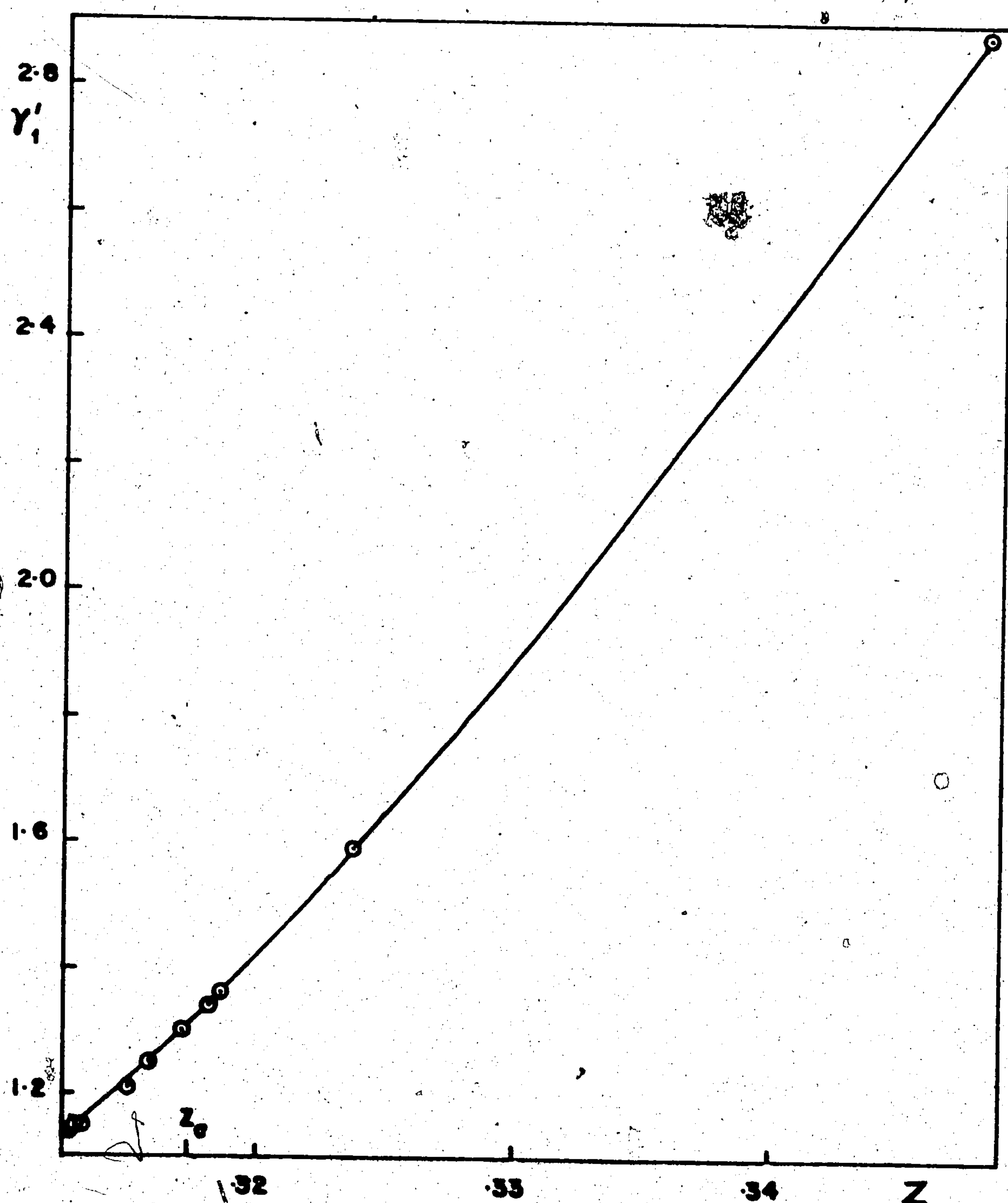

Figure 4.8 Estimates of z_c and γ_2' from poles and residues of Padé approximants to

$$\frac{d}{dz}\left\{\log \frac{1}{z^4}\left[\frac{\partial^2 M(\mu, z)}{\partial \mu^2}\right]_{\mu=\mu_c}\right\}.$$

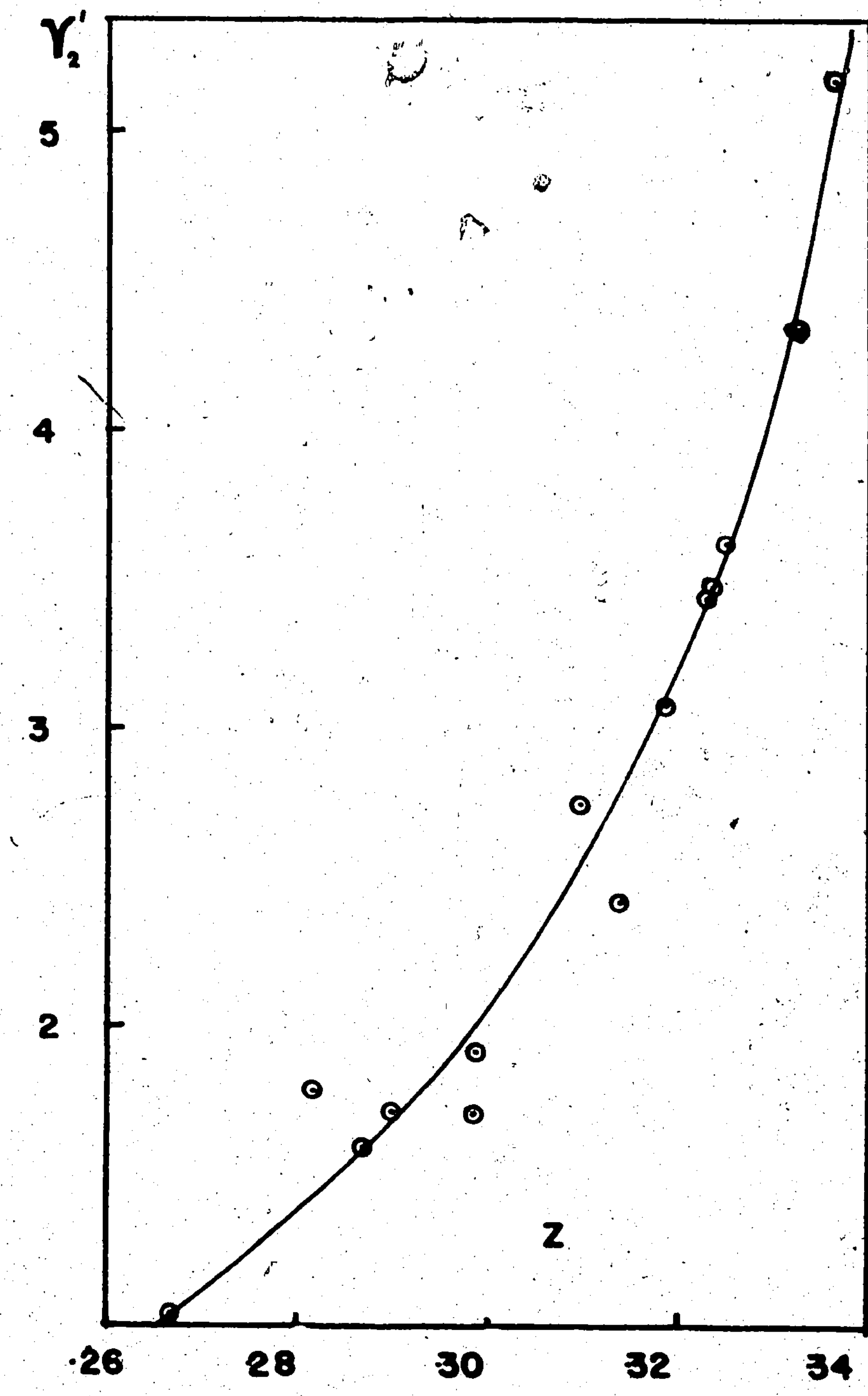

Figure 4.9 Estimates of z_c and γ_3' from poles and residues of Padé approximants to

$$\frac{d}{dz}\left\{\log \frac{1}{z^5}\left[\frac{\partial^3 M(\mu,z)}{\partial\mu^3}\right]_{\mu=\mu_c}\right\}.$$

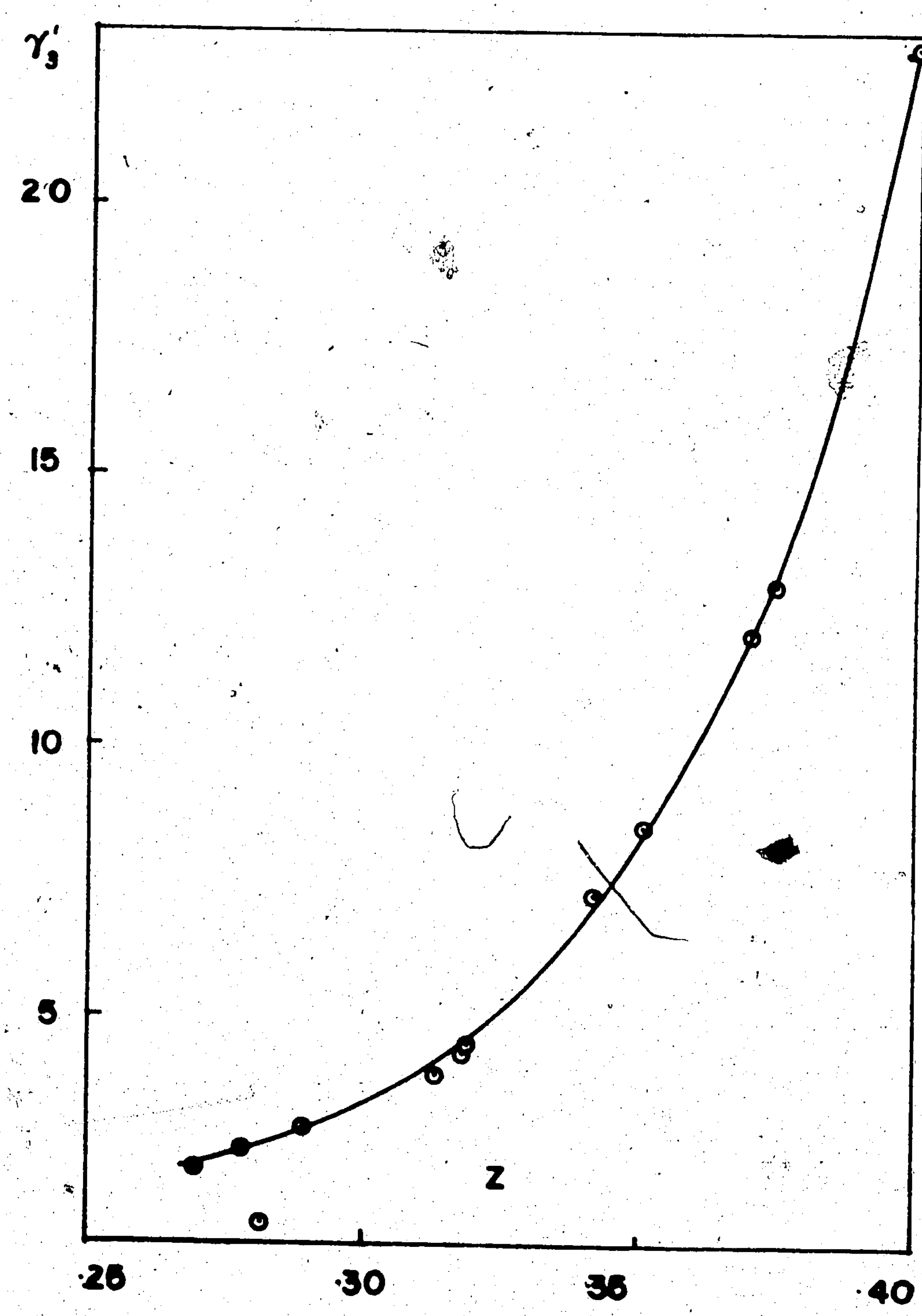

Figure 4.10 Estimates of z_c and γ_4' from poles and residues of Padé approximants to

$$\frac{d}{dz}\left\{\log \frac{1}{z^6}\left[\frac{\partial^4 M(\mu, z)}{\partial\mu^4}\right]_{\mu=\mu_c}\right\}.$$

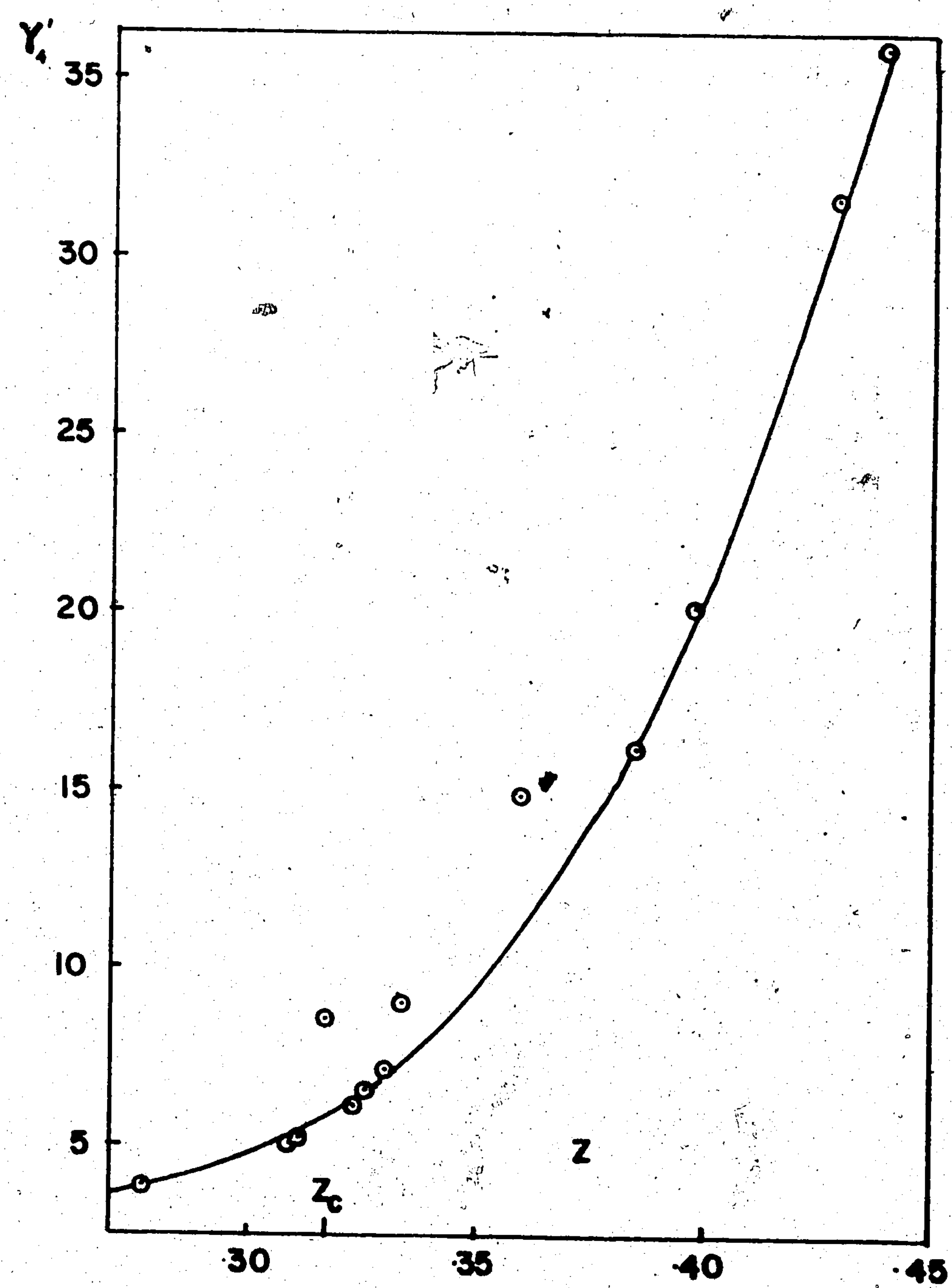

Figure 4.11 Estimates of z_c and γ_5' from poles and residues of Padé approximants to

$$\frac{d}{dz}\left\{\log \frac{1}{z^7}\left[\frac{\partial^5 M(\mu,z)}{\partial\mu^5}\right]_{\mu=\mu_c}\right\}.$$

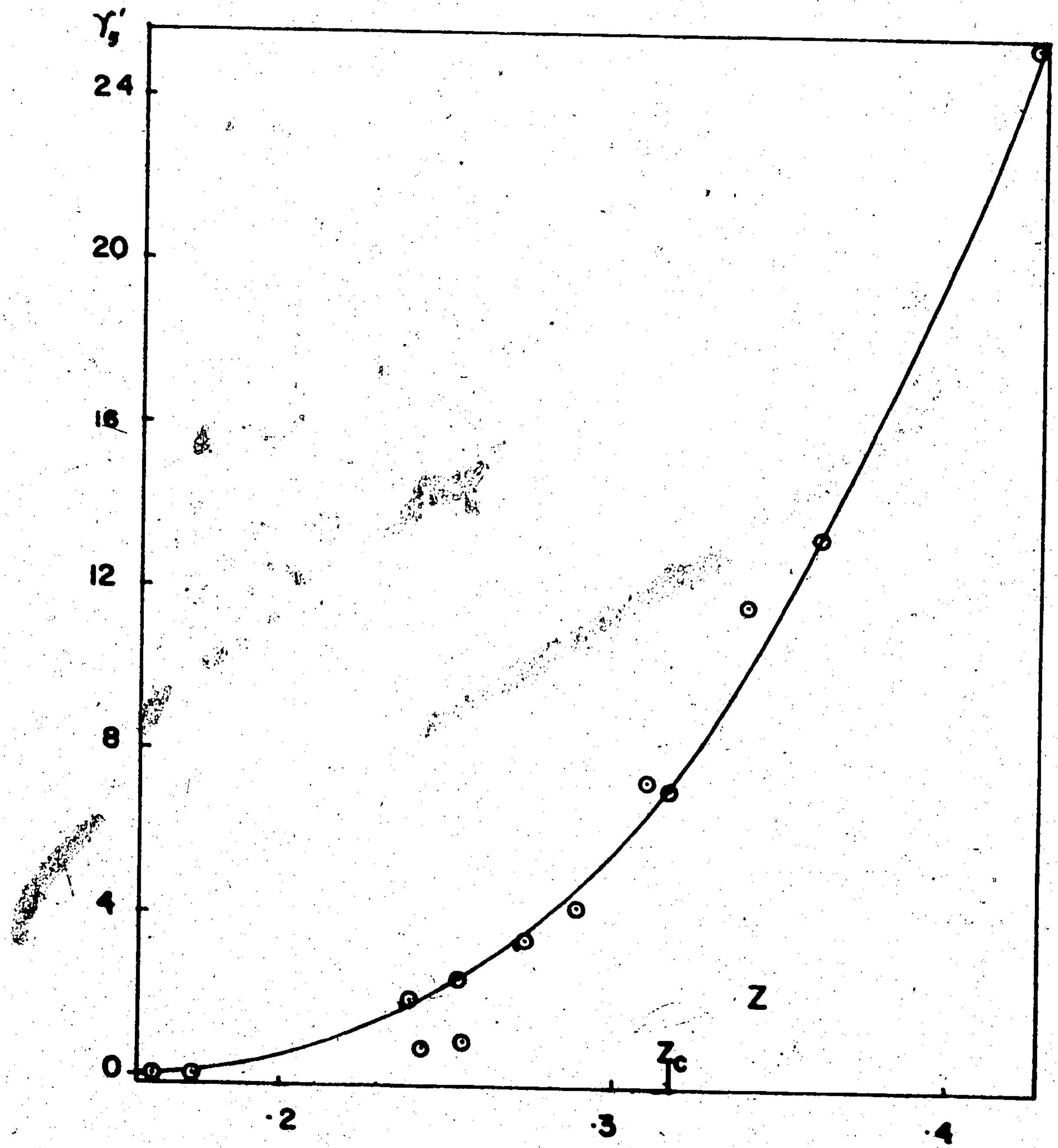

Table 4.1 Estimation of ε_ℓ, by considering residues and poles of Padé approximants to

$$\frac{d}{d\mu}\left\{\log\left[\left.\frac{\partial^\ell M(\mu,z)}{\partial z^\ell}\right|_{z=z_c}\right]\right\},\ \text{for } z_c = 0.317401.$$

ℓ	0	1	2	3	4	5
estimated ε_ℓ	-0.193±0.007	0.491±0.010	0.959±0.010		2.38±0.05	2.85±0.20
scaling ε_ℓ	-0.2	0.44	1.08	1.72	2.36	3

Table 4.2 Estimation of γ_ℓ', by considering residues and poles of Padé approximants to

$$\frac{d}{dz}\left\{\log\left(\left.\frac{\partial^\ell M(\mu,z)}{\partial\mu^\ell}\right|_{\mu=\mu_c}\right)\right\}, \text{ for } \mu_c = 1.$$

ℓ	0	1	2	3	4	5
estimated γ_ℓ'	-0.309 ± 0.002	1.30 ± 0.03	2.82 ± 0.20	4.37 ± 0.10	6.0 ± 0.5	7.4 ± 0.6
scaling γ_ℓ'	-0.3125	1.25	2.8125	4.375	5.9375	7.5

4.3 Neighbouring Powers

In the preceding section, estimates of γ_ℓ' and ε_ℓ were made using the technique of computing Padé approximants to the logarithmic derivatives of (4.8) and (4.7). We recall the divergent behaviour of the most singular parts of (4.8) and (4.7):

$$\left.\frac{\partial^\ell M(\mu,z)}{\partial z^\ell}\right|_{z=z_c} \sim \bar{E}_\ell(1-\mu)^{-\varepsilon_\ell} , \qquad (4.9)$$

$$\left.\frac{\partial^\ell M(\mu,z)}{\partial \mu^\ell}\right|_{\mu=\mu_c} \sim \bar{C}_\ell'(1-z/z_c)^{-\gamma_\ell'} \qquad (4.11)$$

On raising (4.9) to the power $1/\varepsilon_\ell$, and (4.11) to the power $1/\gamma_\ell'$, we get

$$\left(\frac{\partial^\ell M(\mu,z)}{\partial z^\ell}\right)^{1/\varepsilon_\ell} \sim (\bar{E}_\ell)^{1/\varepsilon_\ell}/(1-\mu) \qquad (4.13)$$

and

$$\left(\frac{\partial^\ell M(\mu,z)}{\partial \mu^\ell}\right)^{1/\gamma_\ell'} \sim (\bar{C}_\ell')^{1/\gamma_\ell'}/(1-z/z_c) \qquad (4.14)$$

From tables 4.1 and 4.2 we have best estimates of ε_ℓ and γ_ℓ' by the method of taking logarithmic derivatives. Call these estimates $\hat{\varepsilon}_\ell$ and $\hat{\gamma}_\ell$. In the technique of taking neighbouring powers, we compute Padé approximants to

$[\partial^{\ell}M(\mu,z)/\partial z^{\ell}]_{z=z_c}^{1/\varepsilon_\ell}$ for a series of values of ε_ℓ in the neighbourhood of $\hat{\varepsilon}_\ell$. For each ε_ℓ and each Padé approximant to (4.13) we get a pole which is an estimate of μ_c, and a residue which is an estimate of $(\bar{E}_\ell)^{1/\varepsilon_\ell}$. It is then possible to plot a graph of the estimated $\mu_c([N,D])$ versus ε_ℓ for each Padé approximant, [N,D]. The best estimated ε_ℓ in this technique is that ε_ℓ which corresponds to $\mu_c = 1$.

Similarly, for a fixed ℓ, we form Padé approximants, {[N',D']} to $[\partial^{\ell}M(\mu,z)/\partial\mu^{\ell}]^{1/\gamma'_\ell}$ for a number of values of γ'_ℓ in the neighbourhood of $\hat{\gamma}'_\ell$. This time, for a chosen γ'_ℓ, the simple pole of the Padé approximant to (4.14) yields an estimate of z_c, while the residue calculated at that pole is an estimation of $(\bar{C}'_\ell)^{1/\gamma'_\ell}$. It is again possible to plot for each Padé approximant, [N',D'] a graph of $z_c([N',D'])$ versus γ'_ℓ. The best value of γ'_ℓ is that value which best reproduces $z_c = 0.317401$. It is clear from an inspection of figures 4.12 to 4.22, how we arrive at confidence limits in the estimation of ε_ℓ and γ'_ℓ by this technique of neighbouring powers.

In practice, to improve the graphical resolution, we seldom plot $\mu_c([N,D])$ versus ε_ℓ, nor $z_c([N',D'])$ versus γ'_ℓ. Instead the deviations of the estimations from a reference line are used in place of $\mu_c([N,D])$ and $z_c([N',D'])$; that is we use

$$\Delta\mu_\ell([N,D]) = \mu_C([N,D]) - a\epsilon_\ell - b \tag{4.15}$$

and

$$\Delta z_\ell([N',D']) = z_C([N',D']) - a'\gamma'_\ell - b' \tag{4.16}$$

where $z = a'\gamma'_\ell + b'$, and $\mu = a\epsilon_\ell + b$ are the reference lines mentioned.

Figures 4.12 to 4.15 are graphs of $\Delta\mu_\ell$ versus ϵ_ℓ for $\ell = 1, 2, 4, 5$. The best estimates of ϵ_ℓ are indicated in table 4.3. The graphs of Δz_ℓ versus γ'_ℓ are given in figures 4.16 to 4.21 for $\ell = 0, 1, 2, 3, 4, 5$. The best estimates of γ'_ℓ are indicated in table 4.3.

It is interesting to note that while the method of forming neighbouring powers is more elaborate and precise that of taking logarithmic derivatives is much faster.

Figure 4.12 Deviations, $\Delta\mu$, from a standard line, $\mu = a\epsilon_1 + b$ of poles of Padé approximants to $\left\{ \frac{1}{\mu} \left[\frac{\partial M(\mu, z)}{\partial z}\right]_{z=z_c} \right\}^{1/\epsilon_1}$ versus ϵ_1.

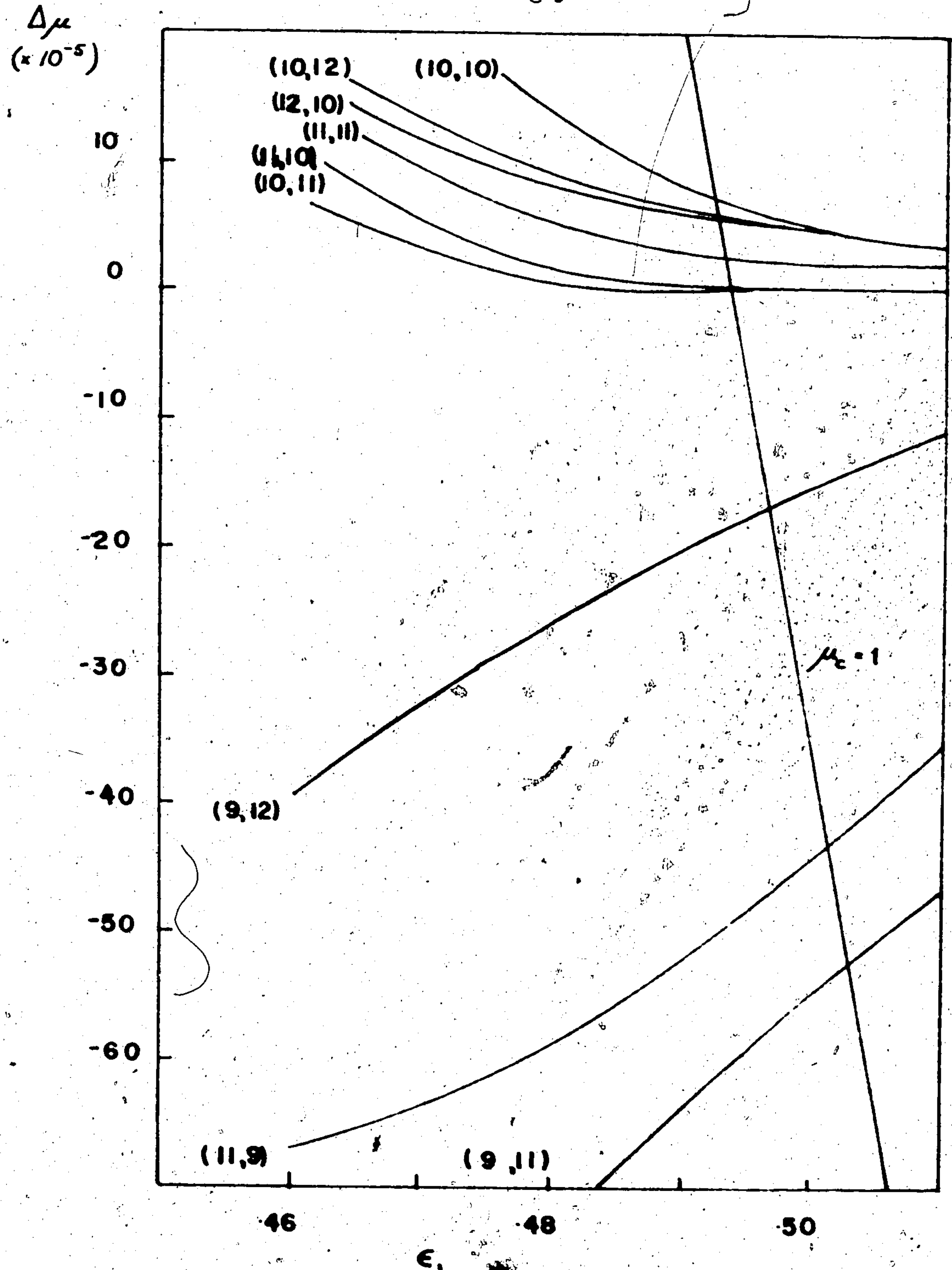

Figure 4.13 Deviations, $\Delta\mu$, from a standard line, $\mu = a\epsilon_2 + b$, of poles of Padé approximants to

$$\left\{ \frac{1}{\mu} \left[\frac{\partial M(\mu,z)}{\partial z^2}\right]_{z=z_c} \right\}^{1/\epsilon_2}$$

versus ϵ_2.

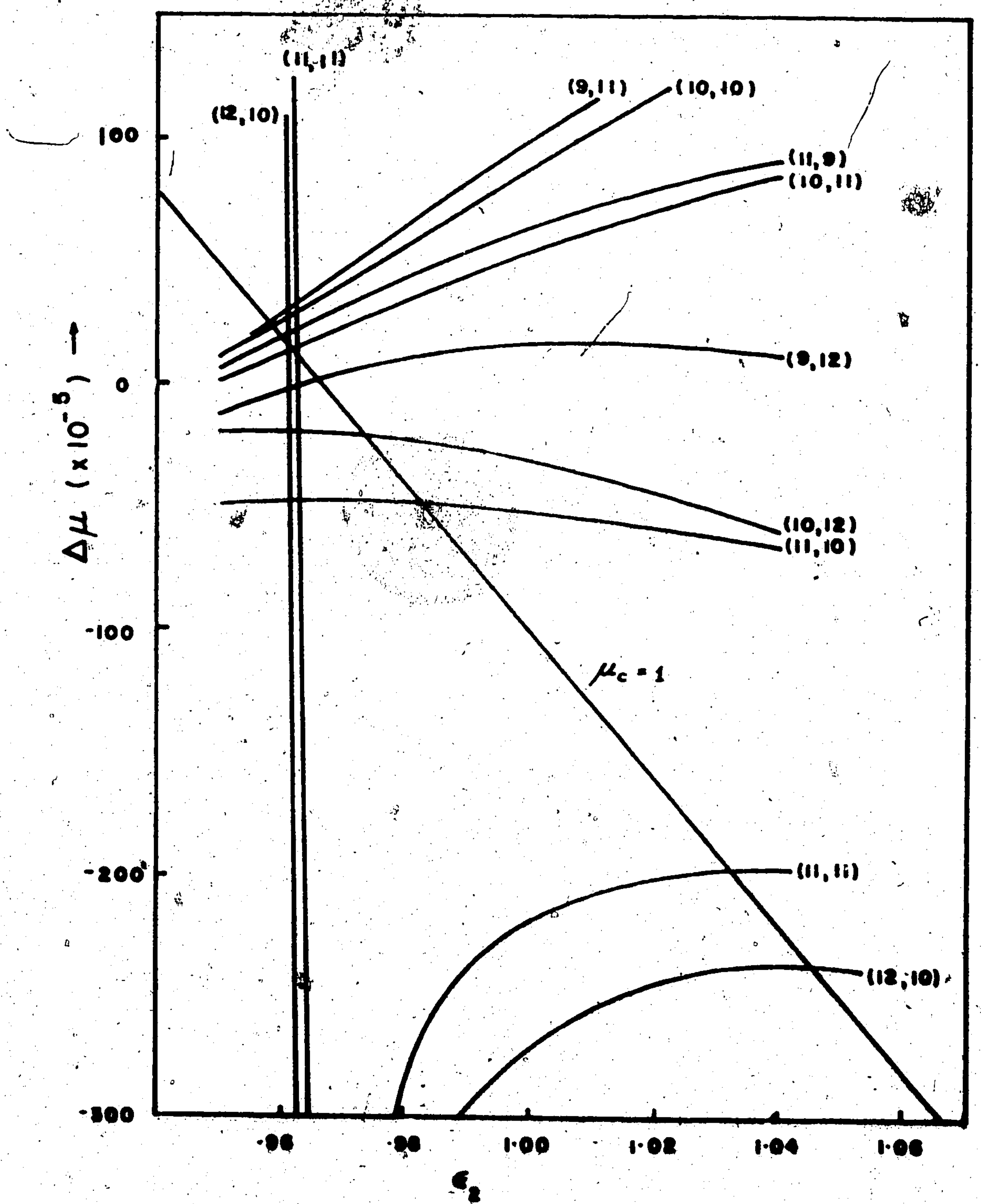

Figure 4.14 Deviations, $\Delta\mu$, from a standard line, $\mu = a\varepsilon_4 + b$, of poles of Pade approximants to $\left\{ \frac{1}{\mu} \left(\frac{\partial^4 M(\mu, z)}{\partial z^4} \right)_{z=z_c} \right\}^{1/\varepsilon_4}$ versus ε_4.

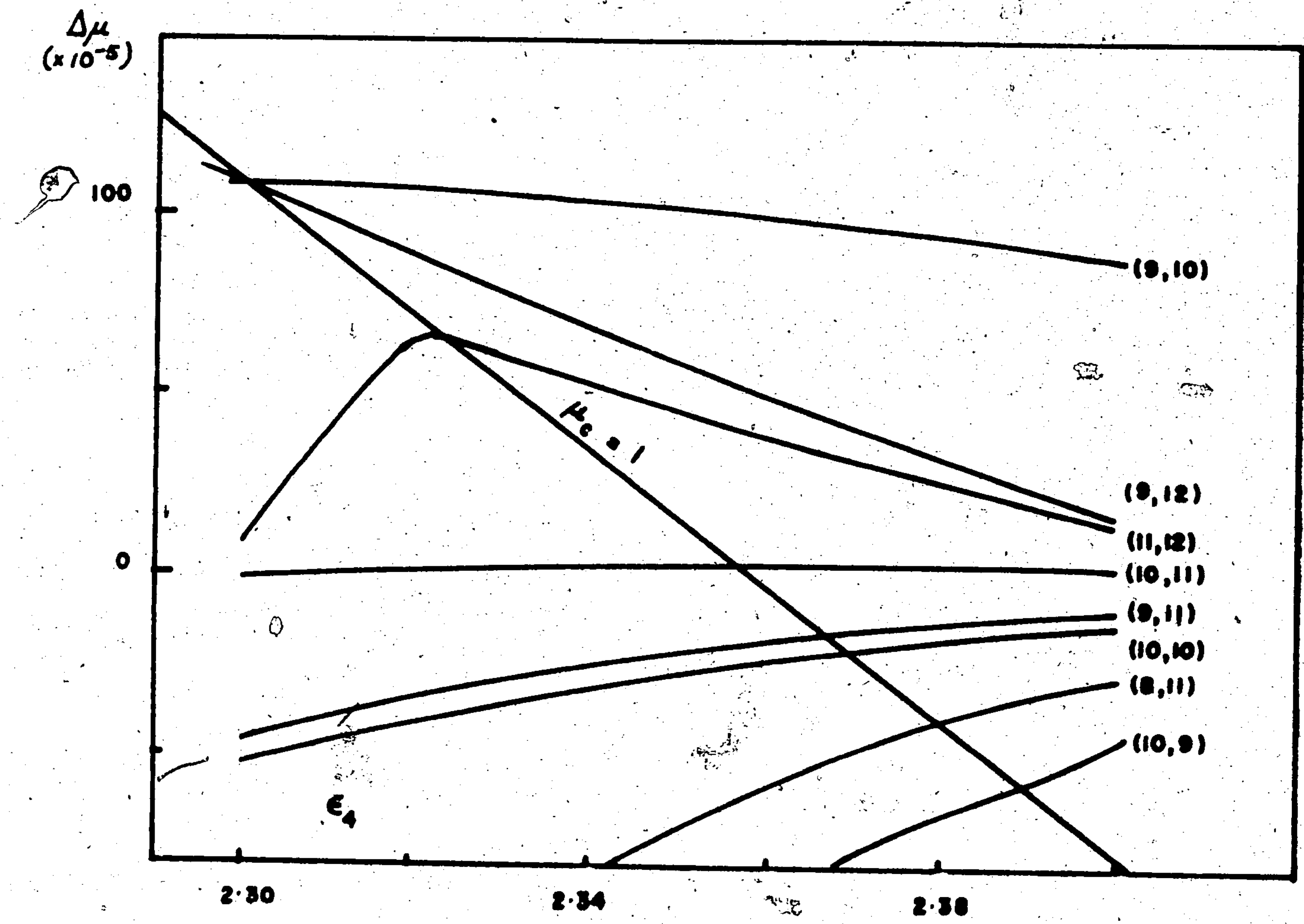

Figure 4.15 Deviations, $\Delta\mu$, from a standard line, $\mu = a\epsilon_5 + b$, of poles of Padé approximants to

$$\left\{ \frac{1}{\mu} \left[\frac{\partial^5 M(\mu, z)}{\partial z^5} \right]_{z=z_c} \right\}^{1/\epsilon_5}$$

versus ϵ_5 .

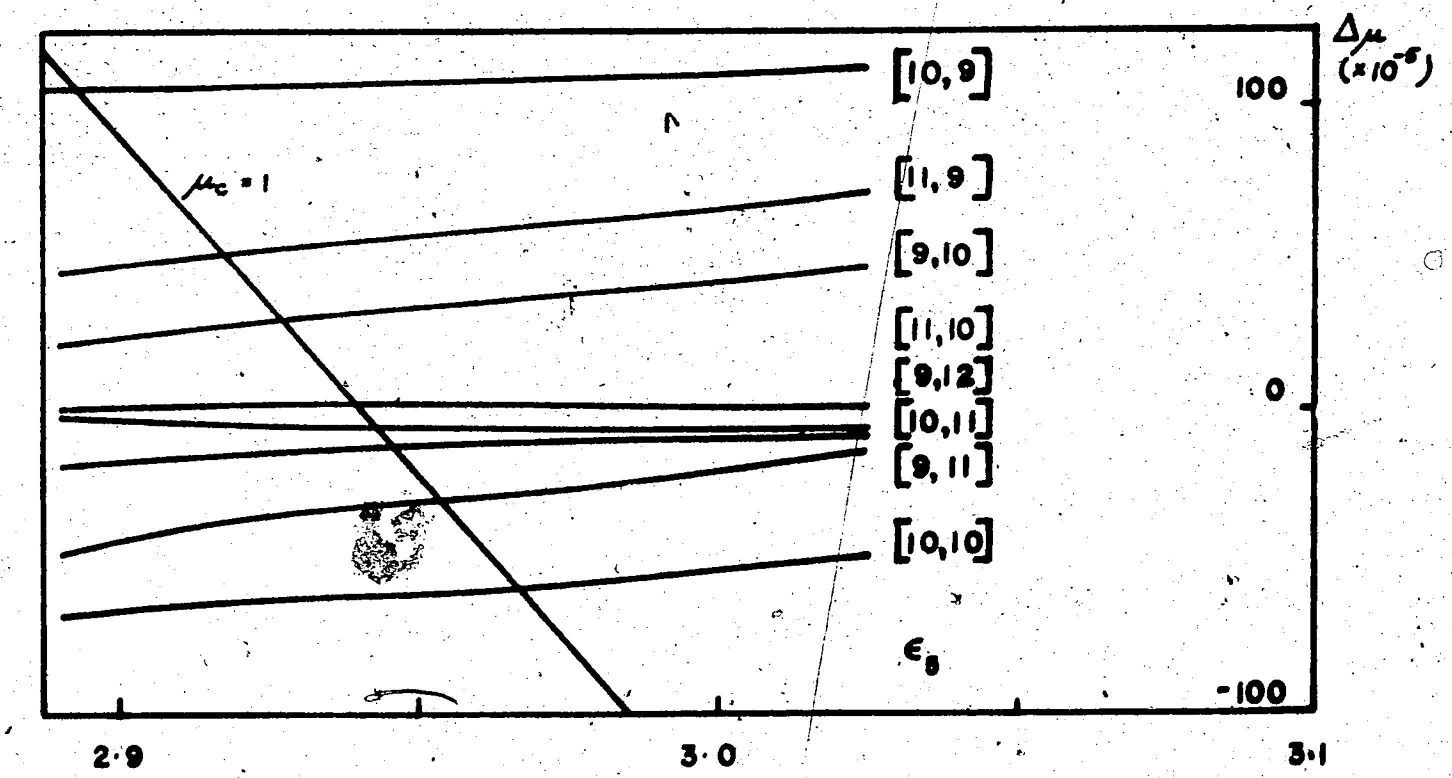

Figure 4.16 Deviations, $\Delta\mu$, from a standard line, $z = a'\gamma_0' + b'$, of poles of Padé approximants to $[M(z)]^{1/\gamma_0'}$.

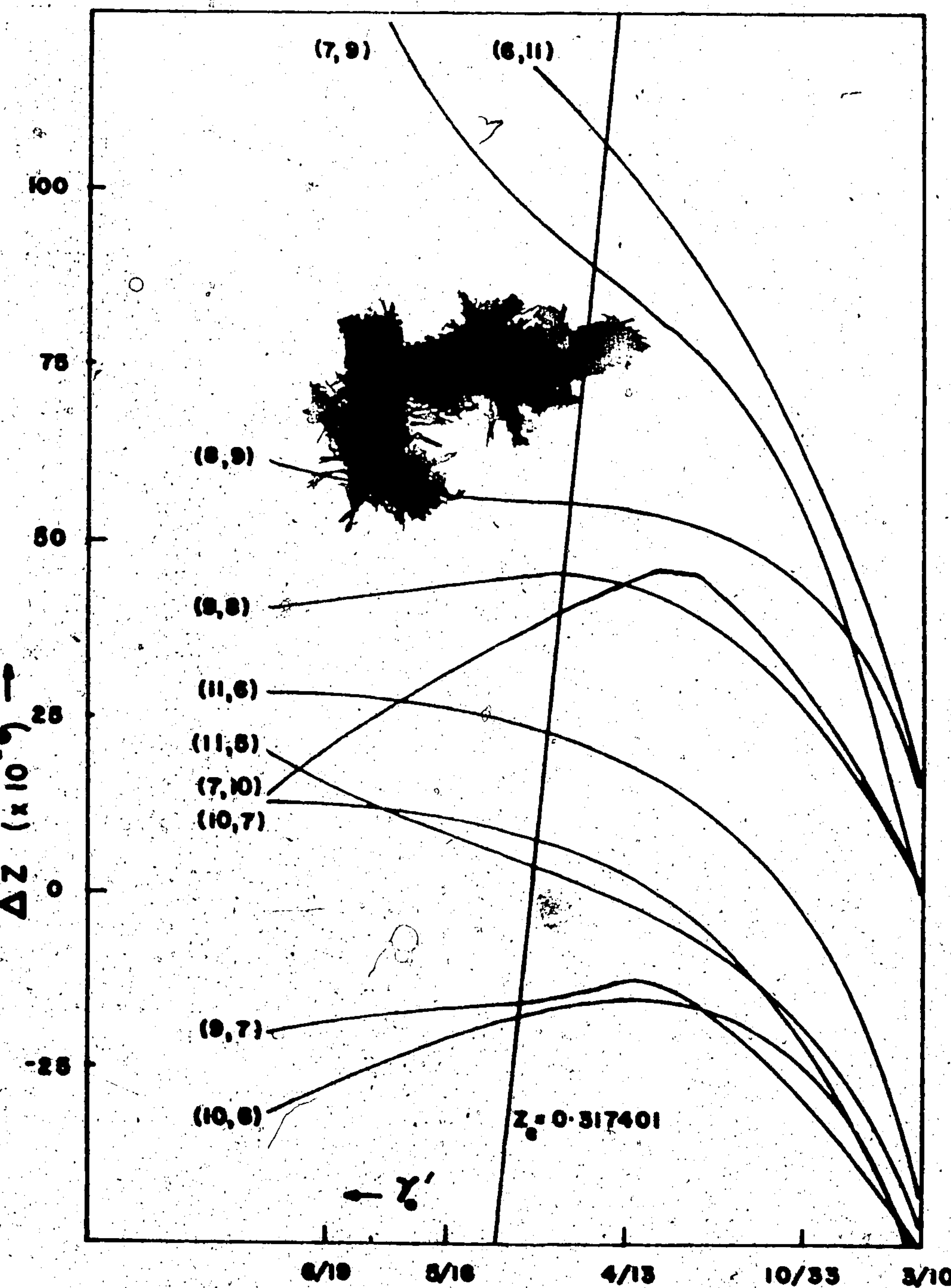

Figure 4.17 Deviations, Δz, from a standard line, $z = a'\,\gamma_1' + b'$, of poles of Padé approximants to $\left\{\frac{1}{z^3}\left|\frac{\partial M(\mu,z)}{\partial \mu}\right|_{\mu=\mu_c}\right\}^{1/\gamma_1'}$ versus γ_1'.

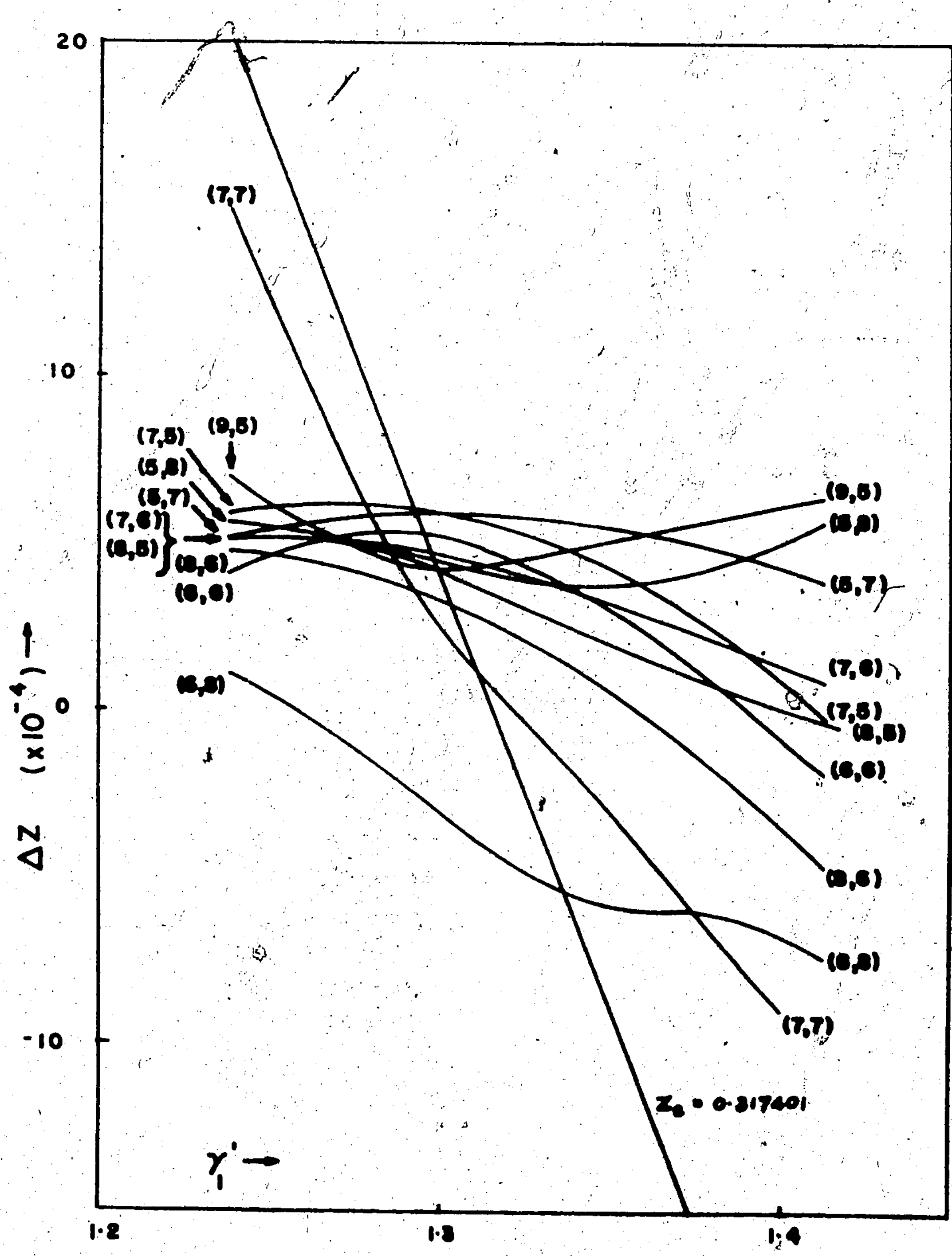

Figure 4.18 Deviations, Δz, from a standard line, $z = a'\gamma_2' + b'$, of poles of Padé approximants to

$$\left\{ \frac{1}{z^4} \left| \frac{\partial^2 M(\mu,z)}{\partial \mu^2} \right|_{\mu=\mu_c} \right\}^{1/\gamma_2'} \quad \text{versus } \gamma_2'.$$

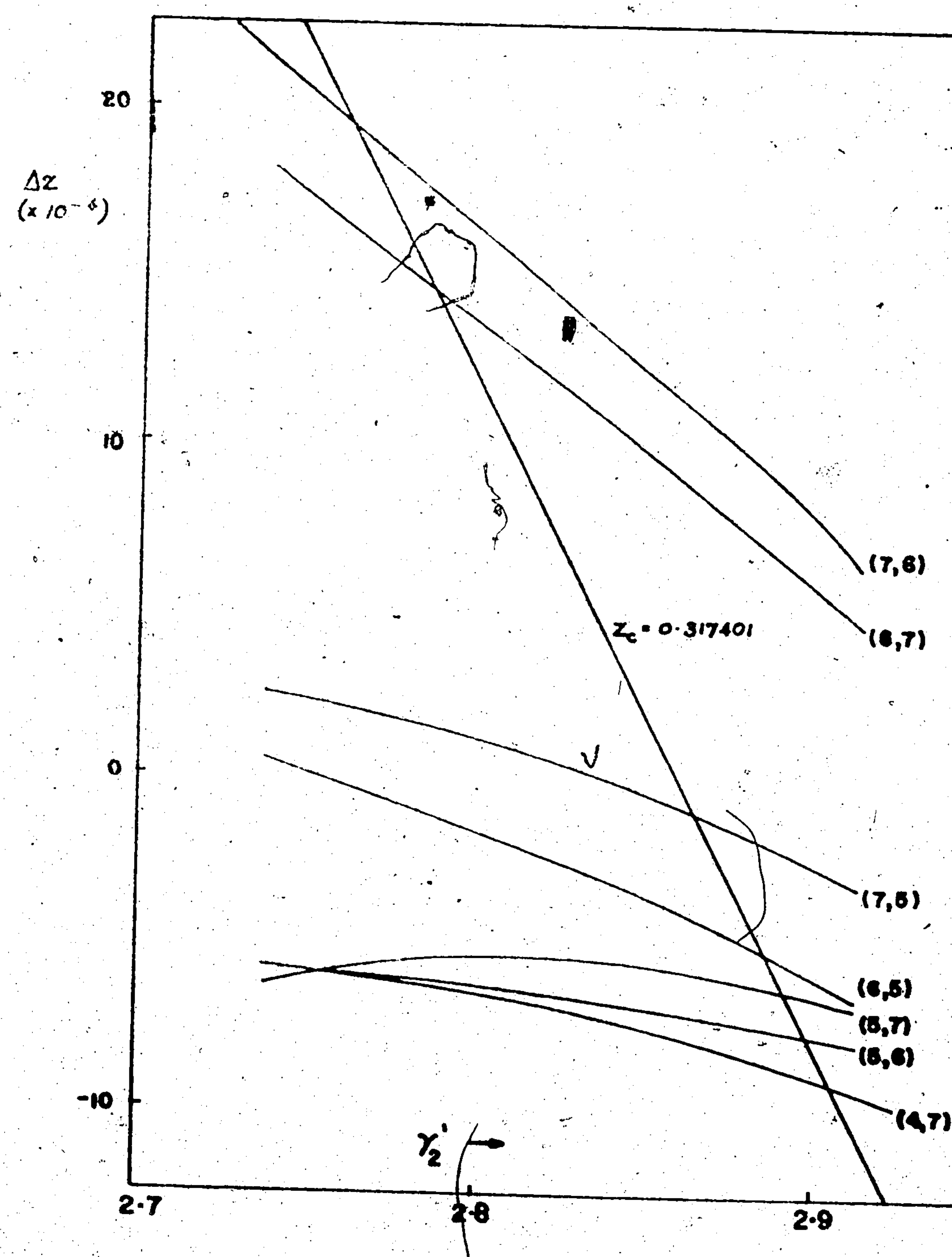

Figure 4.19 Deviations, Δz, from a standard line, $z = a'\gamma_3' + b'$, of poles of Padé approximants to

$$\left\{ \frac{1}{z^5} \left| \frac{\partial^3 M(\mu,z)}{\partial \mu^3} \right|_{\mu=\mu_c} \right\}^{1/\gamma_3'} \quad \text{versus } \gamma_3'.$$

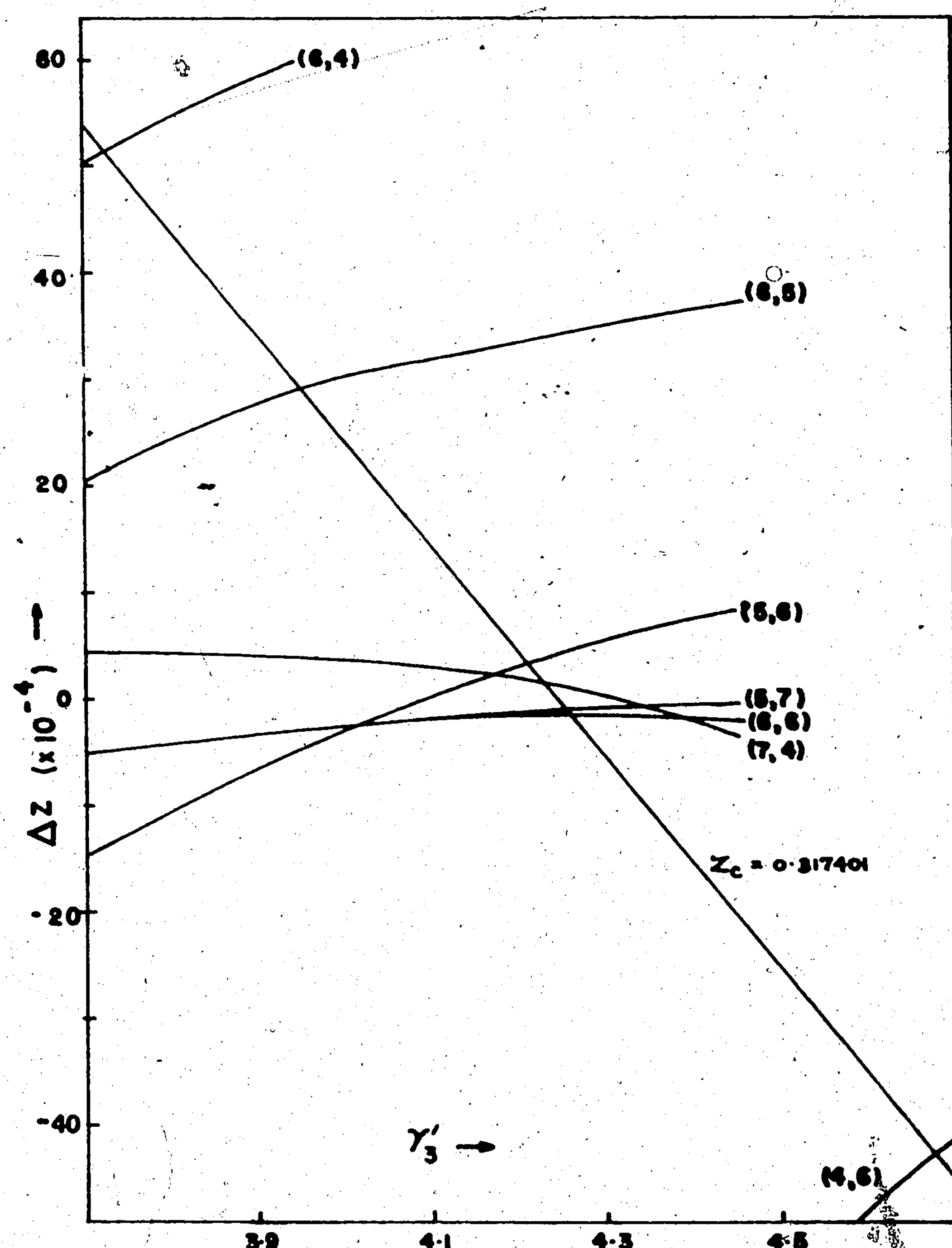

Figure 4.20

Deviations, Δz, from a standard line, $z = a'\gamma_4' + b'$, of poles of Padé approximants to

$$\left\{ \frac{1}{z^6} \left[\frac{\partial^4 M(\mu, z)}{\partial \mu^4} \right]_{\mu=\mu_c} \right\}^{1/\gamma_4'}$$

versus γ_4' .

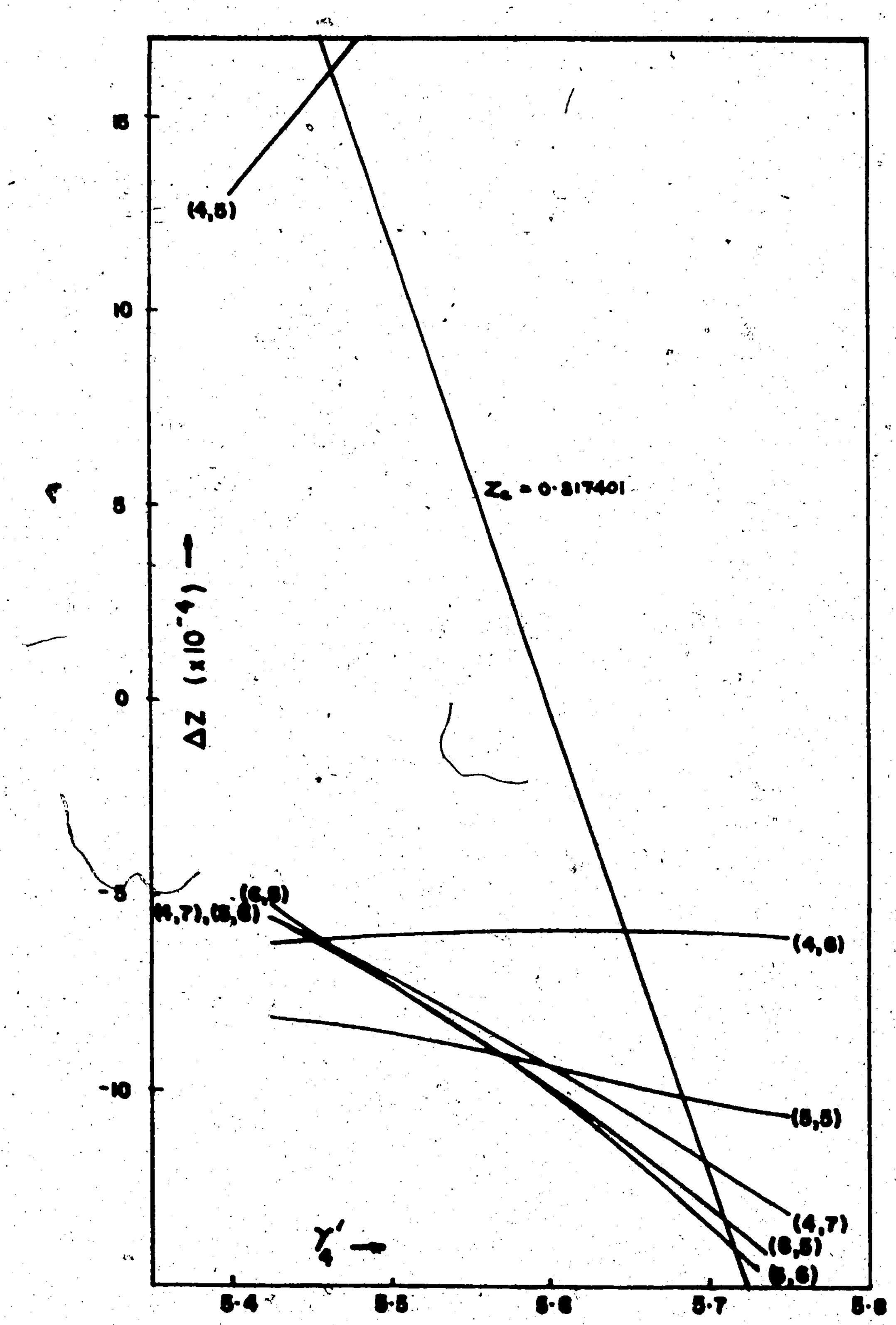
15
10
5
0
-5
-10
ΔZ (x10^-4)
(4,5)
(4,6)
(4,7)
5·4
5·5
5·6
5·7
5·8

Figure 4.21 Deviations, Δz, from a standard line, $z = a' \gamma_5' + b'$, of poles of Padé approximants to

$$\left\{ \frac{1}{z^7} \left. \frac{\partial^5 M(\mu,z)}{\partial \mu^5} \right|_{\mu=\mu_c} \right\}^{1/\gamma_5'}$$

versus γ_5'.

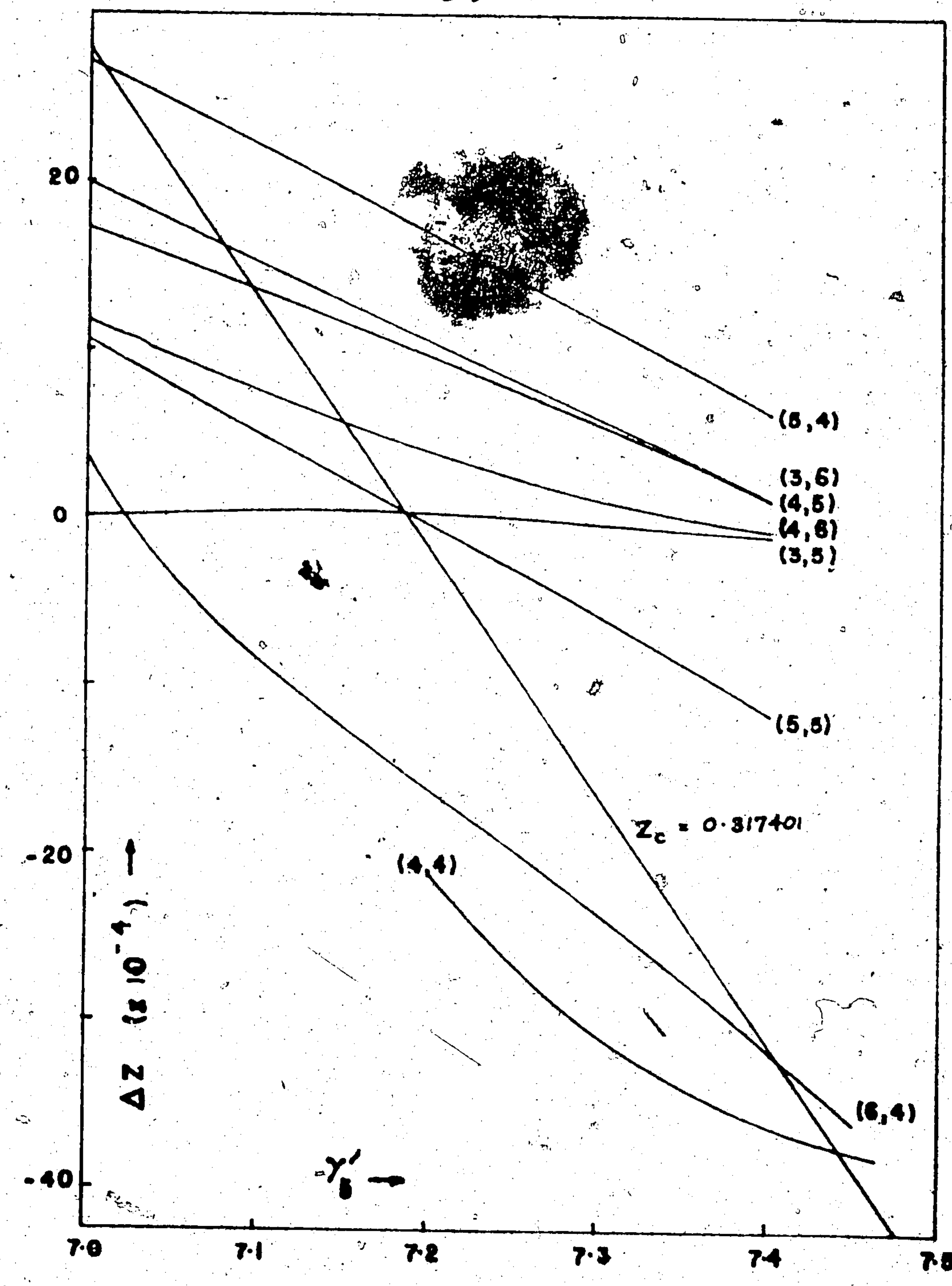

Table 4.3 From Padé approximants to $[\partial^{\ell}M(\mu,z)/\partial z^{\ell}|_{z=z_c}]^{1/\epsilon_\ell}$ and $[\partial^{\ell}M(\mu,z)/\partial\mu^{\ell}|_{\mu=\mu_c}]^{1/\gamma_\ell}$, estimates of critical exponents ϵ_ℓ and γ'_ℓ, via plots of $\Delta\mu_\ell$ versus ϵ_ℓ, and of Δz_ℓ versus γ'_ℓ.

ℓ	0	1	2	3	4	5
ϵ_ℓ		0.493±0.010	0.97±0.02		2.35±0.04	2.93±0.07
γ'_ℓ	0.310±0.003	1.295±0.035	2.86±0.10	4.23±0.40	5.7 ±0.5	7.2 ±0.4

4.4 Transformations

Already in section 4.2 we have seen that the presence of non-physical singularities can prevent the analysis of series expansions from proceeding smoothly. First of all we wish to find out the locations of these singularities. We seek therefore the poles of central, high degree Padé approximants to $(d/dz)\log[\partial^{\ell}M(\mu,z)/\partial\mu^{\ell}|_{\mu=\mu_c}]$. Figure 4.22 depicts the case for $\ell = 4$ and figure 4.23, the case for $\ell = 5$. It appears that there is a pair of singularities in the complex z plane making an angle of about 60° with the positive real axis. In both these cases these non-physical singularities appear nearer to the origin than z_c. This unfortunate situation may account for the greater error we must associate with our estimates of γ_3', γ_4', γ_5'. Moreover, on scrutinizing figure 4.24 we notice the irritating presence of a negative real singularity in $(d/dz)\log[\partial^5 M(\mu,z)/\partial\mu^5|_{\mu=\mu_c}]$.

Many ingenious techniques have been developed for dealing with non-physical singularities (Gaunt and Guttmann, 1974). We follow here the method of conformal mapping as developed by Betts, Elliott and Ditzian (1971). We rewrite the series to be analysed:

$$\left(\frac{\partial^{\ell}M(\mu,z)}{\partial\mu^{\ell}}\right)_{\mu=\mu_c} = \sum_{n=0}^{17} b_n^{(\ell)} z^n. \qquad (4.17)$$

The most general conformal transformation of $[\partial^{\ell}M(\mu,z)/\partial\mu^{\ell}]_{\mu=\mu_c}$ is achieved by the substitution of

$$z = \sum_{n=1}^{L} \lambda_n \bar{z}^n , \qquad (4.18)$$

where L (L = 17 here) is the maximum degree of the known terms in the original series expansion, (4.17).

The resulting new polynomial is obtained

$$\left[\frac{\partial^{\ell}M(\mu,\bar{z})}{\partial\mu^{\ell}}\right]_{\mu=\mu_c} = \sum_{n=0}^{17} \bar{b}_n^{(\ell)} \bar{z}^n \qquad (4.19)$$

For the pair of singularities at an angle of ± 60° to the real axis in the complex z-plane we notice that the transformation:

$$z = \bar{z}/(1 - 27\bar{z}^3) \qquad (4.20)$$

has the following effect on points of distance $|z| = 1/3$ from the origin. Such points on the rays argument z = 0, ± 2π/3 are shifted radially nearer to the origin. Points on the rays argument z = π, ± π/3, however, are pushed radially farther from the origin.

As for the case of $[\partial^3M(\mu,z)/\partial z^3|_{z=z_c}]$, neither the technique of logarithmic derivatives nor that of neighbouring powers were successful in the estimation of

ε_3 (see tables 4.1 and 4.3). Most unfortunately, when the poles of high degree central Padé approximants to $(d/d\mu)\ \ell n\ [\partial^3 M(\mu,z)/\partial z^3]_{z=z_c}$ are examined, a singularity appears on the real μ axis at $\mu = 0.85$. This is rather disconcerting and as yet no simple technique has succeeded in overcoming this impedance to the analysis of the critical behaviour at $\mu_c = 1$ for this function.

Figure 4.22 Poles of Padé approximants to

$$\frac{d}{dz}\left\{\log \frac{1}{z^6}\left[\frac{\partial^4 M(\mu,z)}{\partial \mu^4}\right]_{\mu=\mu_c}\right\}$$ plotted on the

z-plane. The circles drawn have radii z_c.

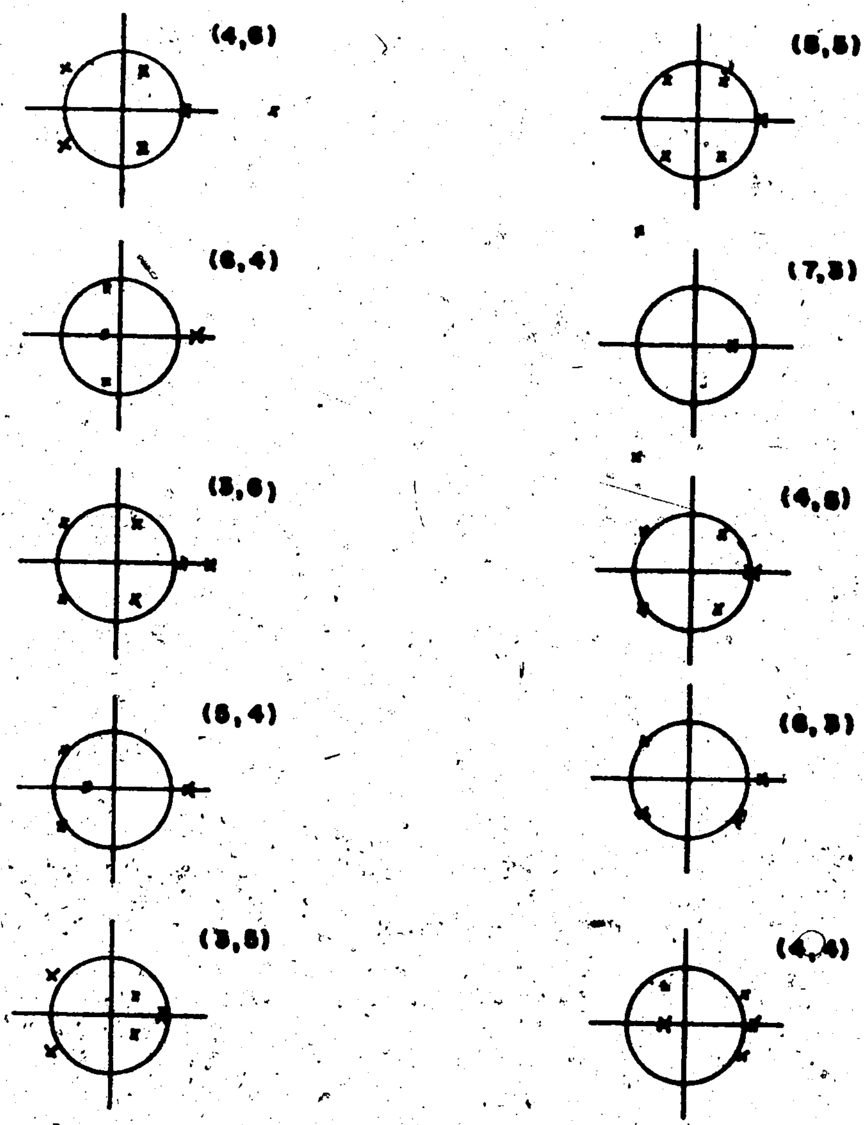

Figure 4.23 Poles of Padé approximants to $\frac{d}{dz}\left\{\log \frac{1}{z^7}\left[\frac{\partial^5 M(\mu,z)}{\partial\mu^5}\right]_{\mu=\mu_c}\right\}$ plotted on the complex z-plane.

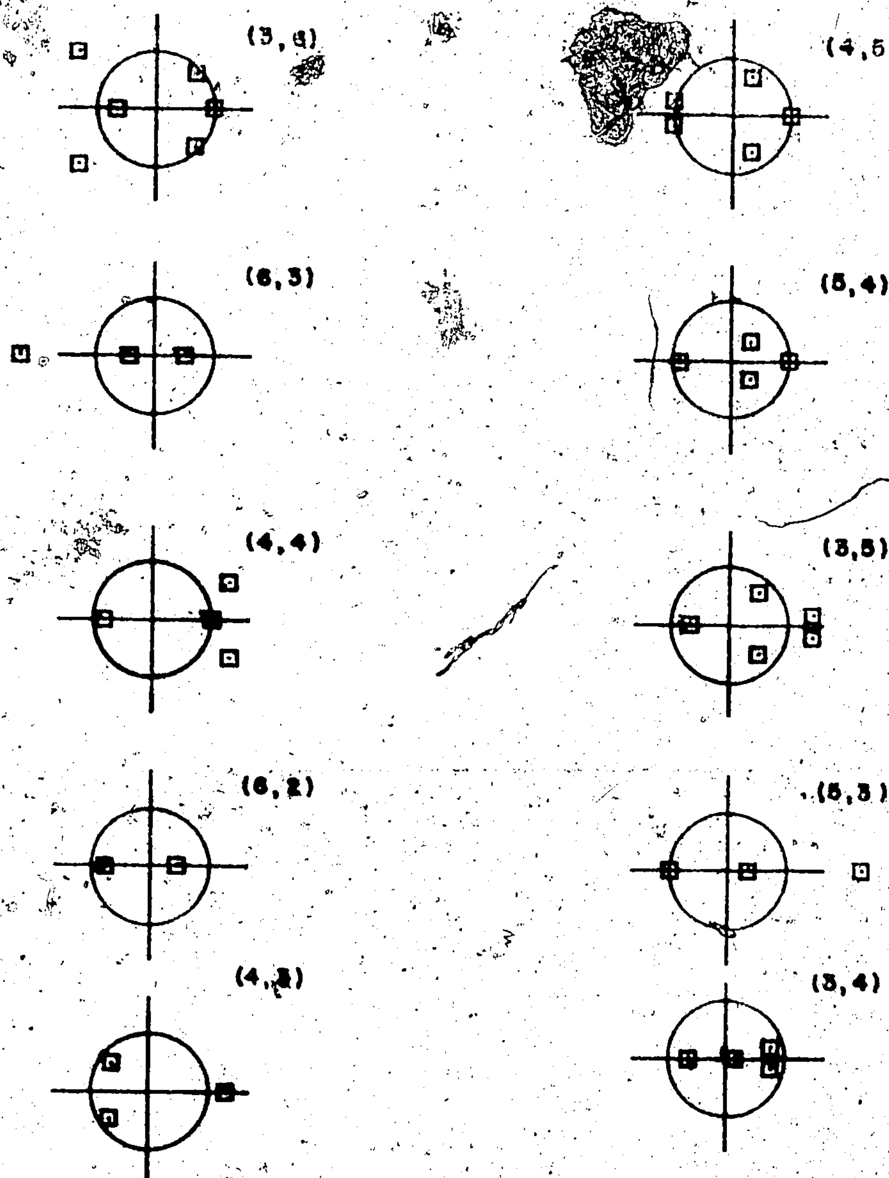

4.5 Results of Transformations

Using the transformation (4.20), $z_c = 0.317401$ is transformed to $\bar{z}_c = 0.222721$. The transformation (4.20) was applied to $[\partial^4 M(\mu,z)/\partial\mu^4]_{\mu=\mu_c}$ and $[\partial^5 M(\mu,z)/\partial\mu^5]_{\mu=\mu_c}$. The resulting estimations of γ_4' and γ_5' from residues and poles of Padé approximants to

$$\frac{d}{d\bar{z}}\left\{\log.\frac{1}{\bar{z}^6}\left[\frac{\partial^4 M(\mu,z)}{\partial\mu^4}\right]_{\mu=\mu_c}\right\}$$

and

$$\frac{d}{d\bar{z}}\left\{\log\frac{1}{\bar{z}^7}\left[\frac{\partial^5 M(\mu,z)}{\partial\mu^5}\right]_{\mu=\mu_c}\right\}$$

are displayed in figures (4.24) and (4.25) respectively.

Next, $[\partial^4 M(\mu,z)/\partial\mu^4]_{\mu=\mu_c}$ and $[\partial^5 M(\mu,z)/\partial\mu^5]_{\mu=\mu_c}$ were analysed by the method of neighbouring powers described in section 4.3, after the transformation (4.20) was applied. The results are illustrated in figures 4.26 and 4.27 respectively. We obtain from these figures the improved estimates of

$$\gamma_4' = 5.85 \pm 0.10$$

and

$$\gamma_5' = 7.12 \pm 0.08$$

The transformation (4.20) appears to improve appreciably the analyses of the series for $[\partial^4 M(\mu,z)/\partial\mu^4]_{\mu=\mu_c}$ and $[\partial^5 M(\mu,z)/\partial\mu^5]_{\mu=\mu_c}$. There is a marked improvement in precision as shown by the better confidence limits we attach to γ_4' and γ_5'. The best estimates of ε_ℓ and γ_ℓ' in the overall analyses are given in table 4.4.

Figure 4.24

Estimations of γ_4' and $\bar{z}_c$ from residues and poles of Padé approximants to $(d/d\bar{z})\ \{\log\ (\partial^4 M/\partial \mu^4)_{\mu=\mu_c}/\bar{z}^6\}$.

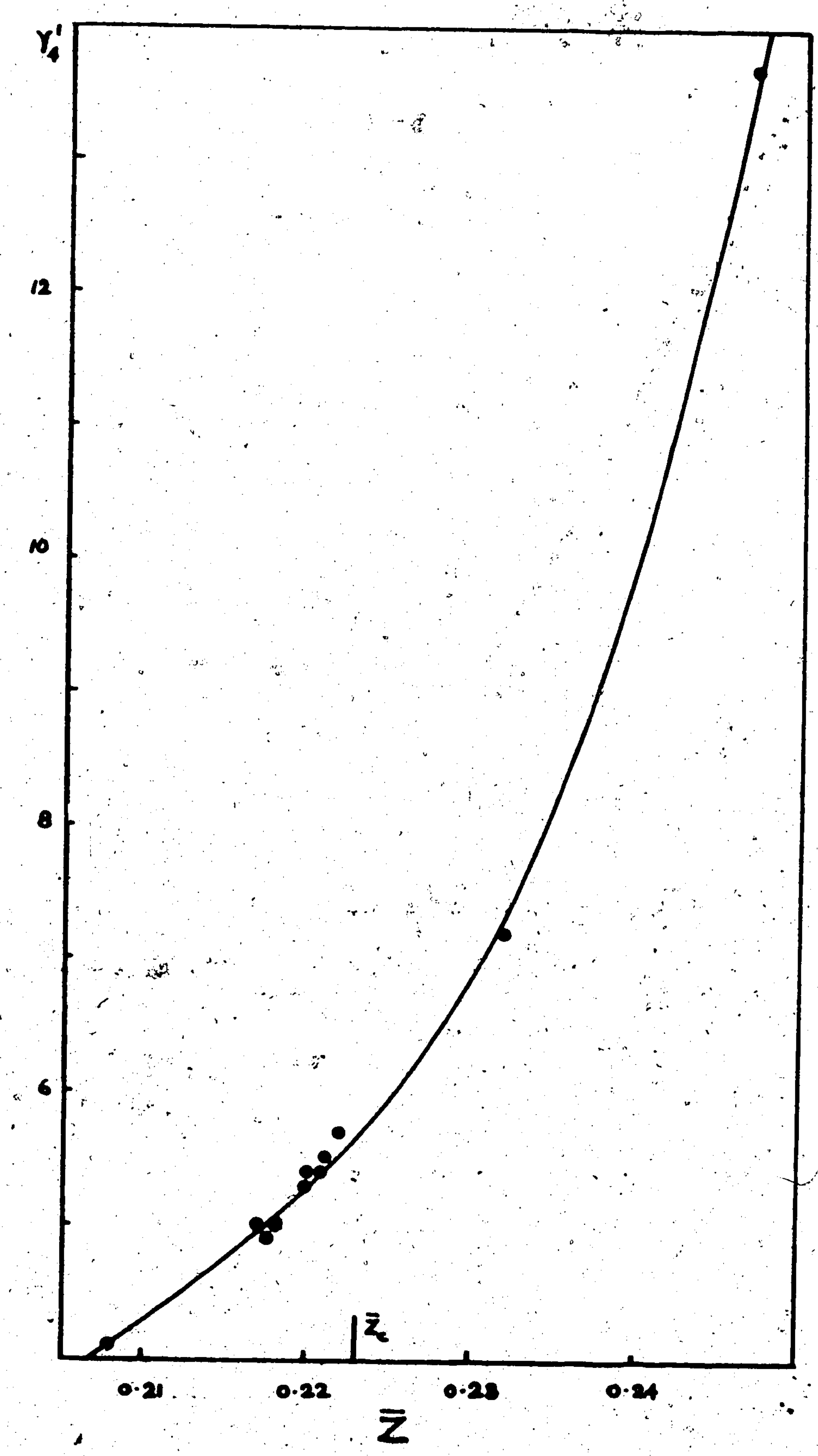
Y_4'
12
10
8
6
$\bar{Z}_c$
0·21
0·22
0·23
0·24
$\bar{Z}$

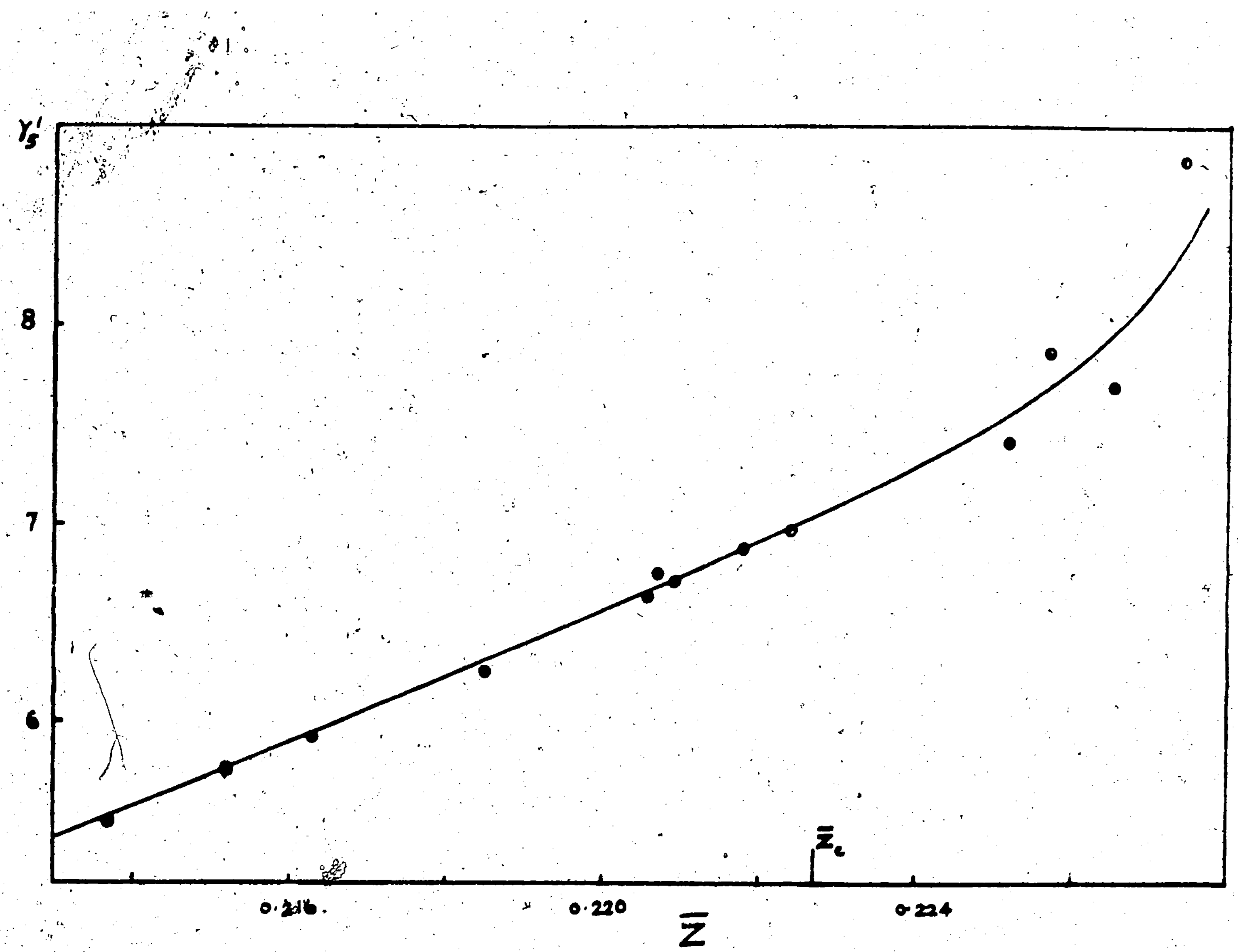

Figure 4.25. Estimation of γ_5' and $\bar{z}_c$ from residues and poles of Padé approximants to $(d/d\bar{z})\{\log (d^5M/d\mu^5)_{\mu=\mu_c}/\bar{z}^7\}$.

Figure 4.26 Deviations, $\Delta\bar{z}$, from a standard line, $\bar{z} = a'\gamma_4' + b'$, of poles of Padé approximants to $\left\{\frac{1}{z^6}\left[\frac{\partial^4 M(\mu,\bar{z})}{\partial\mu^4}\right]_{\mu=\mu_c}\right\}^{1/\gamma_4'}$ versus γ_4'.

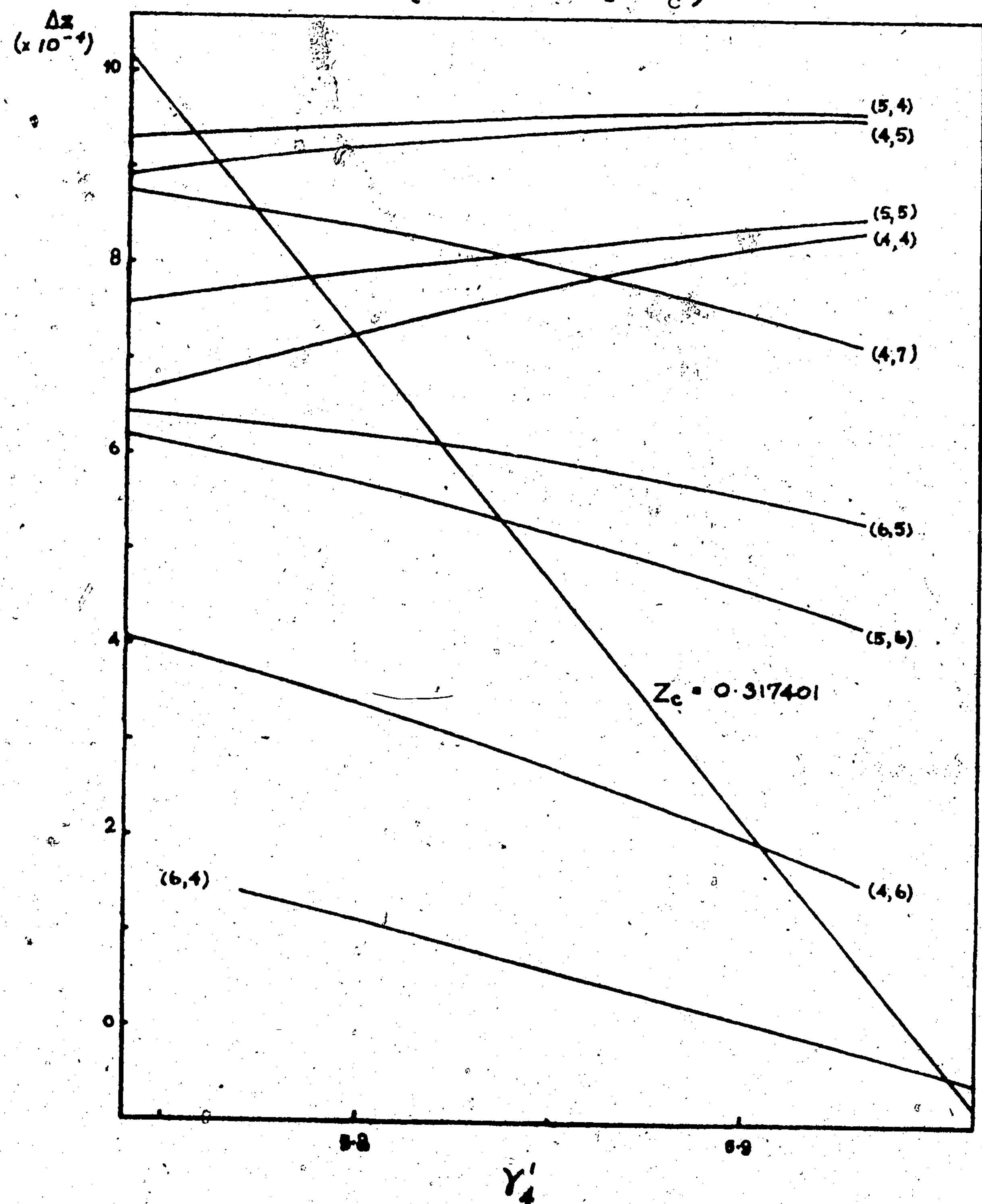

Figure 4.27

Deviations, $\Delta\bar{z}$, from a standard line, $\bar{z} = a'\gamma_5' + b'$, of poles of Padé approximants to

$$\left\{ \frac{1}{\bar{z}^7} \left[\frac{\partial^5 M(\mu,\bar{z})}{\partial \mu^5} \right]_{\mu=\mu_c} \right\}^{1/\gamma_5'}$$

versus γ_5'.

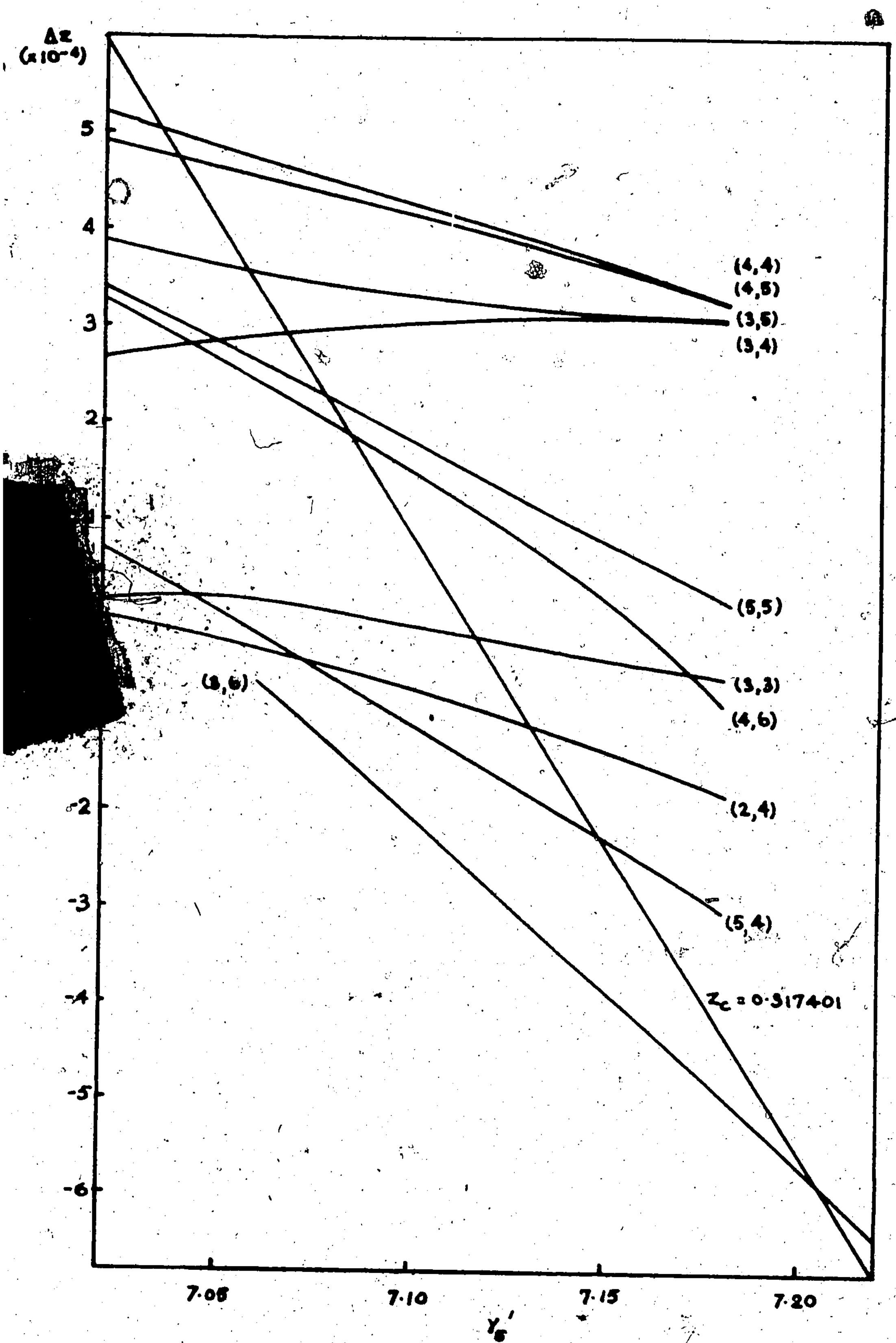

Δz
(x10⁻⁴)
5
4
3
2
-2
-3
-4
-5
-6
(4,4)
(4,5)
(3,5)
(3,4)
(5,5)
(3,3)
(4,6)
(2,4)
(5,4)
(3,6)
Zc = 0·317401
7·05
7·10
7·15
7·20
Y₅'

Table 4.4 Comparison of scaling theory predictions with best estimates from series expansions for the Ising model critical exponents γ'_ℓ of $(\partial^\ell M/\partial h^\ell)_{h=0}$ and ε_ℓ of $(\partial^\ell M/\partial t^\ell)_{t=0}$. Corresponding amplitudes are also included.

ℓ	0	1	2	3	4	5
γ'_ℓ (scaling)	-0.3125	1.25	2.8125	4.375	5.9375	7.5
γ'_ℓ (series)	-0.309±0.002	1.295±0.035	2.86±0.10	4.37±0.10	5.85±0.10	7.12±0.08
C'_ℓ	1.31	0.223	-0.265	0.710	-2.91	34.5
ε_ℓ (scaling)	-0.2	0.44	1.08	1.72	2.36	3
ε_ℓ (series)	-0.193±0.007	0.492±0.010	0.96±0.02	—	2.36±0.04	2.93±0.07
E_ℓ	1.51	-1.06	0.285	—	0.411	-1.02

4.6 Calculation of Critical Amplitudes

We have so far analysed the asymptotic behaviour of $(\partial^{\ell}M/\partial\mu^{\ell})_{\mu=\mu_c}$ and $(\partial^{\ell}M/\partial z^{\ell})_{z=z_c}$. The expected behaviour of the most singular parts of these functions may be expressed as:

$$(\partial^{\ell}M/\partial\mu^{\ell})_{\mu=\mu_c} \sim \bar{C}'_{\ell}\ (1-z/z_c)^{-\gamma'_{\ell}} \qquad (4.21)$$

$$(\partial^{\ell}M/\partial z^{\ell})_{z=z_c} \sim \bar{E}_{\ell}\ (1-\mu)^{-\varepsilon_{\ell}} \qquad (4.22)$$

Theories of critical phenomena are usually expressed in terms of the reduced temperature $t = 1 - T/T_c$, and the reduced magnetic field $h = mH/kT_c$, for a magnetic system. The expected critical behaviour in terms of t and h should then read:

$$(\partial^{\ell}M/\partial h^{\ell})_{h=0} \sim C'_{\ell}\ t^{-\gamma'_{\ell}} \qquad (4.23)$$

$$(\partial^{\ell}M/\partial t^{\ell})_{t=0} \sim E_{\ell}\ h^{-\varepsilon_{\ell}} \qquad (4.24)$$

Equating (4.21) and (4.23) we get:

$$(C'_{\ell})^{1/\gamma'_{\ell}} = (\bar{C}'_{\ell})^{1/\gamma'_{\ell}}\ (d\mu/dh)^{\ell/\gamma'_{\ell}}_{h=0}\ z_c\ (-dt/dz)_{z=z_c}$$

$$= (-2)^{\ell/\gamma'_{\ell}}\ (\bar{C}'_{\ell})^{1/\gamma'_{\ell}}\ (z_c/T_c)\ (dT/dz)_{z=z_c}$$

$$\therefore C'_\ell = (-2)^\ell \, (\bar{C}'_\ell)/(-\log z_c)^{\gamma'_\ell} \qquad (4.25)$$

We note that log z_c is negative, so (-log z_c) is positive. Upon equating (4.22) to (4.24) we get:

$$(E_\ell)^{1/\varepsilon_\ell} = (\bar{E}_\ell)^{1/\varepsilon_\ell} \, (-dh/d\mu)_{\mu=\mu_c} \, (z_c \log z_c)^{\ell/\varepsilon_\ell}$$

$$\therefore E_\ell = (\bar{E}_\ell / 2^{\varepsilon_\ell}) \, (z_c \log z_c)^{\ell} \qquad (4.26)$$

The resulting values of E_ℓ and C'_ℓ estimated are given in table 4.4.

4.7 Investigation of $(\mu\frac{\partial}{\partial\mu})^{\ell}M(\mu,z)|_{\mu=\mu_c}$

We have seen that the series (ℓ = 0, 1, 2, 3, 4, 5)

$$[\partial^{\ell}M(\mu,z)/\partial\mu^{\ell}]_{\mu=\mu_c} = \sum_{n=0}^{17} b_n^{(\ell)} z^n \tag{4.27}$$

has its leading non-zero coefficient, $b_r^{(\ell)}$, at $r = \ell + 2$ for $\ell > 0$. For $\ell = 1$, our truncated series in (4.27) has 15 non-zero terms. Finally, when $\ell = 5$, the series for $\partial^5M/\partial\mu^5|_{\mu=\mu_c}$ has decreased to 11 non-zero terms. We know that the important terms are the higher powers of z, for example terms in z^7 where $p > 17$. Also in general, the longer the series the more accurate the estimations made from the series. To obtain terms involving z^p, where $p > 17$, we would need to have higher $L_s(z)$ polynomials. Since we only know exactly the $L_s(z)$ polynomials up to $s = 23$, we cannot, for the moment, extend the series in (4.27) beyond z^{17}. However, is there a way of increasing the string of non-zero terms in (4.27)?

One method of retaining as many non-zero terms in z as possible is to study instead the series expansions representing the asymptotic behaviour of $(\mu\partial/\partial\mu)^{\ell}M|_{\mu=\mu_c}$. Recall equation (3.11):

$$M(\mu,z) = 1 - 2\sum_{s=1}^{23} s\,L_s(z)\mu^s$$

$$\mu\,\partial M/\partial\mu = -2\sum_{s=1}^{23} s^2 L_s(z)\mu^s$$

In general

$$(\mu \frac{\partial}{\partial\mu})^{\ell} M(\mu,z) = -2 \sum_{s=1}^{23} s^{\ell+1} L_s(z)\mu^s \tag{4.28}$$

In particular, on the coexistence curve:

$$\begin{aligned}(\mu \frac{\partial}{\partial\mu})^{\ell} M(\mu,z)\Big|_{\mu=\mu_c} &= -2 \sum_{s=1}^{23} s^{\ell+1} L_s(z) \\ &= -2 \sum_{p=0}^{17} \beta_p^{(\ell)} z^p\end{aligned} \tag{4.29}$$

The table of coefficients for $-2 \sum_{p=0}^{17} \beta_p^{(\ell)} z^p$, $\ell = 0, 1, 2, 3, 4, 5$, are given in appendix 6.

For $\ell = 0, 1$, the series representing $(\mu\partial/\partial\mu)M|_{\mu=\mu_c}$ and the series representing $\partial^{\ell}M/\partial\mu^{\ell}|_{\mu=\mu_c}$ are the same. For $\ell = 2$, the series representing $(\mu\partial/\partial\mu)^2 M|_{\mu=\mu_c}$ has 15 non-zero terms while the series representing $\partial^2 M/\partial\mu^2|_{\mu=\mu_c}$ has 14 non-zero terms. The truncated series

$$\sum_{n=0}^{17} \beta_n^{(2)} z^n \sim (\mu \frac{\partial}{\partial\mu})^2 M\Big|_{\mu=\mu_c} \tag{4.30}$$

was analysed by computing poles and residues of Padé approximants to:

$$\frac{d}{dz}\left\{\log \sum_{n=3}^{17} \beta_n^{(2)} z^{n-3}\right\}. \tag{4.31}$$

A 3 by 4 Padé (approximant) table was set up and the computed poles and residues are listed in appendix 7. γ_2' estimated by this method was found to be

$$\gamma_2' = 2.98 \pm 0.10 \tag{4.32}$$

Next, poles and residues of Padé approximants to $\left[\sum_{n=3}^{17} \beta_n^{(\ell)} z^{n-3}\right]^{1/\gamma_\ell'}$ were computed. By this method, for a range of values of γ_2' such that $2.90 \leq \gamma_2' \leq 3.00$, it was found that

$$\gamma_2' = 2.94 \pm 0.04 \tag{4.33}$$

In the case of $\ell = 3$, an analysis of the poles and residues to

$$\frac{d}{dz}\left\{\log \sum_{n=3}^{17} \beta_n^{(3)} z^{n-3}\right\}, \tag{4.34}$$

yielded:

$$\gamma_3' = 4.9 \pm 0.7 \tag{4.35}$$

It was suspected from the large uncertainty in (4.35) that troublesome non-physical singularities were hampering the analysis of the series. A natural step to take is to examine the locations of the singularities in the complex z-plane of central high degree Padé approximants to (4.34), for ℓ = 2, 3, 4, 5. However for ℓ = 3, 4, 5, it was found that the series in (4.29) cannot be readily analysed by the usual techniques of series analysis whereas the series in (4.27) can. We have therefore chosen to concentrate on the analysis of the series in (4.27).

4.8 Dropping Off Terms

We have also attempted to investigate the effect of dropping off leading non-zero terms in the field derivatives of the magnetization on the coexistence curve. For example the known non-zero coefficients in the truncated series expansion for

$$(\partial^2 M/\partial \mu^2)_{\mu=\mu_c} \sim \sum_{n=0}^{17} b_n^{(2)} z^n ,$$

are $b_4^{(2)}$ to $b_{17}^{(2)}$. From the poles and residues of Padé approximants to the logarithmic derivatives of the modified series:

$$\sum_{n=5}^{17} b_n^{(2)} z^{n-5}, \quad \sum_{n=6}^{17} b_n^{(2)} z^{n-6}, \quad \sum_{n=7}^{17} b_n^{(2)} z^{n-7},$$

$$\sum_{n=8}^{17} b_n^{(2)} z^{n-8}, \quad \sum_{n=9}^{17} b_n^{(2)} z^{n-9}, \quad \sum_{n=10}^{17} b_n^{(2)} z^{n-10},$$

We found that the estimated γ_2' fluctuated between 2.95 and 2.55. We realise that the important terms are those involving the higher powers of z. If this is the case then dropping off the terms involving the smaller powers of z should not affect adversely the asymptotic behaviour of the series at all.

This procedure of analysis was repeated with the series $\sum_{n=r}^{17} b_n^{(\ell)} z^{n-r}$ where

$r = 6, 7, \ldots 10$ for $\ell = 3$,

$r = 6, \ldots 9$ for $\ell = 4$,

and $r = 8, 9, 10$ for $\ell = 5$.

γ_3' was discovered to vary from 4.2 to 5.2, γ_4' from 6 to 6.8, and γ_5' from 7.8 to 8.5. The fluctuations in γ_ℓ' seems to indicate that the series $\sum_{n=0}^{17} b_n^{(\ell)} z^n$ are too short to represent well the true asymptotic behaviour of the functions $(\partial^\ell M/\partial\mu^\ell)_{\mu=\mu_c}$.

CHAPTER 5

Discussion and Comparison of Model Results with Scaling Theory

Beginning with the spin 1/2 Ising model on the hydrogen peroxide lattice, the low temperature (high field) series expansion for the Gibbs free energy has been obtained from the configurational data of Betts, Elliott and Sykes (1974). The magnetization and its first five field derivatives on the coexistence curve, and the magnetization and its first five derivatives with respect to $z = \exp(-2J/kT)$ on the critical isotherm have been derived. Next, using the techniques of taking logarithmic derivatives and neighbouring powers, the series for $(\partial^{\ell}M/\partial\mu^{\ell})_{\mu=\mu_c}$ and $(\partial^{\ell}M/\partial z^{\ell})_{z=z_c}$ have been analysed. Where the analysis has been impeded by the occurrence of non-physical singularities near the physical singularity, transformations have been sought to facilitate and enhance the analysis. From the residues of Padé approximants to $(\partial^{\ell}M/\partial\mu^{\ell})^{1/\gamma'_{\ell}}_{\mu=\mu_c}$ and $(\partial^{\ell}M/\partial z^{\ell})^{1/\varepsilon_{\ell}}_{z=z_c}$, the critical amplitudes C'_{ℓ} and E_{ℓ} (cf. 4.27 and 4.28) have been computed. Finally, the best estimates of γ'_{ℓ} and ε_{ℓ} (ℓ = 0, 1, 2, 3, 4, 5) have been tabulated in table 4.5 together with those predicted by scaling theory for the purpose of comparison.

If the series for $(\partial^{\ell}M/\partial\mu^{\ell})_{\mu=\mu_c}$ are examined, we find that for approximating M(z) (i.e. the case $\ell = 0$) we have a series of 18 terms (i.e. $\sum_{n=0}^{17} b_n^{(0)} z^n$). At the other extreme, for $\ell = 5$, we are approximating $(\partial^5M/\partial\mu^5)_{\mu=\mu_c}$ by a series of only eleven terms, (i.e. $\sum_{n=7}^{17} b_n^{(5)} z^n$). This means that when we form Padé approximants, to the logarithmic derivative of

$(\partial^5 M/\partial\mu^5)_{\mu=\mu_c}$ or to $(\partial^5 M/\partial\mu^5)^{1/\gamma'_5}_{\mu=\mu_c}$, we are restricted to a smaller Padé table than in the case of $\ell = 0$. This may explain the general trend towards a smaller degree of precision (i.e. wider confidence limits) as ℓ increases. Nevertheless, as has been pointed out by Betts and Chan (1974), all the critical exponents γ'_ℓ ($\ell = 0, 1, 2, 3, 4$) are in good agreement with static scaling predictions where it has been assumed that $\alpha = 1/8$ and $\gamma = 5/4$.

From table 4.4, the γ'_ℓ values agree within confidence limits with scaling predictions for $\ell = 0, 2, 3, 4$. In the cases of $\ell = 1$, and 5, the disagreement with scaling predictions is never greater than 4%. The confidence limits tends to increase with increasing ℓ which is a reason why investigations were confined to $\ell \leq 5$. On the whole the critical exponents, γ'_ℓ, along the coexistence curve are in good agreement with scaling predictions.

In the case of ϵ_ℓ on the critical isotherm, Betts and Filipow (1972) have investigated ϵ_ℓ for a number of two dimensional lattices: the honeycomb, the square and the triangular lattices, using the configurational data of Sykes, Gaunt, Mattingly, Essam and Elliott (1973). They found it impossible to estimate ϵ_4 at all. They obtained quite precisely, estimates of ϵ_0, ϵ_2 and ϵ_5, which agree closely with scaling predictions. Their values for ϵ_1 and ϵ_2 were not so precise but nevertheless the agreement with scaling predictions is still satisfactory. For the three dimensional hydrogen peroxide lattice it was not possible to estimate ε_3 at all. Also, while we could estimate ε_0 by the method of logarithmic derivatives the method of neighbouring powers failed completely to yield an stimate of ε_0. For $\ell = 0, 4, 5$ in the case of the hydrogen peroxide lattice, the agreement with the corresponding ε_ℓ's of scaling is excellent. For ε_1 and ε_2 the agreement is fair. It is clear that there is some qualitative similarity between the two dimensional cases and the three dimensional hydrogen peroxide lattice case. Most of the critical exponents agree very well with scaling. Some agree only satisfactorily, while a few are not even estimatable.

On the whole we conclude that the results obtained in the analyses of the critical exponents, γ'_ℓ and ε'_ℓ for the hydrogen peroxide lattice support static scaling for the three dimensional Ising model. To obtain even more precise results we have to calculate more terms in the low temperature series expansions, especially for the field derivatives of the magnetization on the coexistence curve. A subsequent extension of this work is to test lattice-lattice scaling, or universality theory, using the critical amplitude data obtained here for the hydrogen peroxide lattice and elsewhere for other lattices.

References

ANDREWS, T. (1869) Phil. Trans. R. Soc. 159, 575.

BAKER, G.A. JR. (1961) Phys. Rev. 124, 768.

BAKER, G.A. JR. (1965) Adv. Theor. Phys. 1,1.

BETTS, D.D. and CHAN, C.F.S. (1974) J. Phys. A: Math. Nucl. Gen. 7, (in press).

BETTS, D.D., ELLIOTT, C.J. and DITZIAN, R.V. (1971) Can. J. Phys. 49, 1327.

BETTS, D.D., ELLIOTT, C.J. and SYKES, M.F. (1974) J. Phys. A: Math. Nucl. Gen. 7, (in press).

BETTS, D.D. and FILIPOW, L. (1972) Can. J. Phys. 50, 3117.

BETTS, D.D., GUTTMANN, A.J. and JOYCE, G.S. (1971) J. Phys. C: Solid St. Phys. 4, 1994.

DOMB, C. (1960) Adv. Phys. 9,149.

DOMB, C. (1968) Phys. Rev. Lett. 20, 1425.

DOMB, C. (1970) Adv. Phys. 19, 339.

DOMB, C. and GREEN, M.S. (Ed.) (1974) Phase Transitions and Critical Phenomena, 3, Academic Press, Lond. (in press).

DOMB, C. and GUTTMANN, A.J. (1970) J. Phys. C: Solid St. Phys. 3, 1652.

DOMB, C. and HUNTER, D. L. (1965) Proc. Phys. Soc. 86, 1147.

DOMB, C. and SYKES, M.F. (1957) Proc. Roy. Soc. (London) A, 240, 214.

ESSAM, J.W. and FISHER, M.E. (1963) J. Chem. Phys. 38,802.

ESSAM, J.W. and HUNTER, D.L. (1968) J. Phys. C: Solid St. Phys. 1, 392.

ESSAM, J.W. and SYKES, M.F. (1963) Physica 29, 378.

FISHER, M.E. (1964) J. Math. Phys. 5, 944.

FISHER, M.E. (1965) Lectures in Theoretical Physics 7C, Univ. of Colorado Press, Boulder, Colorado.

FISHER, M.E. (1967) Rep. Prog. Phys. 30, 615.

FISHER, M.E. (1969) Phys. Rev. 180, 594.

GAMMEL, J., MARSHALL, W. and MORGAN, L. (1963) Proc. R. Soc. 275, 257.

GAUNT, D.S. (1967) Proc. Phys. Soc. 92, 150.

GAUNT, D.S. and DOMB, C. (1968) J. Phys. C: Solid St. Phys. 2, 1038.

GAUNT, D.S. and GUTTMANN, A.J. (1974) Phase Transitions and Critical Phenomena, 3, ed. DOMB, C. and GREEN, M.S., Academic Press, Lond., (in press).

GAUNT, D.S. and SYKES, M.F. (1972) J. Phys. C: Solid St. Phys. 5, 1429.

GAUNT, D.S. and SYKES, M.F. (1973) J. Phys. A: Math. Nucl. Gen. 6, 1517.

GRIFFITHS, R.B. (1964) J. Math. Phys. 5, 1215.

GRIFFITHS, R.B. (1965a) Phys. Rev. Lett. 14, 623.

GRIFFITHS, R.B. (1965b) J. Chem. Phys. 43, 1958.

GRIFFITHS, R.B. (1968) Unpublished lectures delivered at the Banff Summer Institute on Critical Phenomena.

GRIFFITHS, R.B., HURST, C.A. and SHERMAN, S. (1970) J. Math. Phys. 11, 790.

GUTTMANN, A.J., THOMPSON, C.J. and NINHAM, B.W. (1970) J. Phys. C: Solid St. Phys. 3, 1641.

HEESCH, H. and LAVES, F. (1933) Z. Krist. 85, 443.

HUANG, K. (1963) Statistical Mechanics, Wiley, New York.

ISING, E. (1925) Z. Phys. 31, 253.

de JONGH, L.J. and MIEDEMA, A.R. (1974) Rep. Prog. Phys. (in press).

KADANOFF, L.P. (1966) Physics 2, 263.

LEU, J.A., BETTS, D.D. and ELLIOTT, C.J. (1969) Can. J. Phys. 47, 1671.

ONSAGER, L. (1944) Phys. Rev. 65, 117.

PATASHINSKII, A.Z. and POKROVSKII, V.L. (1966) Sov. Phys. JETP 23, 292.

PEIERLS, R. (1936) Proc. Camb. Phil. Soc. 32, 477.

RUSHBROOKE, G.S. (1963) J. Chem. Phys. 39, 842.

STANLEY, H.E. (1971) Introduction to Phase Transitions and Critical Phenomena, Clarendon, Oxford.

STEPHENSON, J. (1971) Phys. Chem. 8B, 717.

SYKES, M.F., ESSAM, J.W. and GAUNT, D.S. (1965) J. Math. Phys. 6, 283.

SYKES, M.F., GAUNT, D.S., ESSAM, J.W. and ELLIOTT, C.J. (1973) J. Phys. A: Math. Nucl. Gen. 6, 1507.

SYKES, M.F., GAUNT, D.S., ESSAM, J.W., HEAP, B.R., ELLIOTT, C.J. and MATTINGLY, S.R. (1973) J. Phys. A: Math. Nucl. Gen. 6, 1498.

SYKES, M.F., GAUNT, D.S., ESSAM, J.W., MATTINGLY, S.R. and ELLIOTT, C.J. (1973) J. Math. Phys. 14, 1066.

SYKES, M.F., GAUNT, D.S. and HUNTER, D.L. (1973) J. Math. Phys. 14, 1060.

SYKES, M.F., GAUNT, D.S., MARTIN, J.L., MATTINGLY, S.R. and ESSAM, J.W. (1973) J. Math. Phys. 14, 1071.

SYKES, M.F., GAUNT, D.S., ROBERTS, P.D. and WYLES, J.A. (1972) J. Phys. A: Gen. Phys. 5, 640.

SYKES, M.F., HUNTER, D.L., MCKENZIE, D.S. and HEAP, B.R. (1972) J. Phys. A: Gen. Phys. 5, 667.

van der WAALS, J.D. (1873) Ph.D. Thesis, University of Leiden.

WEISS, P. (1907) J. Phys. Radium, Paris 6, 667.

WELLS, A.F. (1954) Acta. Cryst. 7, 535.

WIDOM, B. (1965a) J. Chem. Phys. 43, 3892.

WIDOM, B. (1965b) J. Chem. Phys. 43, 3898.

APPENDIX 1

Hypertriangular Lattice Graphs and Low Temperature Lattice Constants

(10,5,5,0) 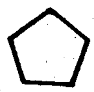 3	(15, 7, 7,1) Σ 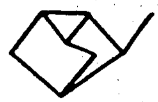 24	Σ 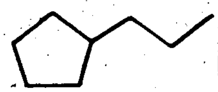 1608
(12,6,6,0) 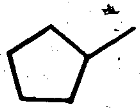 30	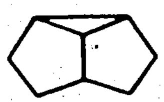 6	(16, 7, 7,2) 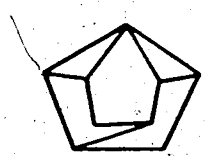 3
(13,6,6,1) 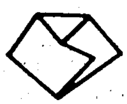 2	(15,6,9,0) 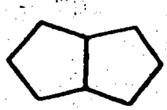 12	(17,8,8,1) 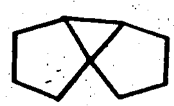 39
(14, 7, 7,0)  3	(16,8,8,0) 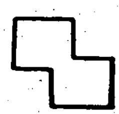 9	Σ 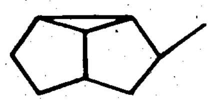 78
Σ  234	 36	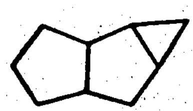 42

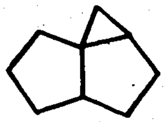
48

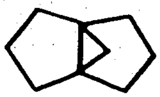
12

Σ 
210

(17, 7,10,0)

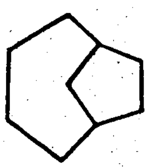
6

Σ 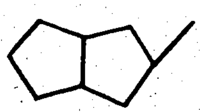
144

(18, 9, 9, 0)

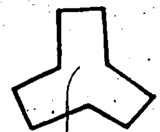
8

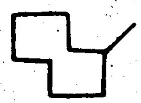
132

Σ 
309

Σ 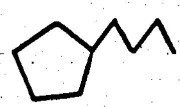
10617

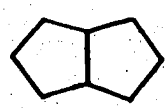
-345

(18, 8, 8, 2)

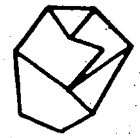
6

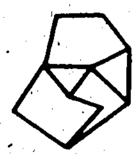
6

Σ 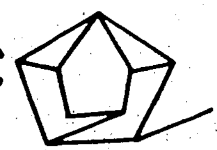
42

(18, 7,10,1)

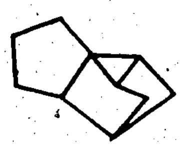
12

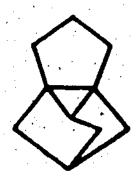
12

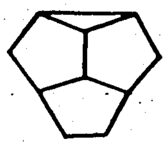 6

(19,9,9,1)

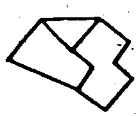 6

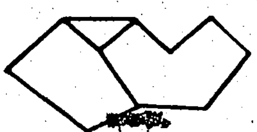 12

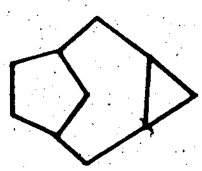 0

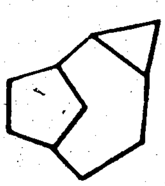 6

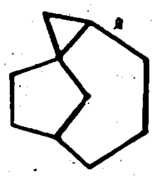 12

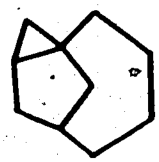 6

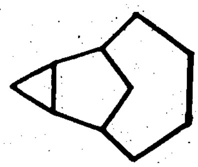 6

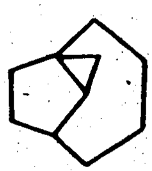 12

Σ  564

Σ  168

Σ 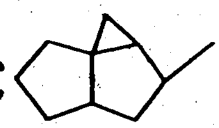 714

Σ 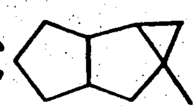 642

Σ 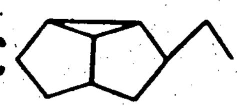 714

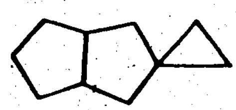 24

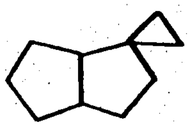 48

Σ  1556

 63

(18, 6, 12, 0)

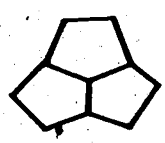 2

(19, 8, 11, 0)

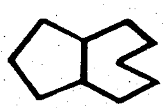 24

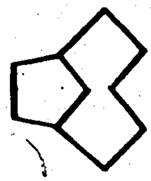 6

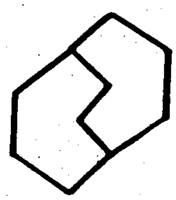 3

Σ 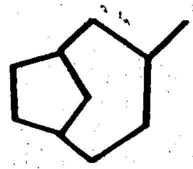 78

Σ 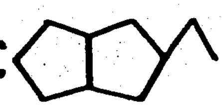 1230

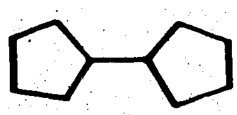 60

(20, 10, 10, 0)

 66

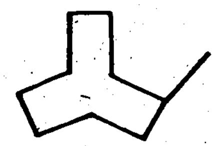 114

Σ 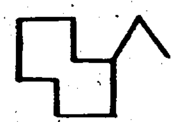 1335

Σ 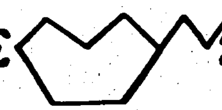 2274

Σ 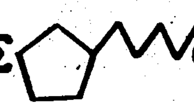 68982

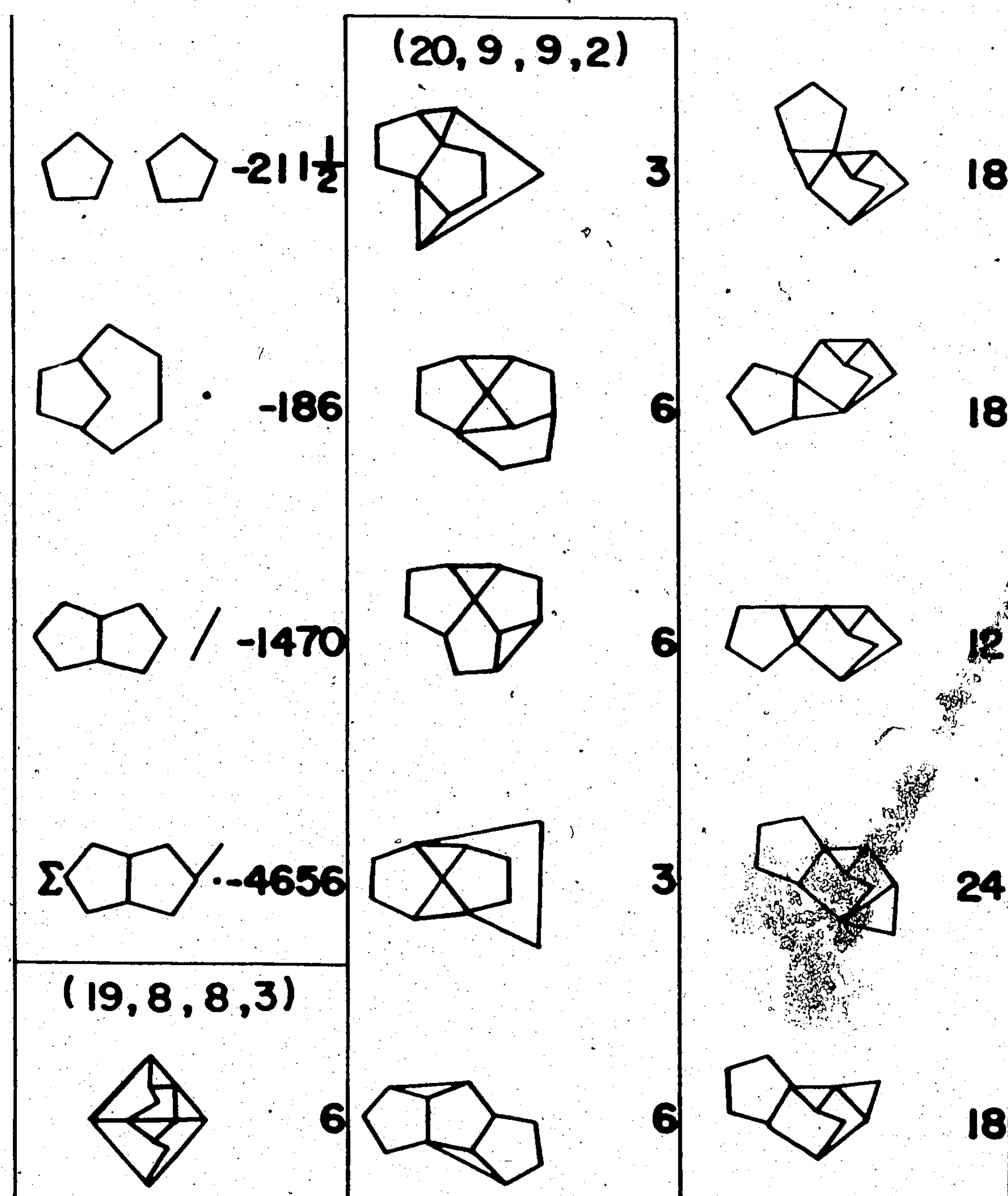
-211 1/2
-186
-1470
Σ
-4656
(19,8,8,3)
6
(20,9,9,2)
3
6
6
3
6
18
18
12
24
18

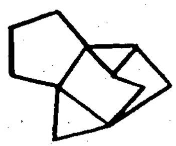
12

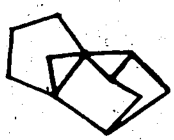
12

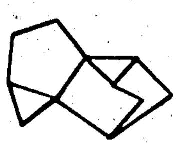
12

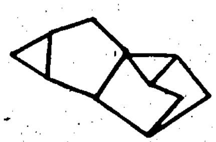
6

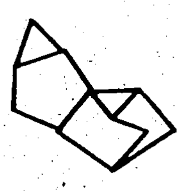
12

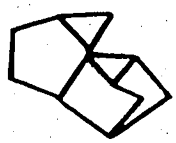
12

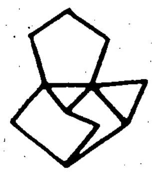
24

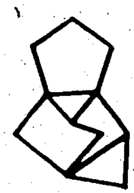
24

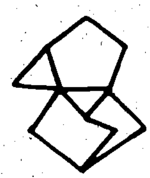
24

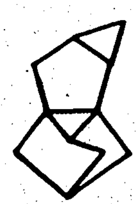
24

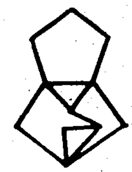
12

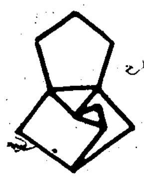
12

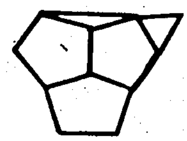
6

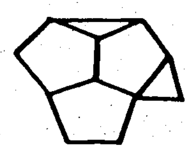
12

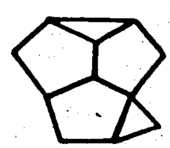
6

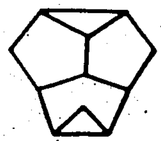	6	Σ 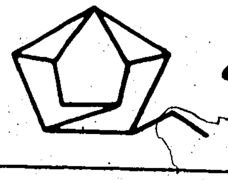	408	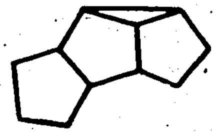	12
		(19, 6, 12, 1)			
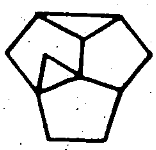	12	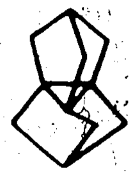	1	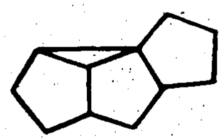	24
		(20, 8, 11, 1)			
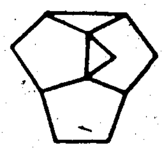	6	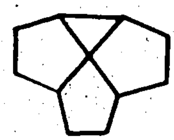	24	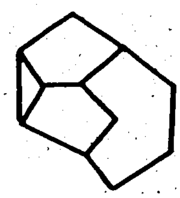	6
Σ 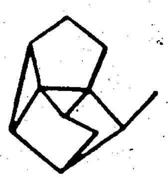	90	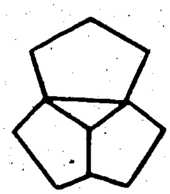	12	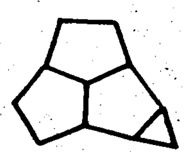	6
Σ 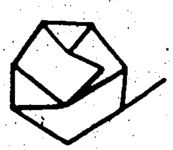	90	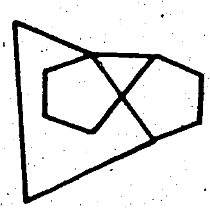	24	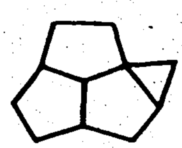	12

(21,10,10,1)

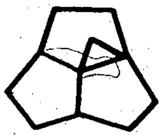 6 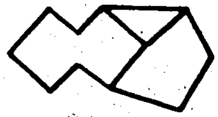 66 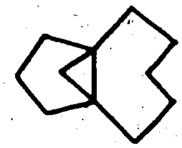 12

Σ 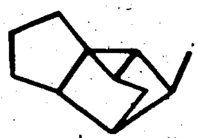 168 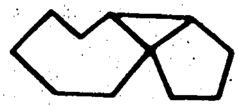 66 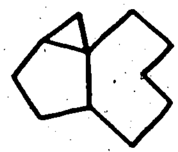 48

Σ 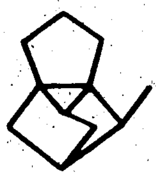 156 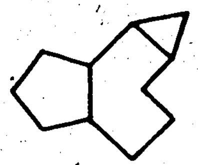 36 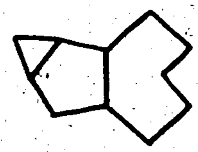 42

Σ 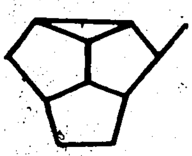 84 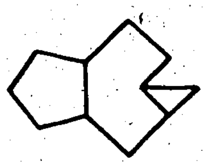 48 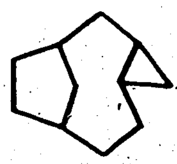 6

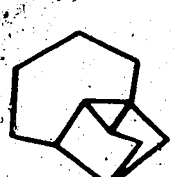 6 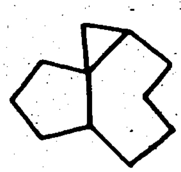 24 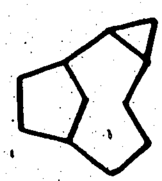 12

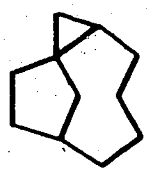
12

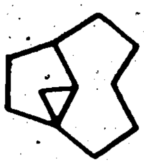
6

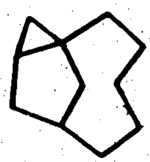
6

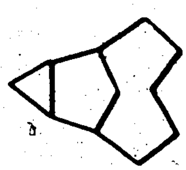
6

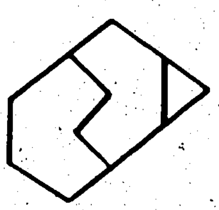
6

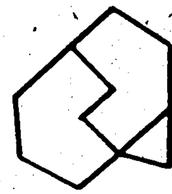
6

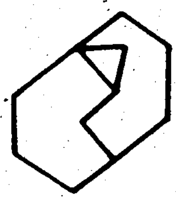
6

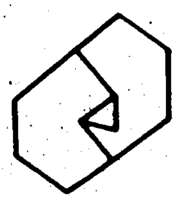
3

Σ
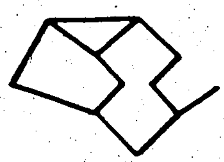
96

Σ
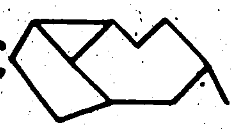
180

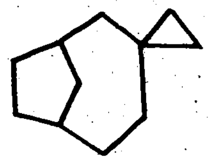
12


12

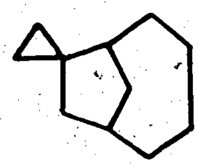
12

Σ
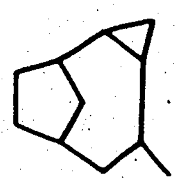
102

Σ
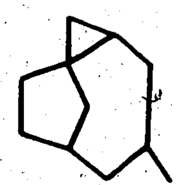
204

Σ 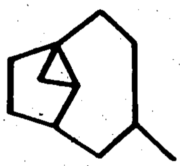 192	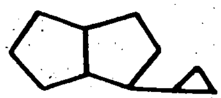 150	Σ 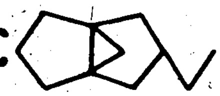 1578
Σ 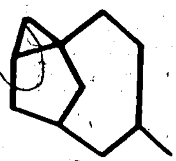 102	Σ 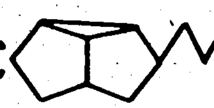 5478	Σ 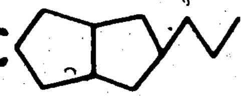 420
Σ 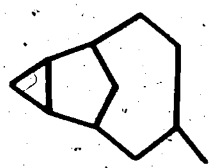 90	Σ 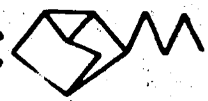 10770	Σ 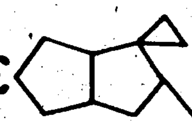 804
Σ 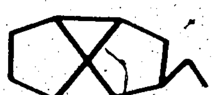 5514	Σ 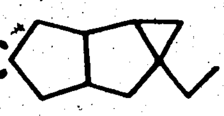 6606	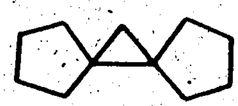 60
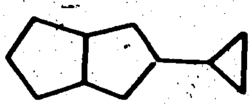 84	Σ 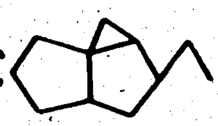 7044	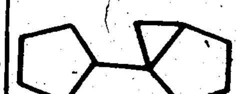 228

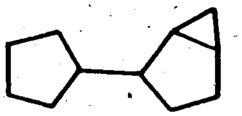
228

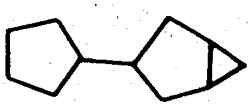
108

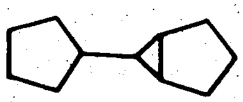
228

Σ 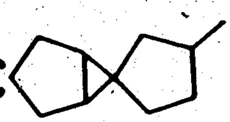
1044

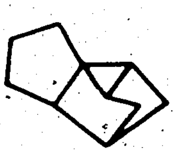
· -402

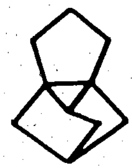
· -402

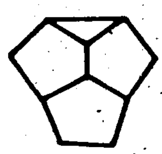
· -198

(20, 7, 13, 0)

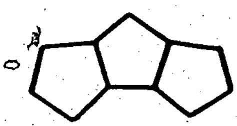
36

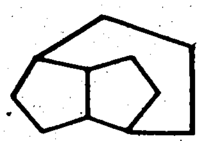
3

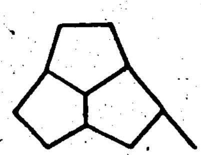
24

(21, 9, 12, 0)

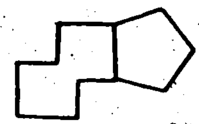
108

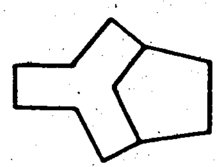
24

Σ 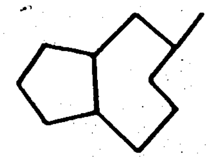
330

Σ 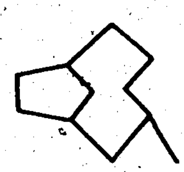
90

Σ 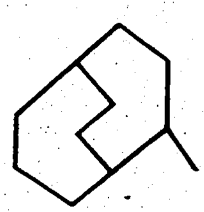
42

	(22,11,11,0)	
Σ 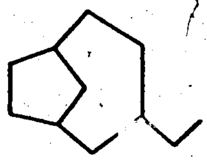 714	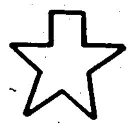 108	Σ  445146
Σ 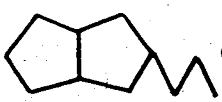 9108	 1158	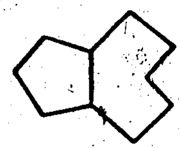 -834
 210	Σ 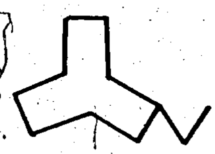 1092	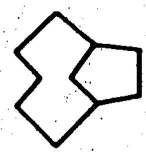 -210
Σ 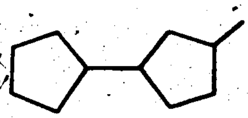 876	Σ 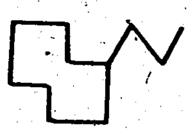 11286	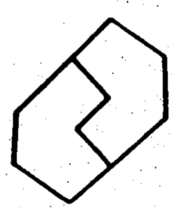 -102
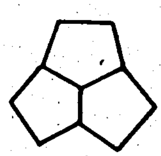 -68	Σ  15759	Σ 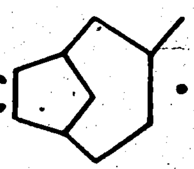 -2706

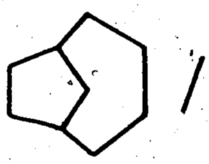

-792

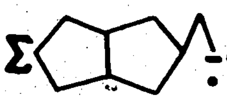

-44109

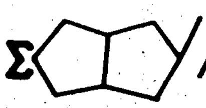

-19680

-7428

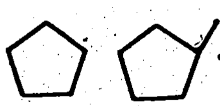

-4878

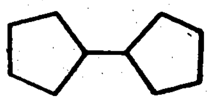

-2160

APPENDIX 2

The Low Temperature, High Field Polynomials

$$L_1 = z^3$$

$$L_2 = 1\tfrac{1}{2}\, z^4 - 2\, z^6$$

$$L_3 = 3\, z^5 - 9\, z^7 + 6\tfrac{1}{3}\, z^9$$

$$L_4 = 7\, z^6 - 33\tfrac{3}{4}\, z^8 + 51\, z^{10} - 24\tfrac{1}{2}\, z^{12}$$

$$L_5 = 18\, z^7 - 121\, z^9 + 288\, z^{11} - 291\, z^{13} + 106\tfrac{1}{5}\, z^{15}$$

$$L_6 = 49\tfrac{1}{2}\, z^8 - 429\, z^{10} + 1410\tfrac{1}{2}\, z^{12} - 2220\, z^{14}$$
$$+ 1684\tfrac{1}{2}\, z^{16} - 495\tfrac{2}{3}\, z^{18}$$

$$L_7 = 143\, z^9 - 1521\, z^{11} + 6420\, z^{13} - 13872\, z^{15}$$
$$+ 16281\, z^{17} - 9888\, z^{19} + 2437\tfrac{1}{7}\, z^{21}$$

$$L_8 = 429\, z^{10} - 5414\tfrac{1}{2}\, z^{12} + 27999\, z^{14} - 77398\tfrac{7}{8}\, z^{16}$$
$$+ 124165\, z^{18} - 116077\tfrac{1}{2}\, z^{20} + 58755\, z^{22} - 12457\tfrac{1}{4}\, z^{24}$$

$$L_9 = 1326\, z^{11} - 19380\, z^{13} + 118864\, z^{15} - 401793\, z^{17}$$
$$+ 822360\, z^{19} - 1047420\, z^{21} + 813216\, z^{23} - 352791\, z^{25}$$
$$+ 65618\tfrac{1}{9}\, z^{27}$$

$$L_{10} = 1\tfrac{1}{2}\, z^{10} + 4184\, z^{12} - 69700\tfrac{1}{2}\, z^{14} + 495463\tfrac{1}{2}\, z^{16}$$
$$- 1984976\, z^{18} + 4959838\tfrac{4}{5}\, z^{20} - 8042325\, z^{22}$$
$$+ 8485862\tfrac{1}{2}\, z^{24} - 5631619\tfrac{1}{2}\, z^{26} + 2137315\tfrac{1}{2}\, z^{28}$$
$$- 354044\tfrac{9}{10}\, z^{30}$$

$$L_{11} = 15\ z^{11} + 13371\ z^{13} - 251461\ z^{15} + 2037402\ z^{17}$$

$$- 9458250\ z^{19} + 27985130\ z^{21} - 55320660\ z^{23}$$

$$+ 74182779\ z^{25} - 66776053\ z^{27} + 38687790\ z^{29}$$

$$- 13048224\ z^{31} + 1948161\tfrac{1}{11}\ z^{33}$$

$$L_{12} = 97\tfrac{1}{2}\ z^{12} + 43029\ z^{14} - 908463\tfrac{3}{4}\ z^{16} + 8286908\tfrac{1}{3}\ z^{18}$$

$$- 43833172\tfrac{1}{2}\ z^{20} + 150201585\ z^{22} - 351274376\tfrac{1}{4}\ z^{24}$$

$$+ 573569217\ z^{26} - 655220490\ z^{28} + 514088399\ z^{30}$$

$$- 264244883\tfrac{1}{4}\ z^{32} + 80188977\ z^{34} - 10896827\tfrac{1}{6}\ z^{36}$$

$$L_{13} = 525\ z^{13} + 138830\ z^{15} - 3281880\ z^{17} + 33392535\ z^{19}$$

$$- 198664785\ z^{21} + 775265400\ z^{23} - 2098448703\ z^{25}$$

$$+ 4050218774\ z^{27} - 5627965959\ z^{29} + 5597194944\ z^{31}$$

$$- 3891121690\ z^{33} + 1797133827\ z^{35} - 495661896\ z^{37}$$

$$+ 61800078\tfrac{1}{13}\ z^{39}$$

$$L_{14} = z^{12} + 2536\tfrac{1}{2}\ z^{14} + 447481\tfrac{1}{2}\ z^{16} - 11841776\ z^{18}$$

$$+ 133444096\tfrac{1}{2}\ z^{20} - 883929669\ z^{22} + 3877211902\ z^{24}$$

$$- 11944978402\tfrac{1}{2}\ z^{26} + 26666016898\tfrac{5}{7}\ z^{28} - 43765361029\tfrac{1}{2}\ z^{30}$$

$$+ 52896457630\tfrac{1}{2}\ z^{32} - 46565296611\ z^{34} + 29055837352\ z^{36}$$

$$- 12182650104\ z^{38} + 3079314606\ z^{40} - 354674912\tfrac{11}{14}\ z^{42}$$

$$L_{15} = 12\ z^{13} + 11425\ z^{15} + 1436253\ z^{17} - 42636642\ z^{19}$$
$$+ 529247008\ z^{21} - 3871587153\ z^{23} + 18889738137\tfrac{3}{5}\ z^{25}$$
$$- 65375406444\tfrac{1}{3}\ z^{27} + 166021444314\ z^{29}$$
$$- 314961411369\ z^{31} + 449306269607\ z^{33}$$
$$- 480296343859\tfrac{4}{5}\ z^{35} + 379171416132\ z^{37}$$
$$- 214589972615\ z^{39} + 82377179820\ z^{41}$$
$$- 19215911169\ z^{43} + 2056526543\tfrac{3}{5}\ z^{45}$$

$$L_{16} = 93\ z^{14} + 49018\tfrac{1}{2} + 4575139\ z^{18} - 153062158\tfrac{1}{2}\ z^{20}$$
$$+ 2084270379\ z^{22} - 16727473621\tfrac{1}{4}\ z^{24} + 90014451033\ z^{26}$$
$$- 346294592671\tfrac{1}{2}\ z^{28} + 987391158963\ z^{30}$$
$$- 2129744151758\tfrac{7}{16}\ z^{32} + 3509772030531\ z^{34}$$
$$- 4425412933290\tfrac{1}{2}\ z^{36} + 4239407973591\ z^{38}$$
$$- 3033241322682\tfrac{3}{4}\ z^{40} + 1570453365285\ z^{42}$$
$$- 555911608111\tfrac{1}{2}\ z^{44} + 120389303730\ z^{46}$$
$$- 12032033468\tfrac{1}{8}\ z^{48}$$

$$L_{17} = 598\ z^{15} + 202764\ z^{17} + 14409894\ z^{19} - 547450096\ z^{21}$$
$$+ 8153604795\ z^{23} - 71405101536\ z^{25} + 420833846469\ z^{27}$$
$$- 1784180286798\ z^{29} + 5651844105765\ z^{31}$$
$$- 13680739580495\ z^{33} + 25620479515527\ z^{35}$$

$$- 37298644730412\, z^{37} + 42120959081893\, z^{39}$$

$$- 36547100200164\, z^{41} + 23906230325115\, z^{43}$$

$$- 11405426399510\, z^{45} + 3745493261637\, z^{47}$$

$$- 756919374921\, z^{49} + 70954769475\tfrac{1}{17}\, z^{51}$$

$$L_{18} = 1\tfrac{1}{2}\, z^{14} + 3433\tfrac{1}{2}\, z^{16} + 814269\, z^{18} + 44669941\tfrac{1}{2}\, z^{20}$$

$$- 1949392143\, z^{22} + 31692763208\, z^{24}$$

$$- 301524958312\tfrac{1}{2}\, z^{26} + 1934917700613\, z^{28}$$

$$- 8975633689717\tfrac{1}{2}\, z^{30} + 31314976037650\tfrac{1}{2}\, z^{32}$$

$$- 84172872303429\, z^{34} + 176820821627237\tfrac{2}{3}\, z^{36}$$

$$- 292389067189908\, z^{38} + 381048704624616\, z^{40}$$

$$- 389545709247428\tfrac{1}{2}\, z^{42} + 308834552509341\, z^{44}$$

$$- 186042063589293\, z^{46} + 82293071837496\, z^{48}$$

$$- 25202642440527\, z^{50} + 4774062085647\, z^{52}$$

$$- 421381862696\tfrac{2}{9}\, z^{54}$$

$$L_{19} = 21\, z^{15} + 18189\, z^{17} + 3188091\, z^{19} + 135471942\, z^{21}$$

$$- 6905938272\, z^{23} + 122423195703\, z^{25}$$

$$- 1260778496526\, z^{27} + 8765897452023\, z^{29}$$

$$- 44222743718502\, z^{31} + 168700384554780\, z^{33}$$

$$- 499182804413709\ z^{35} + 1163951275197360\ z^{37}$$

$$- 2158054973336719\ z^{39} + 3193111724081010\ z^{41}$$

$$- 3765364402180404\ z^{43} + 3515509230247087\ z^{45}$$

$$- 2565449575498857\ z^{47} + 1432096755422085\ z^{49}$$

$$- 590437841068988\ z^{51} + 169401214193559\ z^{53}$$

$$- 30197254445136\ z^{55} + 2518236075263\tfrac{1}{19}\ z^{57}$$

$$L_{20} = 184\tfrac{1}{2}\ z^{16} + 90651\tfrac{1}{2}\ z^{18} + 12201501\tfrac{3}{4}\ z^{20} + 398442687\ z^{22}$$

$$- 24322143193\tfrac{1}{2}\ z^{24} + 470014161397\tfrac{1}{2}\ z^{26}$$

$$- 5224181339661\tfrac{3}{4}\ z^{28} + 39190590764771\tfrac{2}{5}\ z^{30}$$

$$- 213915411067809\tfrac{3}{4}\ z^{32} + 886804880651334\ z^{34}$$

$$- 2867679902319284\ z^{36} + 7357764343318974\ z^{38}$$

$$- 15136198582450644\ z^{40} + 25101400467745347\ z^{42}$$

$$- 33592891698515892\ z^{44} + 36162670173938031\ z^{46}$$

$$- 31064085272018125\tfrac{3}{4}\ z^{48} + 20997085086857609\tfrac{7}{10}\ z^{50}$$

$$- 10919743335146958\tfrac{3}{4}\ z^{52} + 4215633039979898\ z^{54}$$

$$- 1137622611924962\tfrac{1}{4}\ z^{56} + 191500766930638\tfrac{1}{2}\ z^{58}$$

$$- 15134458156494\tfrac{3}{20}\ z^{60}$$

$$L_{21} = 1323\ z^{17} + 430182\ z^{19} + 45718229\ z^{21}$$

$$+ 1120539792\ z^{23} - 85095886233\ z^{25}$$

$$+ 179361948058 2\tfrac{2}{3}\ z^{27} - 21465431325378\ z^{29}$$

$$+ 173127804877254\ z^{31} - 1017935276525102\ z^{33}$$

$$+ 4561835414102031\tfrac{3}{7}\ z^{35} - 16021945036844910\ z^{37}$$

$$+ 44905908255854368\ z^{39} - 101613354282959886\ z^{41}$$

$$+ 186903731997443451\ z^{43} - 280245540313157249\ z^{45}$$

$$+ 342251744594589351\ z^{47} - 338849726998604449\tfrac{2}{7}\ z^{49}$$

$$+ 269498195865459620\ z^{51} - 169636964749506429\ z^{53}$$

$$+ 82572772040916168\ z^{55} - 29970234585965632\ z^{57}$$

$$+ 7634012726533563\ z^{59} - 1217293609514970\ z^{61}$$

$$+ 914218894344323\tfrac{5}{23}\ z^{63}$$

$$L_{22} = 3\ z^{16} + 8370\tfrac{1}{2} + 1959481\tfrac{1}{2}\ z^{20} + 167840194\tfrac{1}{2}\ z^{22}$$

$$+ 2935273028\ z^{24} - 295519270846\tfrac{1}{2}\ z^{26}$$

$$+ 6803493293622\ z^{28} - 87504541802766\tfrac{1}{2}\ z^{30}$$

$$+ 756493598609616\ z^{32} - 4773041146564965\ z^{34}$$

$$+ 23018561402772517\ z^{36} - 87341709282688629\ z^{38}$$

$$+ 268760126833423944\ z^{40} - 656672693675081495\tfrac{1}{2}\ z^{42}$$

$$+\ 1328140280244409195\tfrac{7}{11}\ z^{44} - 2208031854541089061\tfrac{1}{2}\ z^{46}$$

$$+\ 3020206623133842152\tfrac{1}{2}\ z^{48} - 3391105526002817485\tfrac{1}{2}\ z^{50}$$

$$+\ 3107406848381889535\tfrac{1}{2}\ z^{52} - 2300652130584331214\tfrac{1}{2}\ z^{54}$$

$$+\ 1354920776966205385\tfrac{1}{2}\ z^{56} - 619818322654171266\ z^{58}$$

$$+\ 212262173815534014\tfrac{1}{2}\ z^{60} - 51195290584927827\ z^{62}$$

$$+\ 7754484620018985\ z^{64} - 554807062334488\tfrac{2}{11}\ z^{66}$$

$$L_{23} = 48\ z^{17} + 48441\ z^{19} + 8617406\ z^{21} + 603774576\ z^{23}$$

$$+\ 6747317997\ z^{25} - 1017723279317\ z^{27}$$

$$+\ 25651310436624\ z^{29} - 354061536754941\ z^{31}$$

$$+\ 3272477752646354\ z^{33} - 22083326312643045\ z^{35}$$

$$+\ 114155720998785930\ z^{37} - 465813704970417072\ z^{39}$$

$$+\ 1530538682933110038\ z^{41} - 4104128077094857968\ z^{43}$$

$$+\ 9061167056974367956\ z^{45} - 16559112659094354042\ z^{47}$$

$$+\ 25105803765794858595\ z^{49} - 31562148720832543073\ z^{51}$$

$$+\ 32788899493478101590\ z^{53} - 27960461548415023320\ z^{55}$$

$$+\ 19361912137372503092\ z^{57} - 10712589275796094284\ z^{59}$$

$$+\ 4622167746869248128\ z^{61} - 1498274806850039777\ z^{63}$$

$$+\ 34313874792314665 2\ z^{65} - 49495440902354931\ z^{67}$$

$+\ 3381150761398$~~343~~$\frac{1}{23}\ z^{69}$

APPENDIX 3

Coefficients in the series expansions on the critical isotherm for

$$[\partial^{\ell} M(\mu,z)/\partial z^{\ell}]_{z=z_c} = \sum_{n=0}^{23} a_n^{(\ell)} \mu^n$$

n	$a_n^{(0)}$	$a_n^{(1)}$	$a_n^{(2)}$	$a_n^{(3)}$	$a_n^{(4)}$	$a_n^{(5)}$
0	0	0	0	0	0	0
1	-0.0639524	-0.604462	-3.80882	-12.0	0	0
2	-0.0527159	-0.612801	-4.81771	-15.0087	146.142	1828.23
3	-0.0417026	-0.562168	-5.09322	-13.2927	394.675	5717.82
4	-0.0334756	-0.507041	-5.10493	-9.51146	710.037	11520.0
5	-0.0274116	-0.457447	-5.01673	-5.00340	1067.94	19052.4
6	-0.0228616	-0.414762	-4.89428	-0.433923	1452.43	28168.5
7	-0.0193713	-0.378373	-4.76538	3.87211	1852.96	38763.4
8	-0.0166371	-0.347293	-4.64181	7.76505	2262.50	50766.1
9	-0.0144547	-0.320589	-4.52816	11.1866	2676.26	64128.6
10	-0.0127914	-0.300104	-4.47647	13.4903	3090.75	79020.8
11	-0.0114881	-0.283831	-4.45656	15.4096	3522.25	95805.4

APPENDIX 3 (cont'd).

n	$a_n^{(0)}$	$a_n^{(1)}$	$a_n^{(2)}$	$a_n^{(3)}$	$a_n^{(4)}$	$a_n^{(5)}$
12	-0.0104273	-0.270145	-4.44549	17.3700	3976.47	114535
13	-0.00953663	-0.258120	-4.43294	19.4955	4452.03	135106
14	-0.00877872	-0.247452	-4.42022	21.6997	4944.82	157410
15	-0.00812313	-0.237808	-4.40515	23.9951	5453.16	181387
16	-0.00754964	-0.229013	-4.38855	26.3212	5973.90	206956
17	-0.00704498	-0.220997	-4.37283	28.5986	6504.46	234084
18	-0.00659960	-0.213722	-4.36002	30.7826	7044.06	262803
19	-0.00620413	-0.207088	-4.34948	32.9070	7593.90	293174
20	-0.00585053	-0.200995	-4.34020	35.0038	8154.52	325217
21	-0.00553246	-0.195367	-4.33177	37.0826	8725.68	358920
22	-0.00524492	-0.190148	-4.32403	39.1452	9306.96	394272
23	-0.00498373	-0.185288	-4.31675	41.1957	9898.00	431262

APPENDIX 4

Coefficients in the series expansions for zero field for $[\partial^{\ell} M(\mu,z)/\partial\mu^{\ell}]_{\mu=\mu_c} = \sum_n b_n^{(\ell)} z^n$

n	$b_n^{(0)}$	$b_n^{(1)}$	$b_n^{(2)}$	$b_n^{(3)}$	$b_n^{(4)}$	$b_n^{(5)}$
0	1	0	0	0	0	0
1	0	0	0	0	0	0
2	0	0	0	0	0	0
3	-2	-2	0	0	0	0
4	-6	-12	-12	0	0	0
5	-18	-54	-108	-108	0	0
6	-48	-208	-656	-1344	-1344	0
7	-126	-738	-3276	-10476	-21600	-21600
8	-324	-2484	-14580	-64800	-207360	-427680
9	-830	-8078	-60112	-348048	-1536480	-4899840
10	-2154	-25956	-237540	-1719936	-9839232	-43326720
11	-5784	-83784	-918048	-8057232	-57249072	-325864080
12	-16146	-272988	-3499212	-36317616	-310765968	-2189623200
13	-46302	-893682	-13163100	-158511420	-1596048480	-13497864480
14	-134082	-2919180	-48799644	-672173136	-7825830768	-77661583200
15	-387724	-9474856	-178251828	-2778134580	-36896913120	-422346949440
16	-1117164	-30555000	-642594792	-11232603792	-168331650768	-2192689632960
17	-3220146	-98142486	-2292451644	-44595011340	-747155027952	-10953292264560

APPENDIX 5

Coefficients in the series expansion on the coexistence curve for

$$(\mu\frac{\partial}{\partial\mu})^{\ell} M|_{\mu=\mu_c} = -2 \sum_{n=0}^{17} \beta_n^{(\ell)} \cdot z^n$$

n	$\beta_n^{(0)}$	$\beta_n^{(1)}$	$\beta_n^{(2)}$	$\beta_n^{(3)}$	$\beta_n^{(4)}$	$\beta_n^{(5)}$
0	-0.5	0	0	0	0	0
1	0	0	0	0	0	0
2	0	0	0	0	0	0
3	1	1	1	1	1	1
4	3	6	12	24	48	96
5	9	27	81	243	729	2187
6	24	104	432	1760	7104	28544
7	63	369	2007	10521	54063	274689
8	162	1242	8532	55512	350352	2171232
9	415	4039	34095	268231	2026815	14937799
10	1077	12978	131748	1229256	10923792	94153248
11	2892	41892	500916	5447580	56051292	556820052
12	8073	136494	1886100	23544120	276719568	3128992224
13	23151	446841	7028391	99447201	1320076191	16809737481
14	67041	1459590	25859412	410745624	6101693136	86729566560
15	193862	4737428	93863342	1661182460	27411479125	431726348708
16	558582	15277500	336574896	6595471584	120127996032	2083245356160
17	1610073	49071243	1195297065	25785254379	515435199993	9787101372363

APPENDIX 6

Poles and residues of Padé approximants to

$$\frac{d}{dz} \log \sum_{n=3}^{17} \beta_n^{(2)} z^{n-3}$$

	Pole	Residue
PADÉ (6,7)	0.339457840990814	-0.679652664765912D 01
PADÉ (7,6)	0.321357055084527	-0.334813316940444D 01
PADÉ (5,7)	0.295750439416026	-0.185440516806951D 01
PADÉ (6,6)	0.316746646694732	-0.294907918467118D 01
PADÉ (7,5)	0.286112700532900	-0.982988832077769D 00
PADÉ (4,7)	0.303280925282878	-0.213986211[illegible]46816D 01
PADÉ (5,6)	0.301191854662018	-0.203382097354968D 01
PADÉ (6,5)	0.327263151674791	-0.388979824836032D 01
PADÉ (4,6)	0.298259784449363	-0.192092034239890D 01
PADÉ (5,5)	0.289504969941134	-0.159349722735093D 01
PADÉ (6,4)	0.349612674093252	-0.673113035637042D 01
PADÉ (3,6)	0.291765371343721	-0.170975483072717D 01
PADÉ (4,5)	0.249918303485047	-0.534731209974970D 00
PADÉ (5,4)	0.276290868518204	-0.119025228233482D 01